# Breeding of useful bacterial strains in food industry based on the analysis of metabolic systems and phage susceptibilities

**Takura Wakinaka**

**2024**

## CONTENTS

# GENERAL INTRODUCTION

Lactic acid bacteria and bifidobacteria are contained in various fermented foods and contribute to the production of the fermented foods and/or the maintenance of human health. Therefore, understanding the properties of these bacteria is helpful for improving the value of food products and promoting human health.

Bifidobacterum is a Gram-positive bacterium belonging to the genus *Bifidobacterium*. They inhabit the gastrointestinal tract, and are the major bacteria that make up the human intestinal flora. *Bifidobacterium bifidum* is one of the most frequently found bifidobacteria in the intestines of newborn infants (1). *B. bifidum* is commercially used as probiotics since they regulate the host's immune system to enhance resistance to pathogens and reduce inflammation (2, 3).

Since *B. bifidum* is primarily located in the lower intestine where sugars are highly restricted, they utilize indigestible oligosaccharides and glycoconjugates. The gastrointestinal glycoprotein mucin is one such sugar resource and ABH blood group antigens are expressed at the sugar chain termini. *B. bifidum* can degrade B antigens to release galactose, and a candidate gene encoding an α-galactosidase responsible for the degradation of B antigens was discovered from *B. bifidum* (4). To better understand the degradation of gastrointestinal mucin oligosaccharides by Bifidobacterium, the α-galactosidase was constructed as a recombinant protein and investigated in detail (CHAPTER I SECTION 1).

*Tetragenococcus halophilus* is a Gram-positive halophilic lactic acid bacterium that plays an important role in the fermentation of various salted foods such as salted fish, vegetable pickles, and soy sauce (5-7). Lactic acid produced by *T. halophilus* reduces the pH and gives a moderate sour taste to food products.

Certain strains of *T. halophilus* degrade particular amino acids, such as histidine (8), tyrosine (9), arginine (10), and aspartate (11). Histidine and tyrosine are transformed into histamine and tyramine via decarboxylasion by *hdcA* and *tdcA* encoded on the plasmids of *T. halophilus*. Histamine is known as a causative agent of food related intoxication and tyramine is related to food-induced migraines and hypertensive crisis (12-14). Therefore, amino acid decarboxylating strains are generally not preferred for starter cultures, but *T. halophilus* possessing aspartate decarboxylase can transform aspartate into sweet amino acid alanine and can possibly be a desirable fermentation starter (11). In order to elucidate the effects of the aspartate decarboxylation for fish sauce fermentation, aspartate decarboxylating strains were isolated and used as a starter for fish sauce fermentation (CHAPTER II SECTION 1).

Arginine deimination by *T. halophilus* is also disfavored for soy sauce brewing, since it is responsible for the accumulation of citrulline, the main precursor of the potential carcinogen ethyl carbamate (15). *T. halophilus* mutants lacking arginine deiminase activity were generated by UV irradiation, and novel ISs were unexpectedly found by transposition into the arginine deiminase operon. Information about these ISs would contribute to research and strain improvement of *T. halophilus* (CHAPTER II SECTION 2).

Bacteriophages infecting *T. halophilus* are a major industrial problem that causes fermentation failure and decreases the quality of food products (16, 17). Tetragenococcal phages typically display narrow host ranges, but the genetic background for this phenotypical characteristic was not revealed. Adsorption to host cells by bacteriophages largely defines the host range. Host receptors on the cell surface are specifically recognized by their respective bacteriophages. First, ribitol-containing

wall teichoic acid was identified as a receptor for a bacteriophage phiWJ7 (CHAPTER III SECTION 1). Next, capsular polysaccharide was identified as a receptor for a bacteriophage phiYG2_4, and capsular polysaccharide also acts as a barrier to another bacteriophage phiYA5_2. The variety in capsular polysaccharide structures is concluded to be mainly responsible for the narrow host ranges of tetragenococcal phages (CHAPTER III SECTION 2).

In this research, I analyzed the metabolic systems and phage susceptibility of bifidobacteria and lactic acid bacteria, which advanced the understanding of the properties of these bacteria and will serve as the basis for breeding useful bacterial strains in food industry.

**REFERENCES**


1. Benno Y, Sawada K, Mitsuoka T. 1984. The intestinal microflora of infants: Composition of fecal flora in breast-fed and bottle-fed infants. Microbiol Immunol 28:975-986
2. Picard C, Fioramonti J, Francois A, Robinson T, Neant F, Matuchansky C. 2005 Review article: Bifidobacteria as probiotic agents – physiological effects and clinical benefits. Aliment Pharmacol Ther 22:495-512
3. Trebichavsky I, Rada V, Splichalova A, Splichal I. 2009 Cross-talk of human gut with bifidobacteria, Nutr Rev 67:77-82
4. Liu QP, Sulzenbacher G, Yuan H, Bennett EP, Pietz G, Saunders K, Spence J, Nudelman E, Levery SB, White T, Neveu JM, Lane WS, Bourne Y, Olsson ML, Henrissat B, Clausen H. 2007. Bacterial glycosidases for the production of universal red blood cells. Nat Biotechnol 25:454-464
5. Kuda T, Izawa Y, Ishii S, Takahashi H, Torido Y, Kimura B. 2012. Suppressive effect of *Tetragenococcus halophilus*, isolated from fish-nukazuke, on histamine accumulation in salted and fermented fish. Food Chem 130:569-574
6. Chen YS, Yanagida F, Hsu JS. 2006. Isolation and characterization of lactic acid bacteria from suan-tsai (fermented mustard), a traditional fermented food in Taiwan. J Appl Microbiol 101:125-130
7. Tanaka Y, Watanabe J, Mogi Y. 2012. Monitoring of the microbial communities involved in the soy sauce manufacturing process by PCR-denaturing gradient gel electrophoresis. Food Microbiol 31:100-106.
8. Satomi M, Furushita M, Oikawa H, Yoshikawa-Takahashi M, Yano Y. 2008 Analysis of a 30 kbp plasmid encoding histidine carboxylase gene in

*Tetragenococcus halophilus* isolated from fish sauce. Int J Food Microbiol 126:202–209

9. Satomi M, Shozen KI, Furutani A, Fukui Y, Kimura M, Yasuike M, Yano Y. 2014. Analysis of plasmids encoding the tyrosine decarboxylase gene in *Tetragenococcus halophilus* isolated from fish sauce. Fish Sci 804:849-858
10. Iituka, K., Goan, M., 1973. Studies on L-Arginine decomposition in Soy-sauce mash. Chomi Kagaku 20:17-24 (in Japanese).
11. Higuchi, T., Uchida, K., Abe, K., 1998. Aspartate decarboxylation encoded on the plasmid in the soy sauce lactic acid bacterium, *Tetragenococcus halophila* D10. Biosci Biotechnol Biochem 62:1601-1603
12. Rice SL, Eitenmiller RR, Koehler PE. 1976. Biologically active amines in food: a review. J Milk Food Technol 39:353-358
13. Santos MS. 1996. Biogenic amines: their importance in foods. Int J Food Microbiol 29:213-231
14. Taylor SL, Eitenmiller RR. 1986. Histamine food poisoning: toxicology and clinical aspects. CRC Crit Rev Toxicol 17:91-128
15. Matsudo T, Aoki T, Abe K, Fukuta N, Higuchi T, Sasaki M, Uchida K. 1993. Determination of ethyl carbamate in soy sauce and its possible precursor. J Agric Food Chem 41:352-356
16. Uchida K, Kanbe C. 1993. Occurrence of bacteriophages lytic for *Pediococcus halophilus*, a halophilic lactic-acid bacterium, in soy sauce fermentation. J Gen Appl Microbiol 39:429-437.

17. Higuchi T, Uchida K, Abe K. 1999. Preparation of phage-insensitive strains of *Tetragenococcus halophila* and its application for soy sauce fermentation. Biosci Biotechnol Biochem 63:415-417

# CHAPTER I

## A study on bifidobacterial sugar metabolism

## SECTION 1

### Bifidobacterial α-galactosidase with unique carbohydrate-binding module specifically acts on blood group B antigen

*Bifidobacterium bifidum*, the type species of the genus, is one of the most frequently found bifidobacteria in the intestines of newborn infants (1, 2). This bacterium also resides in intestines of adults, although the population diminishes over time (2). *Bifidobacterium bifidum*, as well as other bifidobacteria such as *B. longum*, *B. breve*, and *B. animalis lactis*, gives a health benefit to the hosts, hence they are recognized and commercially used as probiotics. Bifidobacteria lower the intestinal pH to prevent the growth of harmful bacteria by producing lactic acid and acetic acid from sugars via a unique phosphoketolase-dependent hetero lactic acid fermentation (3). In addition, they stimulate the host's immune system to enhance anti-pathogenic and anti-carcinogenic activities; on the other hand, they control unwanted immune responses to reduce chronic inflammation and allergies (4, 5). Since they mainly reside in the lower intestines where the sugars are highly limited, they possess various glycosidases to hydrolyze indigestible oligosaccharides and glycoconjugates. It was previously reported that *B. bifidum* possesses unique metabolic pathways for free oligosaccharides in milk and *O*-linked glycans on gastrointestinal mucin (6-11). It is worth noting that this species expresses two distinct enzymes acting on the core structures in mucin *O*-glycans: glycoside hydrolase (GH) family 101 endo-α-*N*-acetylgalactosaminidase

(EngBF) specific for core 1 structure, also called T-antigen (Galβ1-3GalNAcα1-Ser/Thr) (12, 13), and GH129 α-*N*-acetylgalactosaminidase (NagBb) specific for Tn-antigen (GalNAcα1-Ser/Thr) (14). Whole genomic analysis also revealed that *B. bifidum* is highly adapted to acquire nutrients from *O*-glycans in mucin by producing related glycosidases (15).

The non-reducing termini of *O*-glycans in gastrointestinal mucin are usually covered with various histo-blood glyco-antigens, which confer resistance to digestive enzymes of general commensal bacteria. ABH blood group antigens are the well-known cell surface antigens on red blood cells (RBCs) and other somatic cells. ABH antigens are also expressed as secreted glycoproteins including gastrointestinal mucin in humans with secretor phenotype. H antigen consists of the basic disaccharide α1-2 fucosylgalactose (Fucα1-2Gal), and either GalNAc or Gal is bound to the Gal residue of H antigen via α1-3 linkage to form A [GalNAcα1-3(Fucα1-2)Gal] or B [Galα1-3(Fucα1-2)Gal] antigen (16). GH95 1,2-α-L-fucosidase from *B. bifidum* JCM 1254, which specifically acts on H antigen but not entirely on A and B antigens were previously identified. Therefore, to degrade oligosaccharides with A and B antigens at non-reducing termini, prior elimination of α1,3-linked GalNAc and Gal is required. To better understand the degradation and assimilation of the gastrointestinal mucin oligosaccharides by bifidobacteria, A and B antigen-degrading bifidobacteria were screened and it was found that only *B. bifidum* was capable of releasing Gal from B antigen. Subsequently a candidate gene was found from *B. bifidum* JCM 1254 encoding an α-galactosidase belonging to GH110 that was recently established in the carbohydrate-active enzymes (CAZy) database (17). The enzyme contained a carbohydrate-binding module (CBM) 51 domain that is unique among previously

reported GH110 enzymes. In this chapter, I characterized the hydrolytic specificity of the GH110 domain and binding specificity of the CBM51 domain using recombinant enzymes/proteins, and showed a synergistic effect on degradation of multivalent substrates. I also demonstrated that the recombinant enzyme efficiently converted group B RBCs to O RBCs that are universal for transfusion.

## Materials and methods

### Bacterial strains and culture

The bifidobacterial strains were obtained from the Japan Collection of Microorganisms (JCM, RIKEN Bioresource Center, Japan). The bacteria were cultured in GAM broth (Nissui Pharmaceutical, Japan) for 16 h at 37 °C under anaerobic conditions using Anaeropack (Mitsubishi Gas Chemical, Japan).

### Genome sequence of *B. bifidum* JCM 1254

Draft sequencing of the genome of *B. bifidum* JCM 1254 was performed using a Genome Sequencer 20 System (Roche Applied Science, IN, USA). The details will be reported elsewhere.

### Cloning and expression of AgaBb in *E. coli*

To construct the AgaBb expression vector, a DNA fragment encoding aa 24-1255 (without an N-terminal signal peptide and C-terminal transmembrane region) was amplified by high-fidelity PCR using genomic DNA from *B. bifidum* JCM 1254 as a template and the primers (AgaBb-F and AgaBb-R, Table 1), digested with EcoRI and XhoI, and ligated into pET23b(+). The nucleotide sequence was confirmed by sequencing. *E. coli* BL21(λDE3) was transformed with pET23b/*agabb* and cultured in Luria-Bertani liquid medium containing 100 μg/mL ampicillin at 37 °C until the optical

density at 600 nm reached 0.5. Then, to induce expression, IPTG was added to the culture at a final concentration of 0.5 mM, and the cells were further cultured for 2 h at 37 °C.

**Table 1** Primers list.

| Primer name | Sequence (5'→3') |
|---|---|
| AgaBb-F | TAGAATTCGGCCGGAGGAGACGTCGTC |
| AgaBb-R | AACTCGAGCTGGTTCTTGTCCTTGCCG |
| D328N-F | TACGCCAACTTCGTGCAGATGTCGGGC |
| D328N-R | CACGAAGTTGGCGTATCCTGCGGTGCT |
| H997A-F | GGCACCGCCGCGGCCTCGCGCATCGTG |
| H997A-R | GGCCGCGGCGGTGCCGATGCCCTTGTC |
| H1085A-F | GGCGATGCCGCGGATTGGGCGGACGCC |
| H1085A-R | ATCCGCGGCATCGCCCCACGTCTCGCT |
| D962A-F | TCCGGCGCCCCCAACACCAACCCGGTG |
| D962A-R | GTTGGGGGCGCCGGACGTGGCCGACTC |
| H1031A-F | CGCGACGCCGCAAATGTCGACTTCCAG |
| H1031A-R | ATTTGCGGCGTCGCGGTCGACGCCGGT |
| W1082A-F | GAGACGGCGGGCGATCACGCGGATTGG |
| W1082A-R | ATCGCCCGCCGTCTCGCTGCCCGCGCC |
| DCBM51-F | AAACTCGAGGCCGACCGCGGTGATCGTGCC |
| DCBM51-R | AAACTCGAGCACCACCACCACCACCACTGA |
| CBM51-F | AAAGGATCCGGCGAGACAACGGTCCGCACC |
| CBM51-R | AATAAGCTTCTACTGGTTCTTGTCCTTGCC |

**Purification of the recombinant AgaBb**

After the 2 h-induction, cells were harvested and lysed by BugBuster Protein Extraction Reagent (Novagen, Germany). After centrifugation, the supernatant was

applied to a HisTrap HP column (1 mL, GE Healthcare, UK), and the adsorbed proteins were eluted by a stepwise imidazole concentration gradient in a 50 mM sodium phosphate buffer, pH 7.0, containing 250 mM NaCl. The active fraction (1 mL) was applied onto a Superdex 200 10/300 GL (GE healthcare) gel filtration column with an ÄKTA Explorer system (GE Healthcare). Elution was carried out using a 50 mM sodium phosphate buffer, pH 7.0, containing 150 mM NaCl. Active fractions were collected, concentrated, and desalted using an Amicon Ultra 30K (Merck Millipore, MA, USA).

**Mutants of AgaBb**

To construct various expression vectors, high-fidelity DNA polymerase (PrimeSTAR Max DNA Polymerase, Takara Bio, Japan) and the primers listed in Table 1 were used. For point mutated AgaBb expression vectors, PCR was performed using pET23b/*agabb* as a template. For AgaBb-D328NΔCBM51 (aa 23-701) expression vector, a DNA fragment was amplified using pET23b/*agabb*(D328N) as a template and the primers ΔCBM51-F and ΔCBM51-R, digested with XhoI, and self-ligated. Transformation and expression was performed under the same conditions as the wild-type AgaBb. For TF-tagged CBM51 expression vector, a DNA fragment was amplified using pET23b/*agabb* as a template and the primers CBM51-F and CBM51-R, digested with BamHI and HindIII, and ligated into pCold TF (Takara Bio). *E. coli* BL21(λDE3) was transformed with the plasmid and cultured in Luria-Bertani liquid medium containing 100 μg/mL ampicillin at 37 °C until the optical density at 600 nm reached 0.5. Then, the culture was cooled at 15 °C for 30 min, and incubated for 24 h at 15 °C after the addition of 0.5 mM IPTG.

**Enzyme assay**

Blood group B trisaccharide (Dextra Laboratories, UK) and crude salivary mucin prepared from human saliva by 75% ethanol precipitation were used as substrates for enzyme assay. Substrate was incubated with the enzyme at 37 °C for an appropriate time in 50 mM sodium phosphate buffer (pH 6.0). The reaction products were separated by silica-gel TLC (Merck 5553, Germany) with 1-butanol:acetic acid:water (2:1:1, by volume) as developing solvent and visualized using diphenylamine-aniline-phosphoric acid (18). Released Gal was quantified by the galactose dehydrogenase-coupled method (10, 19) after stopping the reaction by heating.

**Hemagglutination test**

Group B and O RBCs were collected by centrifugation, washed once with PBS, and resuspended in PBS to make a 2% suspension. AgaBb (20 pmol/ml) was added to the suspension and incubated at 37 °C for 10 min. After the enzymatic reaction, the suspension is mixed with mouse anti-B monoclonal antibody (clone 5362B, Funakoshi, Japan) or *Ulex europaeus* agglutinin (UEA)-1 (Seikagaku Biobusiness, Japan) in a V-shape 96-well plate. Anti-B antibody and anti-H lectin were serially diluted twice from 0.125 and 0.25 mg/ml, respectively. After letting the plate stand for 1 h at room temperature, the agglutination was analyzed.

**Dot-blot overlay assay**

Protein concentration was measured using the BCA protein assay reagent (Thermo Scientific, IL, USA). Salivary mucin was blotted onto a PVDF membrane, followed by blocking with 10% skim milk (Wako Pure Chemical Industries, Japan) and 0.05% Tween 20 in PBS. The membranes were then treated with 1 μM purified AgaBb-D328N or AgaBb-D328NΔCBM51 in 50mM sodium phosphate (pH 6.0). After

washing the membrane, subsequent detection was carried out by immunoblotting used a rabbit anti-His-tag polyclonal primary antibody (1/1,000, MBL, Japan), and horseradish peroxidase-conjugated anti-rabbit IgG (1/5,000, Santa Cruz Biotechnology, CA, USA) as the secondary antibody. Detection was carried out using West Pico Chemiluminescent Kit (Thermo Scientific) and LAS Image Analyzer (Fuji Film, Japan).

**ELISA-like assay**

Crude salivary mucin from group B human (50 μg/ml) was dispensed in a 96-well plate and let stand for 1 h at room temperature to adsorb the proteins. After removing the solution, the plate was blocked as for the dot-blot assay. The primary and secondary antibodies were the same as for the dot-blot assay. Measurements were carried out by Powerscan HT (DS Parma Biomedical, Japan) at 415 nm using 2,2'-azino-bis(3-ethylbenzothiazoline-6-sulphonic acid) and $H_2O_2$ as substrates.

**Isothermal titration calorimetry**

ITC experiments were carried out using MicroCal $iTC_{200}$ (GE Healthcare). Proteins were concentrated to approximately 9.0 mg/ml using Amicon Ultra Centrifugal Filters 30K (Merck Millipore) and dialyzed extensively against 50 mM sodium phosphate buffer (pH 7.0). Buffer saved from the dialysis was used to dissolve sugar ligands. All solutions were filtered before use. Each ligand (1 mM) was titrated into the protein solution (68 μM TF-tagged CBM51 or 218 μM TF) filling in the reaction cell under stirring (300 rpm) at 30 °C.

## Results

**Presence of blood group B antigen-degrading α-galactosidase in B. bifidum**

To test whether bifidobacteria possess abilities for degrading blood group A

and B antigens, various bifidobacterial cells were incubated with either blood group A or B trisaccharide, and the products were analyzed by TLC. No bifidobacterial strain tested was able to degrade A trisaccharide, but *B. bifidum* JCM 1254 and *B. bifidum* JCM 1255 (type strain) released Gal from B trisaccharide (Fig. 1). However, *B. bifidum* JCM 7004 and the other bifidobacterial species could not readily hydrolyze it.

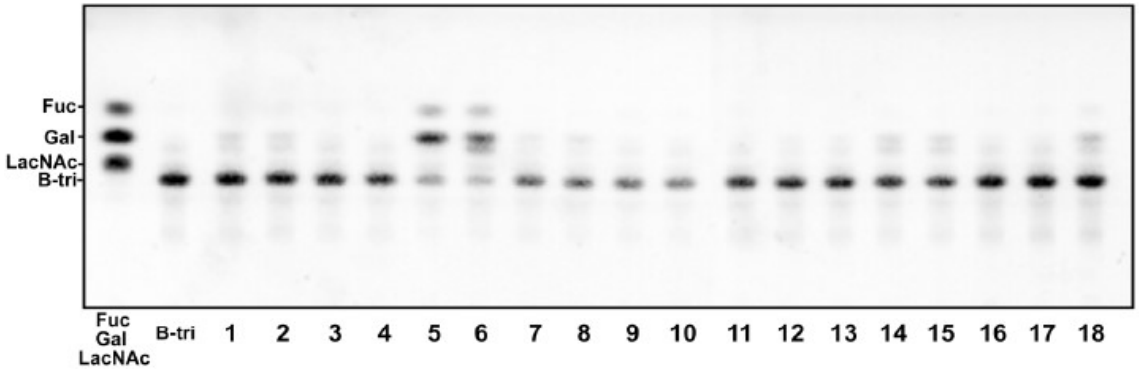


**Fig. 1.** Blood group B trisaccharide-hydrolyzing activity of various bifidobacteria analyzed by TLC. Lane 1, *Bifidobacterium adolescentis* JCM 1275$^{T}$; lane 2, *B. adolescentis* JCM 7046; lane 3, *B. angulatum* JCM 7096$^{T}$; lane 4, *B. animalis* subsp. *lactis* JCM 10602$^{T}$; lane 5, *B. bifidum* JCM 1254; lane 6, *B. bifidum* JCM 1255$^{T}$; lane 7, *B. bifidum* JCM 7004; lane 8, *B. breve* JCM 1192$^{T}$; lane 9, *B. catenulatum* JCM 1194$^{T}$; lane 10, *B. dentium* JCM 1195$^{T}$; lane 11, *B. gallicum* JCM 8224$^{T}$; lane 12, *B. longum* subsp. *infantis* JCM 1210; lane 13, *B. longum* subsp. *infantis* JCM 1222$^{T}$; lane 14, *B. longum* subsp. *longum* JCM 1217$^{T}$; lane 15, *B. longum* subsp. *longum* JCM 7054; lane 16, *B. pseudocatenulatum* JCM 1200$^{T}$; lane 17, *B. pseudolongum* subsp. *pseudolongum* JCM 1205$^{T}$; lane 18, *B. scardovii* JCM 12489$^{T}$. B-tri, blood group B trisaccharide.

I searched the genome of *B. bifidum* JCM 1254, which was previously

sequenced, and found a candidate gene encoding a putative GH110 α-galactosidase and named it *agabb* (accession number AB735681). GH110 was recently established in the CAZy database, in which a few bacterial enzymes were experimentally characterized as α-galactosidases specific for blood group B antigen and the xenotransplantation antigen Galα1-3Galβ1-R (17, 20). The gene *agabb* consists of a 3870 bp open reading frame with an unusual initiation codon GTG, and encodes a polypeptide with 1289 amino acids (aa) containing the following putative sequences/domains: an N-terminal signal sequence (aa 1-23), a GH110 domain (aa 30-600), a carbohydrate-binding module (CBM) 51 domain (aa 943-1095), a bacterial Ig-like (Big) 2 domain (aa 1103-1184), and a C-terminal transmembrane region (aa 1256-1283) (Fig. 2A). The presence of an N-terminal signal sequence and a C-terminal transmembrane region indicates that AgaBb is a membrane-anchored protein with a large extracellular region that includes the GH110 domain.

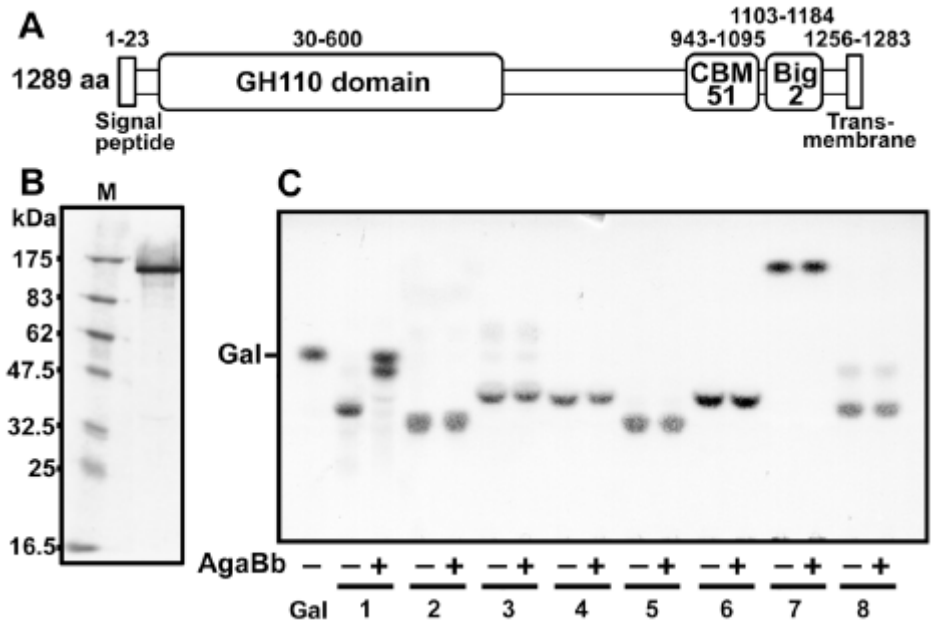


**Fig. 2.** Characterization of AgaBb. (**A**) Domain structure of AgaBb. (**B**) SDS-PAGE of

purified AgaBb. M, marker proteins. (**C**) Substrate specificity of AgaBb. Various oligosaccharides were incubated with purified AgaBb and then analyzed by TLC. Substrate 1, blood group B trisaccharide; 2, linear B-2 trisaccharide (Galα1-3Galβ1-4GlcNAc); 3, α1-3 galabiose (Galα1-3Gal); 4, α1-2 galabiose (Galα1-2Gal); 5, P1 antigen trisaccharide (Galα1-4Galβ1-4GlcNAc); 6 melibiose (Galα1-6Glc); 7, *p*NP-α-Gal; 8, blood group A trisaccharide.

**The substrate specificity and general properties of AgaBb**

A DNA fragment of *agabb* lacking the sequences encoding the N-terminal signal peptide and the C-terminal transmembrane region was amplified by high fidelity PCR and ligated into a pET-23b(+) expression vector to produce C-terminal 6×His-tagged AgaBb. *E. coli* BL21(λDE3) transformed with pET-23b/*agabb* were cultured, and AgaBb expression was induced with isopropyl β-D-1-thiogalactopyranoside (IPTG). The 6×His-tagged protein was purified from cell lysates using immobilized $Ni^{2+}$ affinity chromatography and gel filtration. The purified protein migrated as a single protein band of 130 kDa on reducing SDS-PAGE, which coincides with the calculated molecular mass (132,498 Da) (Fig. 2B). By gel-filtration using Superdex 200 10/300 GE, the molecular weight of the native enzyme was estimated to be around 270 kDa (data not shown), suggesting that AgaBb is a homodimeric enzyme. To examine the enzyme activity of AgaBb, the purified recombinant enzyme was first incubated with various *p*-nitrophenyl (*p*NP)-monosaccharides, but all glycosides including *p*NP-α-Gal were resistant (data not shown). Next, the enzyme was incubated with various oligosaccharides containing α-linked Gal and analyzed the reaction products by TLC (Fig. 2C). Gal was released

only from blood group B trisaccharide. Interestingly, the same α1-3 galactosyl linkage in linear B-2 trisaccharide (Galα1-3Galβ1-4GlcNAc) and α1-3 galabiose (Galα1-3Gal) were not hydrolyzed at all. The other galactosyl linkages such as α1-2, α1-4 and α1-6 were also completely resistant. These results indicate that AgaBb strictly recognizes not only the α1-3 linked Gal but also α1-2 linked Fuc in the trisaccharide antigen. The general properties of AgaBb were determined using blood group B trisaccharide as the substrate (data not shown). The optimum pH and temperature were pH 6.0-6.5 and 30°C, respectively. The divalent cations, $Ca^{2+}$, $Mg^{2+}$, and $Ni^{2+}$, did not affect enzyme activity at 5 mM concentration, whereas 5 mM $Cu^{2+}$ reduced the activity to 30%. The $K_m$ and $k_{cat}$ values were estimated from Hanes-Woolf plot as 1.8 mM and $6.4 \times 10^2$ $s^{-1}$, respectively.

**AgaBb acts on blood group B antigens on glycoconjugates**

Blood group B antigens exist in non-reducing termini of glycan chains on both glycoproteins and glycolipids, but are hardly found in free glycans such as milk oligosaccharides. To test whether AgaBb acts on B antigens on glycoproteins, I used human salivary mucin as a substrate. The crude mucin samples from four volunteers who belong to the group A, B, O and AB with secretor phenotype were incubated with the enzyme. Released Gal was detected in the supernatants of reaction products including the group B and AB mucin samples by TLC analysis but not in those including the groups A and O mucin samples (Fig. 3A).

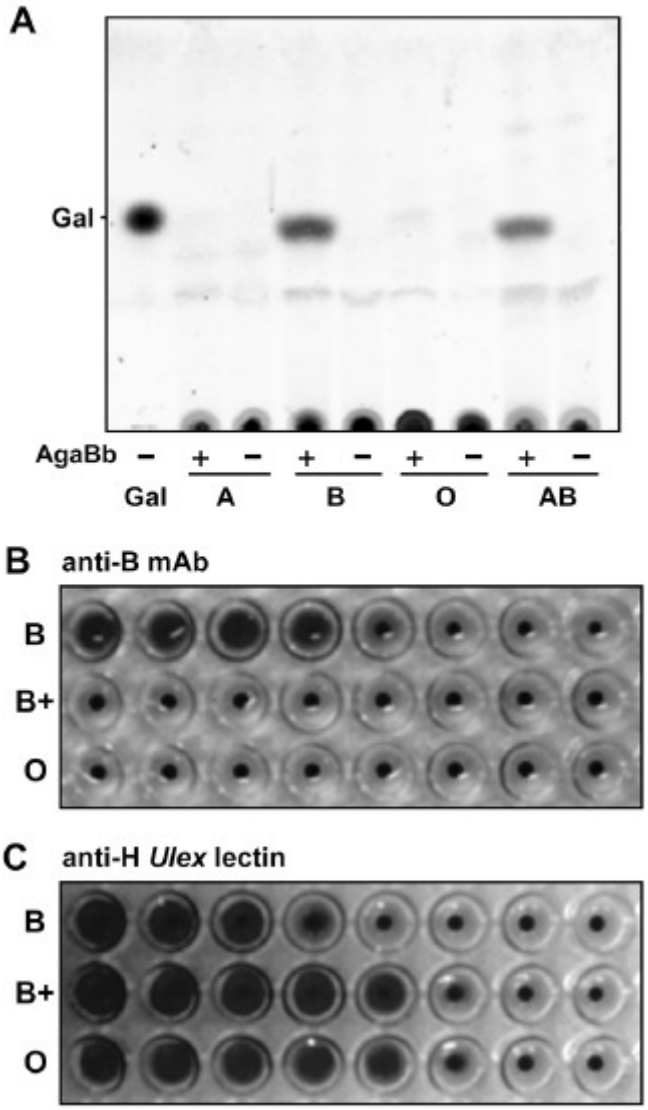


**Fig. 3.** Action of AgaBb on blood group B antigens in glycoconjugates. Crude salivary mucin samples obtained from volunteers (blood group A, B, O, and AB, all of them secretors) were incubated with AgaBb, and the supernatants of the reaction products were analyzed by TLC (**A**). Erythrocyte agglutination test using anti-B monoclonal antibody (**B**) and anti-H *Ulex* lectin (**C**). Upper rows, group B RBCs; middle rows, group B RBCs treated with AgaBb; bottom rows, group O RBCs. Antibody and lectin were serially diluted twice from 0.125 and 0.25 mg/ml, respectively, and were dispensed from left to right columns.

Next, I investigated the enzymatic activity toward B antigens on cell surface glycoconjugates. ABH blood group antigens on red blood cells (RBCs) are found in *O*-glycans and *N*-glycans of membrane glycoproteins and also in glycosphingolipids (21). I treated the blood group B RBCs with AgaBb at 37 °C in PBS and hemagglutination was compared with blood group O RBCs using anti-B monoclonal antibody and anti-H *Ulex* lectin . Agglutination tests were carried out by mixing RBCs with serially diluted antibody and lectin (Fig. 3B and 3C). In both tests, AgaBb-treated B-RBCs behaved indistinguishably from O-RBCs. This result shows that AgaBb removed all cell-surface B antigens, and that it may be a useful tool to make universally transfusable O-RBCs from B-RBCs.

**CBM51 contributes to enhance the affinity of AgaBb toward mucin substrate**

All GH110 enzymes previously reported are single-domain enzymes (17, 20). Therefore, I focused on the function of the CBM51 domain in AgaBb. CBM51 were found in several glycosidases from bacteria, and among them only three proteins, *Clostridium perfringens* (*Cp*) GH95-CBM51 and GH98-CBM51, and *Streptococcus pneumoniae* (*Sp*) GH98-CBM51, were characterized (22, 23). *Cp*GH95-CBM51 was shown to bind mainly β-linked Gal residues, whereas *Cp*GH98-CBM51 and *Sp*GH98-CBM51 specifically bind blood group A and B antigens. However, functions of CBM51 in these glycosidase activities were not investigated.

First, I examined which types of mucin bound to the CBM51 in AgaBb. Catalytically inactivated AgaBb was prepared by replacing conserved acidic aa residues in GH110 domain to prevent degradation of B antigen during the binding assay. Four mutants with single point mutation, AgaBb-D328N, D351N, D352N and E551Q, completely lost activity toward B trisaccharide (data not shown), suggesting that two of

the four are likely the catalytic base and acid residues. Salivary mucin samples of group A, B, and O were dot-blotted onto PVDF membrane, and then catalytically inactivated AgaBb-D328N was overlaid. After washing the membrane thoroughly, AgaBb-D328N was detected to bind to only group B mucin using anti-His antibody (Fig. 4A), while CBM51-deleted AgaBb-D328N (aa 23-701) did not. This result suggests that CBM51 in AgaBb specifically recognizes and binds B antigen.

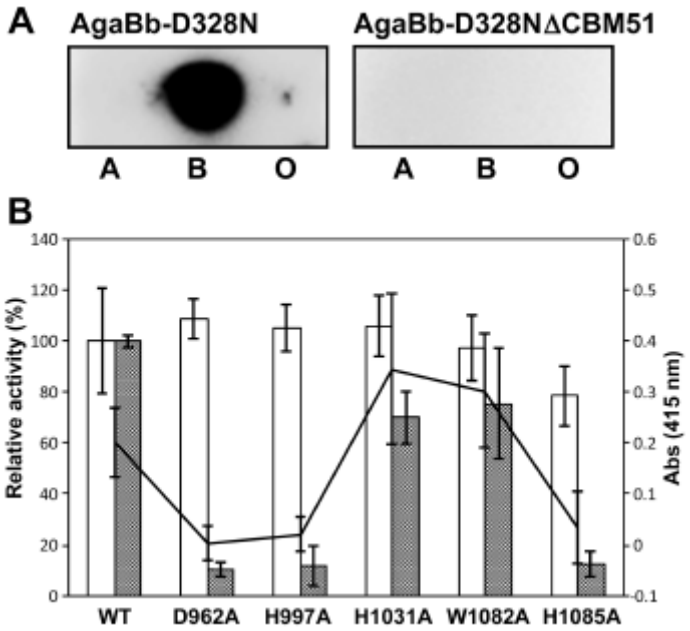


**Fig. 4.** Effect of CBM51 on enzymatic activity of AgaBb. (**A**) Dot-blot overlay assay using anti-His antibody. Crude salivary mucin samples (group A, B, and O) were dot-blotted onto PVDF membrane, and then catalytically inactivated AgaBb-D328N and AgaBb-D328NΔCBM51 were overlaid. (**B**) Correlation of binding activity to group B mucin and hydrolysis activity. Binding activity of CBM51 mutants generated from AgaBb-D328N to group B mucin was measured by ELISA-like assay (bold line): hydrolysis activity of corresponding CBM51 mutants of active form toward blood group B trisaccharide (white bars) and group B mucin (gray bars). Error bars indicate SD.

Next, five CBM51 mutants were generated using both wild-type AgaBb and AgaBb-D328N as templates, by replacing putative important residues such as D962, H997, H1031, W1082, and H1085, based on an alignment with *Cp*GH95-CBM51 and *Cp*GH98-CBM51. Their binding abilities toward group B mucin were quantified by an ELISA-like 96-well plate assay using AgaBb-D328N-based mutants, and also the enzymatic activities toward B trisaccharide and group B mucin were measured using enzymatically active mutants (Fig. 4B). Three CBM51 mutants, D962A, H997A, and H1085A, almost completely lost their binding activity toward group B mucin, but H1031A and W1082A retained activity to some extent. The enzymatic activities of the corresponding active forms toward group B mucin were strongly correlated with their binding activities. Interestingly, however, the hydrolysis activities for B trisaccharide were not affected by mutations in CBM51. This result suggests that CBM51 in AgaBb enhances the enzymatic activity toward multivalent B antigens like mucin.

**Isothermal titration calorimetry**

In order to determine sugar-binding specificity of AgaBb-CBM51 in detail, isothermal titration calorimetry (ITC) was employed. I replaced the GH110 domain of AgaBb with trigger factor (TF), a chaperone in *E. coli*, to eliminate the effect of the GH110 domain. TF-tagged CBM51 was expressed under low temperature condition (15 °C). The purified protein was filled in the reaction cell, and titrated with the following oligosaccharide solutions: blood group B trisaccharide, blood group A trisaccharide, α1-3 galabiose (Galα1-3Gal), and blood group H disaccharide (Fucα1-2Gal). The addition of blood group B trisaccharide (Fig. 5A), but not the others (Fig. 5 B-D), resulted in substantial heat of binding, indicating that CBM51 specifically binds blood group B trisaccharide. These results confirmed that AgaBb-CBM51 strictly recognizes

both α1-3 linked Gal and α1-2 linked Fuc in B antigen. The binding curve obtained for blood group B trisaccharide could be fitted, assuming a one-site binding model (Fig. 5A, bottom panel). The curve could not be fitted into a two-site binding model. The derived thermodynamic values, $K_a$, $\Delta H$, $\Delta S$, and $\Delta G$, for the experiment involving blood group B trisaccharide binding to TF-tagged CBM51 are summarized (Table 2). The binding affinity of CBM51 for blood group B trisaccharide is approximately in the millimolar range. The binding process is enthalpically driven, and the entropy loss opposes binding.

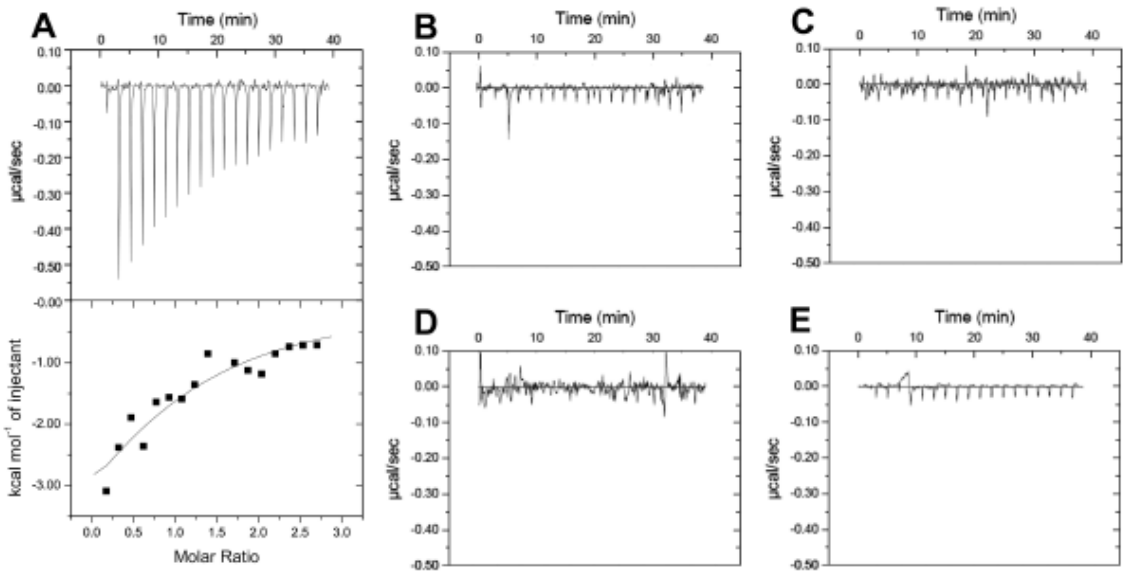


**Fig. 5.** Isothermal titration calorimetry of CBM51. Binding specificity of CBM51 domain was analyzed by ITC. TF-tagged CBM51 was titrated by blood group B trisaccharide (**A**), blood group A trisaccharide (**B**), linear B-2 trisaccharide (Galα1-3Galβ1-4GlcNAc) (**C**), and blood group H disaccharide (Fucα1-2Gal) (**D**). TF only was titrated with blood group B trisaccharide (**E**). Upper panel of **A** and panels **B-E**, raw thermograms; bottom panel of **A**, binding isotherm.

**Table 2.** Thermodynamic parameters for binding of blood group B trisaccharide to TF-tagged CBM51 at 30 °C as determined by isothermal titration calorimetry.

| $K_a$ ($\times 10^3$ $M^{-1}$) | $\Delta G_r^0$ (kcal $mol^{-1}$) | $\Delta H_r^0$ (kcal $mol^{-1}$) | $T\Delta S_r^0$ (kcal $mol^{-1}$) | $\Delta S_r^0$ (cal $mol^{-1}$ $K^{-1}$) |
|---|---|---|---|---|
| 10.7 ± 2.9 | -5.6 ± 0.19 | -6.7 ± 0.88 | -1.1 ± 0.69 | -3.6 ± 2.2 |

## Discussion

In this report, GH110 α-galactosidase from bifidobacteria was identified for the first time. The GH110 family that is exclusively composed of α-galactosidases could be divided into two subfamilies based on their substrate specificities (20). Subfamily GH110a contains the enzymes with strict specificity for B antigen, whereas GH110b contains those with broad specificity for α1,3-linked Gal and also synthetic aryl α-galactoside. AgaBb turned out to belong to the former subfamily because it is strictly specific to B antigen. Phylogenetic analysis also supports the subfamily classification (Fig. 6). The GH110a domain of AgaBb appears to be related to the same Gram-positive actinobacterial enzymes from *Streptomyces avermitilis* (*Sa*GH110a, CAJ33349) and *S. griseoplanus* (*Sg*GH110a, CAJ90659), whose amino acid identities are 46% and 43%, respectively. Intestinal opportunistic pathogens, *Bacteroides thetaiotaomicron* (*Bt*) and *B. fragilis* (*Bf*), possess both GH110a and GH110b enzymes. *Bt*GH110a (CAJ33352)

and *Bf*GH110a (CAH09922) show 37% and 33% amino acid identities with AgaBb. Since the latter *Bt*GH110b (CAJ33353) and *Bf*GH110b (CAJ33351) act on a linear Galα1-3Gal structure that is a xenotransplantation antigen expressed in mammals other than humans and primates, the enzymes may contribute to the association of *Bacteroides* in animal intestines. On the other hand, *B. bifidum* possesses only GH110a AgaBb, which suggests the selective adaptation of the bifidobacterial species to the group B humans and primates. In humans, ABH antigens are frequently found on the terminus of the type 1 chain, whose building unit lacto-*N*-biose I (Galβ1-3GlcNAc) is one of the most effective endogenous bifidogenic factors (24). Once ABH antigens are removed, lacto-*N*-biose I is sequentially released from type 1 chain by an extracellular lacto-*N*-biosidase (11), then incorporated by lacto-*N*-biose I transporter (25) and metabolized by an intracellular lacto-*N*-biose I phosphorylase (26). H antigen-degrading GH95 1,2-α-L-fucosidase is also common in infant-associated bifidobacteria such as *B. breve*, *B. bifidum* and *B. longum infantis* (8). However, as far as I know, no bifidobacterial strain can degrade blood group A antigen, and only *B. bifidum* degrades B antigen. In fact, the cells of *B. bifidum* JCM 1254 released Gal, Fuc, and other sugars from group B and O salivary mucin, but only a trace from group A mucin according to TLC analysis (data not shown). Importantly, other bifidobacterial species released sugars from only group O mucin but not from group A and B salivary mucin, suggesting AgaBb is critical for degrading mucin oligosaccharides from group B humans. Evolutionarily, the *B* and *O* alleles in humans are believed to have derived independently from the ancestral *A* allele by point mutations in α1,3-*N*-acetylgalactosaminyltransferase (27). Dominant association of bifidobacteria to group B and O newborn infants reduces the mortality of infectious diseases in intestines

and might be a driving force of increasing frequency of *B* and *O* alleles in humans. Very recently, the diversity and amount of bifidobacteria in the human intestine was reported to be considerably reduced in non-secretor individuals defined by a mutation in the *FUT2* gene (28). An older report documented that *in vitro* culture of enteric bacteria from B secretors produced greater levels of blood group B-degrading activity (29), suggesting the association of B-degrading bacteria within human intestine. Thus, the relative frequency of AgaBb-expressing *B. bifidum* in B secretors should be studied.

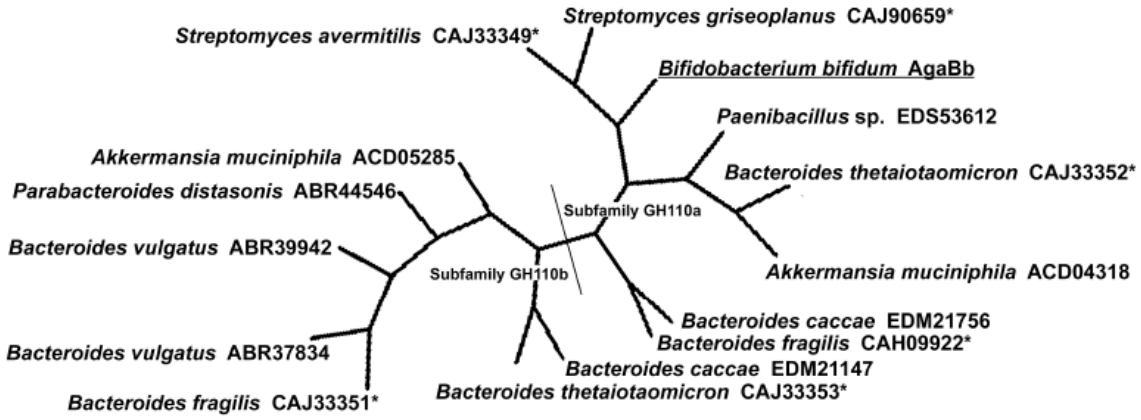


**Fig. 6.** Phylogenetic analysis of GH110 α-galactosidases. The tree was constructed by the neighbor-joining method based on the conserved GH110 domains using the ClustalW program. Bacterial names and accession numbers are shown. Asterisks indicate experimentally characterized enzymes.

Another unique feature of AgaBb is its multidomain structure. AgaBb is a C-terminally membrane-anchored extracellular enzyme containing two accessory domains, CBM51 and Big2, which are located near the membrane. AgaBb-CBM51 was found to specifically bind B antigens but not A and H antigens, as demonstrated by the ITC and solid-phase binding assay. The members of the CBM51 family are distributed

throughout a wide variety of bacteria, and phylogenetically classified into 6 subfamilies tentatively (22). Among them, only two in the CBM51a subfamily and one in the CBM51b subfamily have so far been characterized (22, 23). CBM51a domains were found in GH98 endo-β-galactosidase that is specific to blood group A and B antigens and releases A and B trisaccharides (30). *Cp*GH98-CBM51a and *Sp*CBM51a were shown to bind both A and B trisaccharides by glycan microarray and crystal analyses. On the other hand, CBM51b found in *Cp*GH95 1,2-α-L-fucosidase was reported to have broad binding specificity toward mainly β-linked Gal and also other structures. Although AgaBb-CBM51 seems to be related to the CBM51a subfamily judged from the binding specificity, it shows rather higher sequence identity to the CBM51b subfamily: namely, the identities are 42% to *Cp*GH95-CBM51b (aa 900-1050, ABG82552), 36% to *Cp*GH98-CBM51a (aa 32-211, AAR84225), and 39% to *Sp*GH98-CBM51a (aa 65-233, EDK74349). Three residues, D962, H997, and H1085, in AgaBb-CBM51 were identified to be essential for binding, but they are not completely aligned with these known members. Phylogenetic affiliation is also unclear, because there is no highly conserved motif or region. Thus, the molecular recognition mechanism of B antigen-specific AgaBb-CBM51 may be different from previously reported CBM51 domains and should be an interesting issue in the future. Recently, thermodynamic parameters for binding of blood group A and B antigens to CBM51a of *Sp3*GH98 from *S. pneumoniae* SP3-BS71 have been determined using ITC (23). In this study, I investigated the binding specificity of AgaBb-CBM51 and determined thermodynamic parameters for binding of blood group B trisaccharide to the module. The association constant ($K_a$) found for the binding of blood group B trisaccharide to AgaBb-CBM51 is 7 times lower than that observed for the binding of group B

tetrasaccharide derivative [Galα1-3(Fucα1-2)Galβ1-4GlcNAcβ1-$(CH_2)_6CH=CH_2$] to *Sp*CBM51-1. The reducing end GlcNAc residue of the tetrasaccharide is involved in the fixation of distal trisaccharide conformation. Therefore, the decreased $K_a$ of AgaBb-CBM51 might be due to the lack of this GlcNAc moiety in group B trisaccharide, although direct interaction between the GlcNAc residue and *Sp*CBM51-1 was absent in *Sp*CBM51-1/group B tetrasaccharide derivative complex structure.

The function of CBM domains has been mainly elucidated in polysaccharide-degrading glycosidases such as amylases, chitinases, and cellulases (31, 32). According to the previous studies, CBMs in such enzymes enhance the hydrolytic activity toward insoluble crystallized substrates. By contrast, those in glycosidases acting on glycoconjugates have been poorly investigated (33). In this report, I showed AgaBb-CBM51 enhanced the catalytic activity toward multivalent mucin substrates but not toward monomeric B trisaccharide. Probably the presence of CBM51 could lower the $K_m$ value of AgaBb for mucin, although the value was not determined because of the difficulty of the molecular weight estimation of the mucin.

Enzymatic removal of blood group antigens to prepare universal RBCs for transfusion was a pioneering vision originally proposed about 30 years ago (34). Several α-galactosidases in GH27 and GH36 were investigated for this purpose, but they had problems of low pH optima, broad specificity, and poor kinetic properties with the branched B antigen (35). Recently discovered GH110 enzymes are expected to overcome these problems (17, 36). Newly identified AgaBb from the safe commensal bifidobacteria is inferred to have advantage acting on group B RBCs due to its unique CBM51 domain.

**REFERENCES**


1. Benno Y, Sawada K, Mitsuoka T. 1984. The intestinal microflora of infants: composition of fecal flora in breast-fed and bottle-fed infants. Microbiol Immunol 28:975-986.
2. Turroni F, Peano C, Pass DA, Foroni E, Severgnini M, Claesson MJ, Kerr C, Hourihane J, Murray D, Fuligni F, Gueimonde M, Margolles A, De Bellis G, O'Toole PW, van Sinderen D, Marchesi JR, Ventura, M. 2012. Diversity of Bifidobacteria within the Infant Gut Microbiota. PLoS One 7:e36957.
3. Suzuki R, Katayama T, Kim BJ, Wakagi T, Shoun H, Ashida H, Yamamoto K, Fushinobu S. 2010. Crystal structures of phosphoketolase: thiamine diphosphate-dependent dehydration mechanism. J Biol Chem 285:34279-34287.
4. Picard C, Fioramonti J, Francois A, Robinson T, Neant F, Matuchansky C. 2005. Review article: bifidobacteria as probiotic agents – physiological effects and clinical benefits. Aliment Pharmacol Ther 22:495-512.
5. Trebichavsky I, Rada V, Splichalova A, Splichal I. 2009. Cross-talk of human gut with bifidobacteria. Nutr Rev 67:77-82.
6. Asakuma S, Hatakeyama E, Urashima T, Yoshida E, Katayama T, Yamamoto K, Kumagai H, Ashida H, Hirose J, Kitaoka M. 2011. Physiology of consumption of human milk oligosaccharides by infant gut-associated bifidobacteria. J Biol Chem 286:34583-34592.
7. Ashida H, Miyake A, Kiyohara M, Wada J, Yoshida E, Kumagai H, Katayama T, Yamamoto K. 2009. Two distinct α-L-fucosidases from *Bifidobacterium bifidum* are essential for the utilization of fucosylated milk oligosaccharides and

glycoconjugates. Glycobiology 19:1010-1017.

8. Katayama T, Sakuma A, Kimura T, Makimura Y, Hiratake J, Sakata K, Yamanoi T, Kumagai H, Yamamoto K. 2004. Molecular cloning and characterization of *Bifidobacterium bifidum* 1,2-α-L-fucosidase (AfcA), a novel inverting glycosidase (glycoside hydrolase family 95). J Bacteriol 186:4885-4893.

9. Kiyohara M, Tanigawa K, Chaiwangsri T, Katayama T, Ashida H, Yamamoto K. 2011. An exo-α-sialidase from bifidobacteria involved in the degradation of sialyloligosaccharides in human milk and intestinal glycoconjugates. Glycobiology 21:437-447.

10. Miwa M, Horimoto T, Kiyohara M, Katayama T, Kitaoka M, Ashida H, Yamamoto K. 2010. Cooperation of β-galactosidase and β-*N*-acetylhexosaminidase from bifidobacteria in assimilation of human milk oligosaccharides with type 2 structure. Glycobiology 20:1402-1409.

11. Wada J, Ando T, Kiyohara M, Ashida H, Kitaoka M, Yamaguchi M, Kumagai H, Katayama T, Yamamoto K. 2008. *Bifidobacterium bifidum* lacto-*N*-biosidase, a critical enzyme for the degradation of human milk oligosaccharides with a type 1 structure. Appl Environ Microbiol 74:3996-4004.

12. Ashida H, Maki R, Ozawa H, Tani Y, Kiyohara M, Fujita M, Imamura A, Ishida H, Kiso M, Yamamoto K. 2008. Characterization of two different endo-α-*N*-acetylgalactosaminidases from probiotic and pathogenic enterobacteria, *Bifidobacterium longum* and *Clostridium perfringens*. Glycobiology 18:727-734.

13. Fujita K, Oura F, Nagamine N, Katayama T, Hiratake J, Sakata K, Kumagai H, Yamamoto K. 2005. Identification and molecular cloning of a novel glycoside

hydrolase family of core 1 type *O*-glycan-specific endo-α-*N*-acetylgalactosaminidase from *Bifidobacterium longum*. J Biol Chem 280:37415-37422.

14. Kiyohara M, Nakatomi T, Kurihara S, Fushinobu S, Suzuki H, Tanaka T, Shoda S, Kitaoka M, Katayama T, Yamamoto K, Ashida H. 2012. α-*N*-acetylgalactosaminidase from infant-associated bifidobacteria belonging to novel glycoside hydrolase family 129 is implicated in alternative mucin degradation pathway. J Biol Chem 287:693-700.

15. Turroni F, Bottacini F, Foroni E, Mulder I, Kim JH, Zomer A, Sanchez B, Bidossi A, Ferrarini A, Giubellini V, Delledonne M, Henrissat B, Coutinho P, Oggioni M, Fitzgerald GF, Mills D, Margolles A, Kelly D, van Sinderen D, Ventura M. 2010. Genome analysis of *Bifidobacterium bifidum* PRL2010 reveals metabolic pathways for host-derived glycan foraging. Proc Natl Acad Sci USA 107:19514-19519.

16. Yamamoto F, Clausen H, White T, Marken J, Hakomori S. 1990. Molecular genetic basis of the histo-blood group ABO system. Nature 345:229-233.

17. Liu QP, Sulzenbacher G, Yuan H, Bennett EP, Pietz G, Saunders K, Spence J, Nudelman E, Levery SB, White T, Neveu JM, Lane WS, Bourne Y, Olsson ML, Henrissat B, Clausen H. 2007. Bacterial glycosidases for the production of universal red blood cells. Nat Biotechnol 25:454-464.

18. Anderson K, Li SC, Li YT. 2000. Diphenylamine-aniline-phosphoric acid reagent, a versatile spray reagent for revealing glycoconjugates on thin-layer chromatography plates. Anal Biochem 287:337-339.

19. Yoshida E, Sakurama H, Kiyohara M, Nakajima M, Kitaoka M, Ashida H,

Hirose J, Katayama T, Yamamoto K, Kumagai H. 2012. *Bifidobacterium longum* subsp. *infantis* uses two different β-galactosidases for selectively degrading type-1 and type-2 human milk oligosaccharides. Glycobiology 22:361-368.

20. Liu QP, Yuan H, Bennett EP, Levery SB, Nudelman E, Spence J, Pietz G, Saunders K, White T, Olsson ML, Henrissat B, Sulzenbacher G, Clausen H. 2008. Identification of a GH110 subfamily of α1,3-galactosidases: novel enzymes for removal of the α3Gal xenotransplantation antigen. J Biol Chem 283:8545-8554.

21. Clausen H, Hakomori S. 1989. ABH and related histo-blood group antigens; immunochemical differences in carrier isotypes and their distribution. Vox Sang 56:1-20.

22. Gregg KJ, Finn R, Abbott DW and Boraston AB. 2008. Divergent modes of glycan recognition by a new family of carbohydrate-binding modules. J Biol Chem 283:12604-12613.

23. Higgins MA, Ficko-Blean E, Meloncelli PJ, Lowary TL, Boraston AB. 2011. The overall architecture and receptor binding of pneumococcal carbohydrate-antigen-hydrolyzing enzymes. J Mol Biol 411:1017-1036.

24. Kiyohara M, Tachizawa A, Nishimoto M, Kitaoka M, Ashida H, Yamamoto K. 2009. Prebiotic effect of lacto-*N*-biose I on bifidobacterial growth. Biosci Biotechnol Biochem 73:1175-1179.

25. Suzuki R, Wada J, Katayama T, Fushinobu S, Wakagi T, Shoun H, Sugimoto H, Tanaka A, Kumagai H, Ashida H, Kitaoka M, Yamamoto K. 2008. Structural and thermodynamic analyses of solute-binding protein from *Bifidobacterium*

*longum* specific for core 1 disaccharide and lacto-*N*-biose I. J Biol Chem 283:13165-13173.

26. Kitaoka M, Tian J, Nishimoto M. 2005. Novel putative galactose operon involving lacto-*N*-biose phosphorylase in *Bifidobacterium longum*. Appl Environ Microbiol 71:3158-3162.

27. Saitou N, Yamamoto F. 1997. Evolution of primate ABO blood group genes and their homologous genes. Mol Biol Evol 14:399-411.

28. Wacklin P, Makivuokko H, Alakulppi N, Nikkila J, Tenkanen H, Rabina J, Partanen J, Aranko K, Matto J. 2011. Secretor genotype (FUT2 gene) is strongly associated with the composition of bifidobacteria in the human intestine. PLoS One 6:e20113.

29. Hoskins LC, Boulding ET. 1976. Degradation of blood group antigens in human colon ecosystems. I. In vitro production of ABH blood group-degrading enzymes by enteric bacteria. J Clin Invest 57:63-73.

30. Anderson KM, Ashida H, Maskos K, Dell A, Li SC, Li YT. 2005. A clostridial endo-β-galactosidase that cleaves both blood group A and B glycotopes: the first member of a new glycoside hydrolase family, GH98. J Biol Chem 280:7720-7728.

31. Guillen D, Sanchez S, Rodriguez-Sanoja R. 2010. Carbohydrate-binding domains: multiplicity of biological roles. Appl Microbiol Biotechnol 85:1241-1249.

32. Shoseyov O, Shani Z, Levy I. 2006. Carbohydrate binding modules: biochemical properties and novel applications. Microbiol Mol Biol Rev 70:283-295.

33. Fujita M, Tsuchida A, Hirata A, Kobayashi N, Goto K, Osumi K, Hirose Y, Nakayama J, Yamanoi T, Ashida H, Mizuno M. 2011. Glycoside hydrolase family 89 α-*N*-acetylglucosaminidase from *Clostridium perfringens* specifically acts on GlcNAcα1,4Galβ1R at the non-reducing terminus of *O*-glycans in gastric mucin. J Biol Chem 286:6479-6489.

34. Goldstein J, Siviglia G, Hurst R, Lenny L, Reich L. 1982. Group B erythrocytes enzymatically converted to group O survive normally in A, B, and O individuals. Science 215:168-170.

35. Olsson ML, Hill CA, de la Vega H, Liu QP, Stroud MR, Valdinocci J, Moon S, Clausen H, Kruskall MS. 2004. Universal red blood cells – enzymatic conversion of blood group A and B antigens. Transfus Clin Biol 11:33-39.

36. Olsson ML, Clausen, H. 2008. Modifying the red cell surface: towards an ABO-universal blood supply. Br J Haematol 140:3-12.

**SUMMARY**

*Bifidobacterium bifidum* is one of the most frequently found bifidobacteria in the intestines of newborn infants. It was previously reported that *B. bifidum* possesses unique metabolic pathways for *O*-linked glycans on gastrointestinal mucin (Kiyohara et al. 2012. J Biol Chem 287:693-700). Non-reducing termini of *O*-linked glycans on mucin are frequently covered with histo-blood group antigens. Here, a gene *agabb* was identified from *B. bifidum* JCM 1254, which encodes glycoside hydrolase (GH) family 110 α-galactosidase. AgaBb is a 1289-amino acid polypeptide containing an N-terminal signal sequence, a GH110 domain, a carbohydrate-binding module (CBM) 51 domain, a bacterial Ig-like (Big) 2 domain, and a C-terminal transmembrane region, in this order. The recombinant enzyme expressed in *Escherichia coli* hydrolyzed α1,3-linked Gal in branched blood group B antigen [Galα1-3(Fucα1-2)Galβ1-R], but not in linear xenotransplantation antigen (Galα1-3Galβ1-R). The enzyme also acted on group B human salivary mucin and erythrocytes. I also revealed that CBM51 specifically bound blood group B antigen using both isothermal titration calorimetry (ITC) and a solid-phase binding assay, and it enhanced the affinity of the enzyme toward substrates with multivalent B antigens. I suggest that this enzyme plays an essential role in degrading B antigens to acquire nutrients from mucin oligosaccharides in the gastrointestinal tracts.

# CHAPTER II

## Studies on tetragenococcal amino acid metabolism

## SECTION 1

## Isolation of halophilic lactic acid bacteria possessing aspartate decarboxylase and application to fish sauce fermentation starter

Fish sauce is a common, traditional seasoning produced by the fermentation of fish, widely used in Southeast and East Asia. During the fermentation process, fish protein is hydrolyzed by the digestive enzymes of fish, resulting in peptides and amino acids, which give a strong umami and unique complex taste to fish sauce. Fish sauce also contains high concentrations of NaCl, which prevents rotting and allows halophilic bacteria to reside. As fish sauce production solely depends on a natural fermentation process, its quality is seriously affected by microbes in the fish sauce mash.

Halophilic lactic acid bacteria, mainly *Tetragenococcus* spp., were isolated from the fish sauce and other fermented sea foods as the dominant microbe (1-5). Lactic acid produced by lactic acid bacteria reduces the pH and gives a moderate sour taste to fish sauce. However, certain strains of *Tetragenococcus* spp. degrade particular amino acids, such as histidine (6, 7), tyrosine (8), arginine (9), serine, threonine, phenylalanine (10) and aspartate (11). Although the degradation pathways of these amino acids are not fully clarified, some of them become amines by decarboxylation. Previous reports demonstrated that histidine is transformed into histamine by histidine decarboxylase, encoded by *hdcA* on plasmids of *Tetragenococcus halophilus* (12) and *Tetragenococcus muriaticus* (13) and that tyrosine is converted to tyramine by tyrosine decarboxylase,

encoded by *tdcA* on the plasmids of *T. halophilus* (8).

Histamine is known as a causative agent of food related intoxication, participating in allergic and inflammatory responses, whereas tyramine is related to food-induced migraines and hypertensive crisis (14-16). Tyramine and other biogenic amines, such as phenethylamine, cadaverine, putrescine, spermidine and spermine, can enhance the toxicity of histamine by inhibiting histamine-metabolizing enzymes in the small intestine (17, 18). Furthermore, these amines potentially react with nitrous acid and make carcinogenic nitrosamines (19-21). In addition to their potential toxicity, biogenic amines are used for the evaluation of the hygienic quality of a marine species (17). Therefore, amino acid-decarboxylating bacteria are generally not preferred for fish sauce fermentation. To prevent the accumulation of biogenic amines, selected strains of *Tetragenococcus* incapable of amine production are often used as starter cultures for fermented fish foods, including fish sauce (22-24).

It is also known that aspartate is transformed into another amino acid, alanine, via decarboxylation by *T. halophilus* possessing aspartate decarboxylase encoded by *aspD* on plasmids (11). The conversion of aspartate to alanine potentially makes the taste milder by combination of a decrease in the amount of the sour amino acid aspartate and an increase in the amount of the sweet amino acid alanine (25). This reaction is highly similar to malolactic fermentation, which is often performed for red wine brewing. The reaction is conducted by lactic acid bacteria, such as *Oenococcus oeni*, which transforms malic acid into lactic acid by decarboxylation (26). The conversion of malic acid, a dicarboxylic acid, to lactic acid, a monocarboxylic acid, deacidifies wine, resulting in a milder taste. Hence, for fish sauce fermentation, aspartate decarboxylating bacteria can possibly be considered as a desirable starter. However, while a few strains

of *T. halophilus* possessing aspartate decarboxylase were isolated from soy sauce mash (10, 11), such strains have never been isolated from fish sauce or any other sea foods, nor applied to fish sauce fermentation so far.

The aims of this study were to isolate halophilic lactic acid bacteria possessing aspartate decarboxylase from fermented fish foods, to apply to starter cultures for fish sauce fermentation and to elucidate the effects of the isolates on taste improvement and biogenic amine reduction.

## Materials and methods

### Samples

Samples used for this study are shown in Table 1. All fish sauces were obtained from a fish sauce manufacturing company in Japan, and fish *nukazuke* (salted and fermented fish with rice bran) were collected from markets in Japan.

**Table 1** List of the sources from which aspartate decarboxylating bacteria were isolated.

| Sample number | Sample | Fish material | The number of the isolates |
|---|---|---|---|
| 1[a] | Fish sauce mash | Deep-sea smelt | 14 |
| 2[a] | Fish sauce mash | Deep-sea smelt | 12 |
| 3[a] | Fish sauce mash | Deep-sea smelt | 15 |
| 4 to 12[a] | Fish sauce mash | Deep-sea smelt | 0 |
| 13 to 17 | Fish *Nukazuke* | Mackerel | 0 |
| 18 | Fish *Nukazuke* | Sardine | 1 |
| 19 to 20 | Fish *Nukazuke* | Sardine | 0 |
| 21 | Fish *Nukazuke* | Sardine | 13 |
| 22 | Fish *Nukazuke* | Sardine | 19 |

[a] Same manufacturer but different lots.

**Isolation of aspartate decarboxylating bacteria**

Aspartate decarboxylating bacteria were isolated in aspartate indicator broth containing bromocresol purple (11). pH reduction by lactic acid production makes the color of this medium yellow, but when aspartate is decarboxylated, the color remains purple. Samples were properly diluted with 10% saline, inoculated in the broth and incubated at 30°C for 6 days with an AnaeroPack (Mitsubishi Gas Chemical, Tokyo, Japan) in a hermetically sealed box.

**Detection of aspartate decarboxylase and other genes**

Specific detection of *aspD*, *hdcA* and *tdcA* was performed using PCR amplification with oligonucleotide primer sets aspF-aspR, hdcF-hdcR and tdcF-tdcR, respectively (Table 2). A brief identification of *T. halophilus* or not was performed using

PCR amplification with *T. halophilus* species-specific oligonucleotide primer Th67F and Th800R, which amplifies the 16S rRNA gene (Table 2).

Each PCR reaction mixture (50 µl) consisted of 25 µl of SapphireAmp (Takara Bio, Kusatsu, Japan), 25 pmol of each primer and only a few cells. PCR was performed for 30 cycles after preincubation at 94°C for 1 min using the following conditions: denaturation at 98°C for 5 s; annealing at 54°C for 5 s; and extension at 72°C for 10 s. The PCR products were visualized by electrophoresis with 0.9% agarose gel (Nippon Gene, Tokyo, Japan), which was stained with ethidium bromide. Strains decarboxylating aspartate, histidine or tyrosine were used as positive controls for PCR detection of *aspD*, *hdcA* and *tdcA* (Table 3).

The 16S rRNA gene amplicons were purified using the Wizard SV Gel and PCR Clean-Up System (Promega, Madison, USA), and their DNA sequences were determined by commercial DNA sequencing service (Fasmac, Atsugi, Japan) and analyzed using the Blast program.

**Table 2** Primers list.

| Primer name | Sequence (5'→3') |
|---|---|
| aspF | AATGTTTTCCCTACTGAAGG |
| aspR | CCTGTTGCACCATAAAGTTT |
| hdcF | ACTTGGGGTTGACCGTATCTCAGTGAGTC |
| hdcR | TCTTCGTTAGGAGTCTCCCAAACACCAGC |
| tdcF | CGTGGTGGCATGGATCTTTC |
| tdcR | GCACCCTCTTCAGTTGAACCAG |
| Th67F | ACGCTGCTTAAGAAGAAACTTCGG |
| Th800R | TGGACTACCAGGGTATCTAATCC |
| aspInvF | CATTGGCTAACCAACCAGCTG |
| aspInvR | GACATACCTTTTAATTGTTCAATATCTAATGATTCC |
| repInvF | GCAAAAAGAAGACGAACGCAAC |
| repInvR | TTTTTGATTATGGCAATTAAATAAACTCCC |
| pinInvF | GATTGAACGAAAAACAGGCATTAGTG |
| pinInvR | TTGATCTTGTGTACTTACCCTAGCATAACC |

**Table 3** Strains used in this study.

| Strain | Relevant features | Source or reference |
|---|---|---|
| *Tetragenococcus halophilus* C1 | Not aspartate-, histidine- or tyrosine-decarboxylating strain | Isolated from fish sauce mash. Kept in my laboratory. |
| *Tetragenococcus halophilus* A-24 | Aspartate-decarboxylating strain | Isolated from soy sauce mash. Kept in my laboratory. |
| *Tetragenococcus halophilus* H | Histidine-decarboxylating strain | (7) |
| *Tetragenococcus halophilus* TyrA | Tyrosine-decarboxylating strain | (8) |

**Plasmid typing**

For plasmid typing, specific oligonucleotide primer sets aspInvF-aspInvR, repInvF-repInvR and pinInvF-pinInvR were designed at *aspD*, *repA* (encoding rolling-circle replication type plasmid replication initiation protein) and *pinR* (encoding site-specific recombinase), respectively (Table 2). These three primer sets were mixed, and direct colony PCR was performed on all isolates using KOD FX Neo (Toyobo, Osaka, Japan) with 25 pmol of each primer. PCR was performed for 35 cycles after pre-incubation at 94°C for 2 min using the following conditions: denaturation 98°C for 10 s; annealing at 67°C for 30 s; and extension at 68°C for 40 min. The PCR products were detected with 0.7% agarose gel (Nippon Gene), and the isolates were classified based on their amplified DNA fragment patterns.

**Preparation of starter cultures**

Starter strains were cultured in fish sauce medium, which contains fish sauce (BlessingFavour, Kumamoto, Japan) with the same composition as that of soy sauce medium for halophilic lactic acid bacteria (27). Concretely, fish sauce was diluted so that the total nitrogen concentration becomes 0.4%, added NaCl to make the final concentration 10%, and added 1% glucose. The pH was adjusted to 8.0 with NaOH before sterilization by autoclave. Cultures were incubated at 30°C for 5 days without stirring, additional pH adjustment or making anaerobic conditions.

**Fish sauce manufacturing**

Minced anchovy (*Engraulis japonicus*) was mixed with NaCl (final concentration 17%) and glucose (final concentration 0.5%). The mixture, fish sauce mash, was stored at 5°C until use. In small-scale fermentation, 2 ml of starter cultures prepared in fish sauce medium were added to 200 g of fish sauce mash. In large-scale

fermentation, 30 ml of starter cultures prepared in fish sauce medium were added to 20 kg of fish sauce mash and fermented at 30°C for 28 days.

As the fermentation indicator strain, *T. halophilus* C1 was used. C1 was previously confirmed not to produce gas in Durham tube with aspartate, histidine nor tyrosine (Table 3).

**Chemical analysis**

The fish sauce mash was filtered through filter paper (No. 2; Toyo Roshi, Tokyo, Japan), and the pH of the filtrate was determined using pH meter F-52 (Horiba, Kyoto, Japan). Amino acid composition was analyzed by high-performance liquid chromatography (HPLC) with ninhydrin detection. The HPLC system used was Hitachi ELITE LaChrom (Hitachi High-Technologies, Tokyo, Japan). The concentration of biogenic amines was also determined by HPLC with post-column *o*-phthalaldehyde derivatization and fluorescence detection. The HPLC system used was SCL-10$A_{VP}$ (Shimadzu, Kyoto, Japan). Total nitrogen content was measured by the Dumas combustion method using SUMIGRAPH NC-220F (Sumika Chemical Analysis Service, Osaka, Japan). The NaCl concentration was determined from chlorine content measured by potentiometric titration using an automatic titration apparatus COM-1700 (Hiranuma, Mito, Japan). Reducing sugar concentrations were assayed using the ferricyanide method (28). Lactic acid and acetic acid content was determined using Shodex OA (Shodex, Tokyo, Japan) following the instructions of the manufacturer.

**Bacterial count**

The population of halophilic lactic acid bacteria was monitored using LA13 medium (29) with a slight modification, containing 1% polypeptone, 0.4% yeast extract, 1% $KH_2PO_4$, 12% NaCl, 0.5% glucose, 5% soy sauce (Yamasa, Choshi, Japan) and

1.5% agar. Starter cultures or fish sauce mashes taken at various fermentation periods were diluted with 10% saline, spread on the LA13 medium and incubated at 30°C for 5 days with an AnaeroPack (Mitsubishi Gas Chemical) in a hermetically sealed box.

**Sensory evaluation**

After 28 days fermentation, fish sauce mash was filtered through a filter paper (No. 2; Toyo Roshi), and the filtrate was heated till it reached 90°C. Then, the resulting fish sauce was dialyzed by the electrodialysis system Micro Acilyzer S3 (Astom Corp., Tokyo, Japan) and adjusted to total nitrogen 1.5% and NaCl 1.5%. The fish sauce fermented with control strain C1 and with the isolated strain 1-1 or 21-11 were scored in 5-point scales to characterize the quality (salty, umami, sweet, bitter and sour). Fish sauce was served to panelists at room temperature in a random order. All nine panelists (men 24-38 years old) were the members of Yamasa Corporation.

**Statistical analysis**

The data were analyzed using SPSS software (SPSS Inc., Chicago, USA). Comparison of the two groups was performed using an unpaired t-test. The data involving more than two groups were assessed using a one-way ANOVA followed by post hoc Dunnett's or Bonferroni's multiple comparison test. Statistical significance was considered at $p < 0.05$. All experiments were carried out in triplicate. Exceptional sensory evaluation tests were carried out using fish sauce obtained by mixing three samples inoculated with the same strains.

## Results and discussion

**Isolation and identification of aspartate decarboxylating bacteria**

Seventy-four candidates of aspartate decarboxylating halophilic bacteria were

isolated as purple colonies on aspartate indicator broth, 41 from fish sauce and 33 from fish *nukazuke* (Table 1). All of the candidates were confirmed to possess *aspD,* but not *hdcA* or *tdcA*, and were estimated as *T. halophilus* by PCR amplification using gene or species-specific primer sets (data not shown). The strains were named by connecting the sample numbers from which they were isolated and using consecutive numbers with hyphens (Table 4).

**Table 4** Classification of isolated strains based on PCR.

| PCR | Strains |
|---|---|
| A | 1-1, 1-7, 1-9, 1-10, 1-14, 2-1, 2-5, 3-15 |
| B | 1-2, 1-3, 1-5, 1-6, 2-2, 2-6, 2-7, 2-8, 2-10, 3-4, 3-6, 3-8, 3-9, 3-14 |
| C | 1-4, 1-12 |
| D | 1-8, 3-2, 3-5 |
| E | 1-11, 2-3, 2-4, 2-11, 2-12, 3-3, 3-7, 3-10, 3-11, 3-12, 3-13 |
| F | 1-13 |
| G | 2-9 |
| H | 3-1 |
| I | 18-1, 21-2, 21-6, 21-8, 22-14, 22-18 |
| J | 21-1, 22-2 |
| K | 21-3, 21-5, 21-7, 21-9, 21-10, 21-12, 22-4, 22-5, 22-6, 22-8, 22-9, 22-10, 22-11, 22-12, 22-13, 22-15, 22-16, 22-17, 22-19 |
| L | 21-4, 22-1, 22-7 |
| M | 21-11, 22-3 |
| N | 21-13 |

Underlined strains were selected for subsequent experiments.

**Classification of the isolated strains**

Because the isolates from same samples may be genetically identical to each

other, I tried to classify these isolates. First, to classify the isolates based on their plasmid construction, PCR from three genes *aspD*, *repA* and *pinR* was conducted. *AspD* is a structural gene of aspartate decarboxylase and confirmed to be possessed by all of the isolates in a preceding experiment. *repA* exists on plasmids of *T. halophilus* encoding *hdcA* and *tdcA* with slight exceptions, and *pinR* exists on those plasmids with no exception so far (7, 8). Thus, this PCR from three genes was expected to generate three DNA fragments. And considering the length of plasmids encoding *hdcA* (21-37 kb) and *tdcA* (27-29 kb), the total length of the three fragments was expected to appear within this range. Although not all isolates made clear three fragments, their fragment patterns could be typed into 14 groups (Fig. 1, Table 4).

Eight different types of strains were isolated from fish sauces, and six types of strains were isolated from fish *nukazuke*. While multiple strains were isolated from five samples, no strain was isolated from 16 samples. This result suggests the possibility that the residence of halophilic bacteria possessing aspartate decarboxylase depends on the property of the samples. For example, shortage of glucose would provide an advantage to aspartate decarboxylating bacteria because the aspartate alanine conversion cycle contributes to ATP synthesis (30). This cycle is also involved in acid tolerance by extruding protons from cells (31). In addition, starter cultures naturally outcompete wild strains. The samples from which the isolates were obtained in this study might have met some of these conditions.

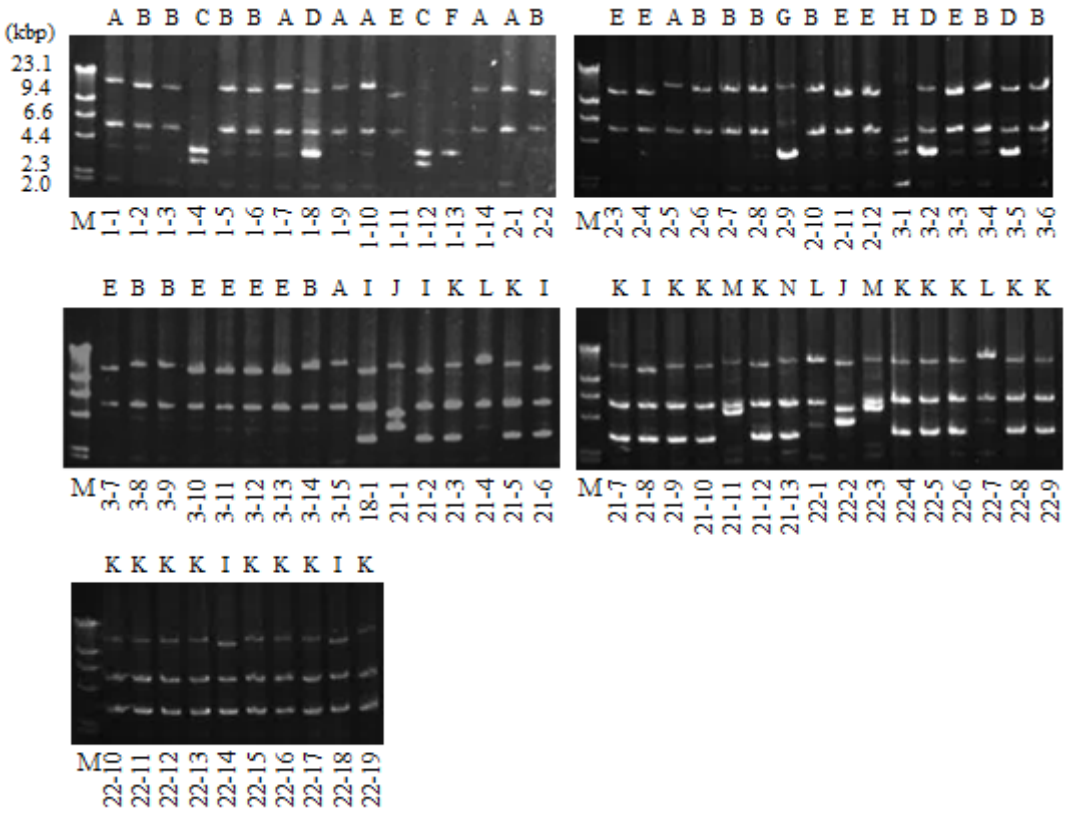


**Fig. 1.** Amplified DNA fragment patterns of PCR for classification of the isolated strains. Strain names are shown under the lanes (M: Molecular weight marker Lambda HindIII). The upper letters indicate groups corresponding to Table 4.

**Amino acid conversion and biogenic amines accumulation**

A total of 14 strains were selected, generally one from each group (Table 4). Their 16 rDNA sequences were determined, all of which showed more than 99.8% identity to that of *T. halophilus* (DDBJ accession numbers LC430618 - LC430631). To evaluate the property of *T. halophilus* possessing aspartate decarboxylase as a fish sauce fermentation starter, I performed small scale fermentation. The selected 14 strains and strain C1, incapable of aspartate, histidine or tyrosine decarboxylation (Table 2), were cultured in fish sauce medium and inoculated in fish sauce mash. After 28 days

fermentation, the amino acid content and biogenic amines accumulated in the fish sauce mash were analyzed. All 14 strains possessing aspartate decarboxylase decreased aspartate by 28.0-31.6 mM and increased alanine by 28.2-37.2 mM compared to that of the control strain C1 (Table 5).

Strains 1-11 diminished arginine levels in addition to aspartate levels, probably by the arginine deiminase pathway, which converts arginine to ornithine. It has been known that most strains of *T. halophilus* possess an arginine deiminase system, but some strains do not (9, 10, 24). In contrast, 13 out of 14 isolates used in this experiment did not decrease the arginine levels. Arginine deimination and aspartate decarboxylation are both used to complement the pH reduction occurring with lactic acid fermentation. Considering that arginine deimination and histidine decarboxylation are reciprocally regulated in *Lactobacillus hilgardii* (32), possessing both arginine deimination and amino acid decarboxylation systems may not be so beneficial for lactic acid bacteria. *T. halophilus* strains decarboxylating multiple amino acids have never been found, even though they could possess a multitude of plasmids (11). It may be the survival strategy of *T. halophilus* that each of the strains utilizes different amino acids to adapt to various environments.

In the fish sauce mash without starters, arginine and histidine levels significantly decreased, and various biogenic amines were remarkably accumulated (Table 5). Compared to this result, the accumulation of biogenic amines was entirely suppressed in fish sauce mash with starters, indicating that they were most probably produced by a contaminated wild microbe. Tyramine, histamine, phenylethylamine, tryptamine and spermidine levels tended to increase with certain strains, such as 1-4, 21-1 and 21-3. Given that these amines were also produced by wild microbes, such strains should have

allowed slight growth for some reason. Not much is known about the way these amines accumulate at high NaCl concentration, except for tyramine and histamine. In this study, I did not determine which bacteria participated in producing these biogenic amines, but further research is necessary from the point of food hygiene.

The cadaverine content increased in fish sauce mash inoculated with C1 more than that in other strains. Udomsil et al. also reported that using certain strains of *T. halophilus* increased the cadaverine content in fish sauce. C1 and such strains may possess lysine decarboxylase activity (24).

**Table 5** Amino acid and biogenic amine content in the small-scale fermentation of fish sauce.

| | C1 | 1-1 | 1-2 | 1-4 | 1-8 | 1-11 | 1-13 | 2-9 | 3-1 | 18-1 | 21-1 | 21-3 | 21-4 | 21-11 | 21-13 | NS |
|---|---|---|---|---|---|---|---|---|---|---|---|---|---|---|---|---|
| Amino acid (mM) | | | | | | | | | | | | | | | | |
| Aspartic acid | 31.6 | 0.1* | 0.2* | 0.1* | 0.0* | 2.1* | 3.6* | 1.0* | 1.2* | 1.9* | 1.7* | 1.8* | 0.1* | 0.3* | 1.4* | 31.7 |
| Threonine | 19.7 | 19.3 | 19.9 | 20.4 | 20.1 | 20.7 | 20.9 | 20.1 | 19.9 | 19.2 | 20.3 | 20.4 | 18.9 | 19.3 | 19.6 | 21.1 |
| Serine | 19.8 | 19.6 | 19.8 | 20.4 | 20.4 | 20.1 | 20.2 | 20.3 | 19.7 | 18.9 | 19.6 | 19.9 | 19.1 | 19.6 | 19.4 | 17.5 |
| Glutamic acid | 34.3 | 33.6 | 34.6 | 35.4 | 35.1 | 34.9 | 35.3 | 34.9 | 34.2 | 32.9 | 34.6 | 34.8 | 33.5 | 35.0 | 34.1 | 35.1 |
| Glycine | 14.8 | 14.7 | 15.5 | 15.2 | 15.3 | 15.4 | 15.4 | 15.2 | 14.9 | 14.3 | 14.9 | 14.8 | 14.6 | 15.2 | 14.6 | 16.0 |
| Alanine | 35.8 | 69.0* | 70.2* | 71.5* | 73.0* | 68.2* | 67.0* | 68.9* | 67.5* | 64.0* | 68.5* | 68.8* | 67.0* | 69.8* | 66.7* | 39.1 |
| Cysteine | 0.4 | 0.4 | 0.4 | 0.4 | 0.3 | 0.5 | 0.5 | 0.3 | 0.3 | 0.6 | 0.5 | 0.4 | 0.5 | 0.4 | 0.6 | 0.6 |
| Valine | 22.0 | 21.5 | 22.0 | 22.5 | 22.2 | 22.5 | 22.7 | 22.1 | 21.9 | 21.0 | 22.4 | 22.4 | 21.2 | 22.4 | 21.8 | 23.3 |
| Methionine | 11.4 | 11.6 | 11.8 | 12.1 | 11.9 | 12.1 | 12.1 | 12.0 | 11.7 | 10.9 | 11.7 | 12.0 | 11.2 | 11.6 | 11.3 | 12.1 |
| Isoleucine | 16.3 | 15.9 | 16.3 | 16.6 | 16.5 | 16.6 | 16.7 | 16.5 | 16.2 | 15.5 | 16.4 | 16.4 | 15.7 | 16.6 | 16.2 | 16.9 |
| Leucine | 31.6 | 30.8 | 31.3 | 32.4 | 31.9 | 32.1 | 32.3 | 32.0 | 31.5 | 30.3 | 31.8 | 32.0 | 30.2 | 31.9 | 31.5 | 32.6 |
| Tyrosine | 1.3 | 1.1 | 1.2 | 1.2 | 1.2 | 1.1 | 1.3 | 1.1 | 1.0 | 1.0 | 1.3 | 1.2 | 1.1 | 1.1 | 1.0 | 0.4 |

| | | | | | | | | | | | | | | | | |
|---|---|---|---|---|---|---|---|---|---|---|---|---|---|---|---|---|
| Phenylalanine | 10.6 | 10.2 | 10.2 | 10.8 | 10.3 | 10.8 | 10.6 | 10.4 | 10.4 | 9.9 | 10.3 | 10.7 | 9.8 | 10.8 | 10.5 | 9.5 |
| Lysine | 29.4 | 30.4 | 31.2 | 31.6 | 31.6 | 31.7 | 31.6 | 31.4 | 30.9 | 29.8 | 31.5 | 31.3 | 30.0 | 31.6 | 31.0 | 27.4 |
| Histidine | 14.3 | 14.4 | 15.1 | 14.5 | 15.1 | 15.1 | 14.7 | 15.2 | 15.1 | 13.9 | 13.7 | 13.4 | 14.7 | 15.0 | 13.8 | 2.6* |
| Arginine | 15.9 | 16.2 | 16.8 | 15.4 | 17.1 | 0.2* | 16.1 | 16.8 | 16.6 | 15.7 | 14.9 | 14.4 | 16.2 | 16.8 | 15.5 | 0.0* |
| Biogenic amine (ppm) | | | | | | | | | | | | | | | | |
| Tyramine | 21 | 5 | 4 | 42 | 4 | 4 | 26 | 8 | 4 | 12 | 41 | 46 | 4 | 6 | 21 | 1172* |
| Putrescine | 125 | 22 | 22 | 110 | 17 | 78 | 345 | 21 | 12 | 31 | 153 | 185 | 18 | 23 | 64 | 2888* |
| Cadaverine | 215 | 16* | 15* | 50* | 18* | 15* | 49* | 15* | 14* | 21* | 51* | 61* | 16* | 18* | 35* | 770* |
| Histamine | 73 | 16 | 14 | 105 | 12 | 10 | 71 | 20 | 11 | 43 | 159 | 190 | 28 | 30 | 78 | 1510* |
| Agmatine | 0 | 0 | 1 | 0 | 1 | 0 | 0 | 0 | 0 | 0 | 0 | 0 | 0 | 0 | 0 | 0 |
| Phenethylamine | 5 | 5 | 2 | 9 | 6 | 1 | 9 | 1 | 2 | 1 | 14 | 15 | 1 | 1 | 5 | 209* |
| Tryptamine | 154 | 20* | 4* | 275* | 8* | 7* | 239* | 37* | 9* | 68* | 261* | 270* | 20* | 46* | 172 | 419* |
| Spermidine | 13 | 13 | 12 | 13 | 14 | 10 | 15 | 10 | 111 | 13 | 25 | 28* | 13 | 10 | 15 | 57* |

Values are expressed as the mean (n=3).

Values with an asterisk are significantly different from samples fermented with C1 at $p<0.05$ by Dunnett's multiple test.

NS: Fermented without starter cultures.

**Fish sauce manufacturing**

To elucidate the effects of aspartate decarboxylation in more detail, larger-scale fish sauce manufacturing was carried out using strains C1, 1-1 and 21-11. In the small-scale experiment mentioned earlier, it was confirmed that 1-1 and 21-11 converted aspartate to alanine almost completely and that C1 did not. Although C1 slightly changed some amine content compared to that of the others, it did not change any amino acid content other than that of aspartate and alanine (Table 5). Therefore, I decided to use C1 as a control strain to assess the effects of aspartate decarboxylation on sensory characteristics.

The bacterial counts of C1, 1-1 and 21-11 in fish sauce medium just before inoculation in fish sauce mash were $1.3\times10^7$, $1.4\times10^8$ and $1.0\times10^8$ CFU/ml, respectively. The counts of fish sauce mash samples inoculated with 1-1 and 21-11 were higher than those inoculated with C1 throughout the fermentation, which probably resulted in higher organic acid and lower reducing sugar levels (Fig. 2a, Table 6). This result should be due to the acid tolerance caused by aspartate decarboxylation of 1-1 and 21-11. Aspartate decarboxylation eliminates protons from cells and generates the more alkaline alanine while simultaneously producing carbonic acid that would be released into the air. This effect can also explain the higher pH in fish sauce mash inoculated with 1-1 and 21-11, even though their organic acid content increased (Fig. 2b).

In fish sauce mash inoculated with 1-1 and 21-11, aspartate levels decreased more than 95% and alanine levels increased more than 107% compared to those in control samples treated with C1 at 28 days. In fact, at 14 days after inoculation, the aspartate content in fish sauce mash treated with 1-1 and 21-11 was below detection limit (data not shown). Therefore, the aspartate that remained in these products must be released from

fish protein or peptides after bacterial growth was completed. The amount of increased alanine was slightly larger than the amount of decreased aspartate, as also occurred in the preceding small-scale test, possibly because the activities of aspartate-generating enzymes might be higher when the concentration of aspartate is low. Other amino acid compositions did not significantly differ.

All amines in fish sauce mash inoculated with 1-1 and 21-11 were suppressed to less than 100 ppm. The histamine and tryptamine content slightly differs between samples, but this tendency is not consistent with the preceding results. This result might have been caused by a slight difference of microbiota in fish sauce mash samples unrelated to the starter inoculations. C1 increased the levels of putrescine and cadaverine, which also occurred in the small-scale experiments (Table 5). These compounds may have been produced by the same enzyme because it is reported in another species that lysine decarboxylase can also have ornithine decarboxylase activity (33).

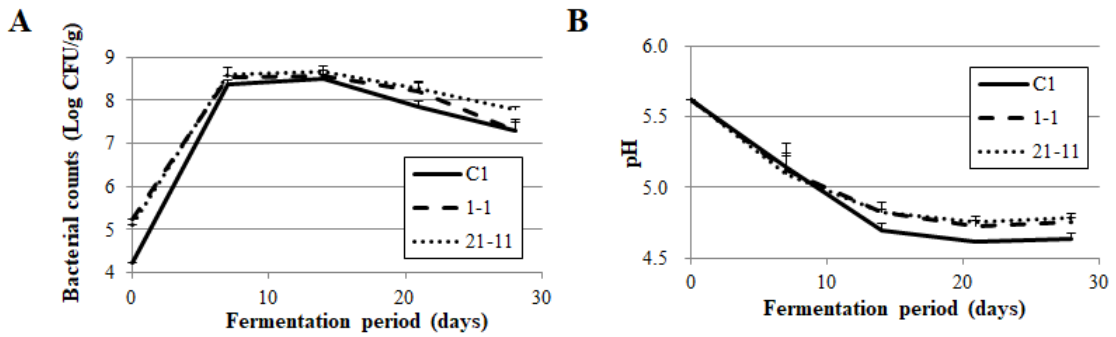


**Fig. 2.** Bacterial counts (A) and pH (B) evolution of fish sauce mush treated with each strain. Data are expressed as the mean with error bars representing +1 SD (n=3). Since no bacterium was detected in the fish sauce mash before starter inoculation ($<5\times10^{1}$ CFU/g), the initial bacterial counts are calculated from the values in the cultures.

**Table 6** Profiles of free amino acids, biogenic amines and other components in the large-scale fermentation of fish sauce.

| Item | C1 | 1-1 | 21-11 |
|---|---|---|---|
| Total nitrogen (%) | 1.44 ± 0.01 | 1.39 ± 0.04 | 1.42 ± 0.01 |
| NaCl (%) | 16.5 ± 0.5 | 16.9 ± 0.4 | 16.7 ± 0.4 |
| pH | 4.64 ± 0.03 [a] | 4.76 ± 0.03 [b] | 4.79 ± 0.03 [b] |
| Reducing sugar (%) | 0.70 ± 0.11 [a] | 0.48 ± 0.03 [b] | 0.51 ± 0.03 [b] |
| Lactic acid (%) | 1.19 ± 0.01 [a] | 1.29 ± 0.03 [b] | 1.30 ± 0.03 [b] |
| Acetic acid (%) | 0.10 ± 0.01 | 0.11 ± 0.00 | 0.11 ± 0.00 |
| Amino acid (mM) | | | |
| Aspartate | 30.7 ± 0.8 [a] | 1.4 ± 1.0 [b] | 1.4 ± 0.4 [b] |
| Threonine | 18.3 ± 0.5 | 19.8 ± 2.2 | 20.0 ± 0.6 |
| Serine | 19.4 ± 0.5 | 20.9 ± 2.1 | 21.2 ± 0.7 |
| Glutamate | 31.1 ± 1.2 | 33.5 ± 3.5 | 33.9 ± 1.4 |
| Glycine | 14.0 ± 0.3 | 15.3 ± 1.4 | 15.3 ± 0.7 |
| Alanine | 35.5 ± 0.4 [a] | 73.5 ± 6.8 [b] | 74.1 ± 3.6 [b] |
| Cysteine | 0.9 ± 0.0 | 0.9 ± 0.1 | 0.9 ± 0.0 |
| Valine | 21.1 ± 0.7 | 22.4 ± 2.2 | 22.6 ± 1.0 |
| Methionine | 11.9 ± 0.2 | 12.8 ± 1.4 | 12.9 ± 0.5 |
| Isoleucine | 15.2 ± 0.4 | 16.1 ± 1.6 | 16.2 ± 0.7 |
| Leucine | 29.7 ± 0.7 | 31.8 ± 3.2 | 31.9 ± 1.3 |
| Tyrosine | 0.9 ± 0.1 | 1.4 ± 0.4 | 1.1 ± 0.1 |
| Phenylalanine | 10.2 ± 0.3 | 10.7 ± 1.3 | 10.8 ± 0.4 |

| | | | |
|---|---|---|---|
| Lysine | 27.7 ± 0.7 | 31.8 ± 3.1 | 31.8 ± 1.2 |
| Histidine | 12.6 ± 0.3 | 14.1 ± 1.6 | 13.8 ± 0.5 |
| Arginine | 16.4 ± 0.4 | 17.5 ± 1.6 | 18.0 ± 1.2 |
| Total amino acids (mg/ml) | 38.7 ± 0.9 | 40.8 ± 4.2 | 41.1 ± 1.7 |
| Biogenic amine (ppm) | | | |
| Tyramine | 90 ± 4 | 91 ± 3 | 96 ± 4 |
| Putrescine | 26 ± 1 [a] | 10 ± 0 [b] | 11 ± 1 [b] |
| Cadaverine | 383 ± 43 [a] | 48 ± 1 [b] | 52 ± 4 [b] |
| Histamine | 3 ± 0 [a] | 7 ± 0 [b] | 7 ± 0 [b] |
| Agmatine | 21 ± 2 | 17 ± 1 | 18 ± 2 |
| Phenethylamine | 0 ± 0 | 7 ± 4 | 0 ± 0 |
| Tryptamine | 14 ± 2 [a] | 11 ± 0 [b] | 12 ± 1 [ab] |
| Spermidine | 18 ± 1 | 16 ± 1 | 17 ± 1 |

Values are expressed as the mean ± SD (n=3).

Values not sharing common superscripts are significantly different at $p<0.05$ by Bonferroni's multiple test.

**Sensory evaluation**

Fish sauce samples were dialyzed and adjusted to a total nitrogen of 1.5% and NaCl of 1.5%. The purpose of dialysis was to evaluate a sensory property with low NaCl concentration, avoiding an extreme salty taste. As a matter of fact, the fish sauce before dialysis was so salty that it was not easy to recognize the taste properties of each sample. Concentration by evaporation and removal of the separated salt is actually practiced by Japanese fish sauce manufacturers.

As a result of sensory evaluation, fish sauce treated with 1-1 or 21-11 was sweeter than the control sample treated with C1 was. On the other hand, saltiness, bitterness and sourness tended to be intensified in the control sample (Fig. 3). The reducing sugar content was higher and the lactic acid and acetic acid content was lower in the control sample, which suggests the attenuated sweetness and intensified saltiness, bitterness and sourness were not caused by differences in these components but by the conversion of aspartate to alanine. Considering the taste qualities and threshold of aspartate (sour, slightly bitter; 0.182-0.226 mM) and alanine (sweet; 6.7-16.2 mM), this result appears to be reasonable (34, 35).

The sweetness of fish sauce does not necessarily correspond to its quality. Sourness and bitterness are a part of the factors behind the unique and complex taste of the fish sauce. Hence, I do not insist that aspartate-decarboxylating bacteria are superior to others as a fish sauce fermentation starter. Nevertheless, this approach can provide alternatives to modify taste and enrich a variety of fish sauce items. There are various fermented marine food products by country or region, and the effects of use of aspartate-decarboxylating starters should be different in each product.

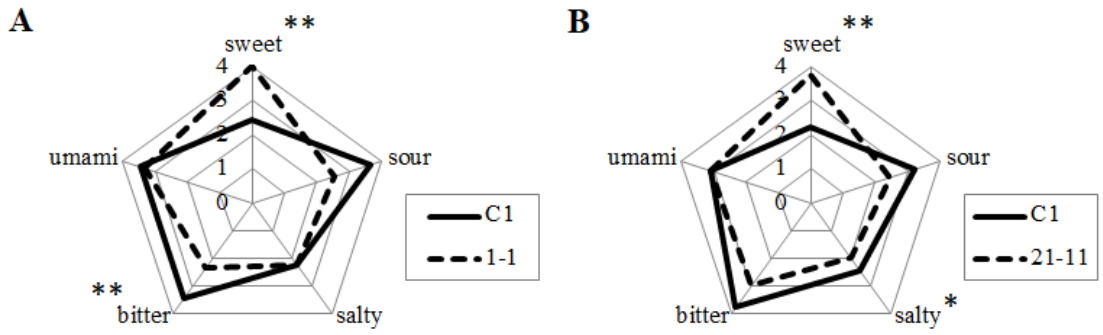


**Fig. 3.** Sensory evaluation of fish sauce comparing starter 1-1 to C1 (A) and 21-11 to

C1 (B). Solid line: C1, Broken line: 1-1 (A) and 21-11 (B). Data are expressed as the mean (nine panelists). Items with asterisks are significantly different (t-test; *$p$<0.05, **$p$<0.01).

**REFERENCES**


1. Kobayashi T, Kimura B, Fujii T, 2000. Differentiation of *Tetragenococcus* populations occurring in products and manufacturing processes of puffer fish ovaries fermented with rice-bran. Int J Food Microbiol 56:211-218.
2. Sato T, Kimura B, Fujii T, 1995. Histamine contents and histamine-metabolizing bacterial flora of fish sauce during fermentation. J Food Hyg Soc Jpn 36:763–768 (in Japanese).
3. Satomi M, Kimura B, Mizoi M, Sato T, Fujii T, 1997. *Tetragenococcus muriaticus* sp. nov, a new moderately halophilic lactic acid bacterium isolated from fermented squid sauce. Int J Syst Bacteriol 47:832–836.
4. Taira W, Funatsu Y, Satomi M, Takano T, Abe H, 2007. Changes in extractive components and microbial proliferation during fermentation of fish sauce from underutilized fish species and quality of final products. Fish Sci 73:913-923.
5. Thongsanit J, Tanasupawat S, Keeratipibul S, Jatikavanich S, 2002. Characterization and identification of *Tetragenococcus halophilus* and *Tetragenococcus muriaticus* strains from fish sauce (Nam-pla). Jpn J Lactic Acid Bact 13:46-52.
6. Kimura B, Konagaya Y, Fujii T, 2001. Histamine formation by *Tetragenococcus muriaticus*, a halophilic lactic acid bacterium isolated from fish sauce. Int J Food Microbiol 70:71–77.
7. Satomi M, Furushita M, Oikawa H, Yoshikawa-Takahashi M, Yano Y, 2008. Analysis of a 30 kbp plasmid encoding histidine carboxylase gene in *Tetragenococcus halophilus* isolated from fish sauce. Int J Food Microbiol 126:202–209.

8. Satomi M, Shozen KI, Furutani A, Fukui Y, Kimura M, Yasuike M, Yano Y, 2014. Analysis of plasmids encoding the tyrosine decarboxylase gene in *Tetragenococcus halophilus* isolated from fish sauce. Fish Sci 804:849-858.

9. Iituka K, Goan M, 1973. Studies on L-Arginine decomposition in Soy-sauce mash. Chomi Kagaku 20:17-24 (in Japanese).

10. Uchida K, 1982. Diversity of lactic acid bacteria in soy sauce and their application to brewing. J Brew Soc Jpn. 77:740-742 (in Japanese).

11. Higuchi T, Uchida K, Abe K, 1998. Aspartate decarboxylation encoded on the plasmid in the soy sauce lactic acid bacterium, *Tetragenococcus halophila* D10. Biosci Biotechnol Biochem 62:1601-1603.

12. Satomi M, Furushita M, Oikawa H, Yano Y, 2011. Diversity of plasmids encoding histidine decarboxylase gene in *Tetragenococcus* spp. isolated from Japanese fish sauce. Int J Food Microbiol 148:60-65.

13. Satomi M, Mori-Koyanagi M, Shozen KI, Furushita M, Oikawa H, Yano Y, 2012. Analysis of plasmids encoding the histidine decarboxylase gene in *Tetragenococcus muriaticus* isolated from Japanese fermented seafoods. Fish Sci 78:935-945.

14. Rice SL, Eitenmiller RR, Koehler PE, 1976. Biologically active amines in food: a review. J Milk Food Technol 39:353-358.

15. Santos MS, 1996. Biogenic amines: their importance in foods. Int J Food Microbiol 29:213-231.

16. Taylor SL, Eitenmiller RR, 1986. Histamine food poisoning: toxicology and clinical aspects. CRC Crit Rev Toxicol 17:91-128.

17. Prester L, 2011. Biogenic amines in fish, fish products and shellfish: a review.

Food Addit Contam Part A 28:1547-1560.

18. Stratton JE, Hutkins RW, Taylor SL, 1991. Biogenic amines in cheese and other fermented foods: a review. J Food Prot 54:460-470.

19. Nagahara A, Ohshita K, Nasuno S, 1986. Relation of nitrite concentration to mutagen formation in soy sauce. Food Chem Toxicol 24:13-15.

20. Sen NP, Baddoo PA, Weber D, Helgason T, 1990. Detection of a new nitrosamine, N-nitroso-N-methylaniline, and other nitrosamines in Icelandic smoked mutton. J Agric Food Chem 38:1007-1011.

21. Shalaby AR, 1996. Significance of biogenic amines to food safety and human health. Food Res Int 29:675-690.

22. Kimura M, Furutani A, Fukui Y, Shibata Y, Nei D, Yano Y, Satomi M, 2015. Isolation and identification of the causative bacterium of histamine accumulation during fish sauce fermentation and the suppression effect of inoculation with starter culture of lactic acid bacterium on histamine accumulation in fish sauce processing. Nippon Suisan Gakkaishi 81:97-106 (in Japanese with English abstract).

23. Kuda T, Izawa Y, Ishii S, Takahashi H, Torido Y, Kimura B, 2012. Suppressive effect of *Tetragenococcus halophilus*, isolated from fish-nukazuke, on histamine accumulation in salted and fermented fish. Food Chem 130:569-574.

24. Udomsil N, Rodtong S, Choi YJ, Hua Y, Yongsawatdigul J, 2011. Use of *Tetragenococcus halophilus* as a starter culture for flavor improvement in fish sauce fermentation. J Agric Food Chem 59:8401-8408.

25. Uchida K, 2000. Diversity and ecology of salt tolerant lactic acid bacteria:

*Tetragenococcus halophilus* in Soy Sauce fermentation. Jpn J Lactic Acid Bact 11:60-65.

26. Nielsen JC, Richelieu M, 1999. Control of flavor development in wine during and after malolactic fermentation by *Oenococcus oeni*. Appl Environ Microbiol 65:740-745.

27. Noda Y, Inoue H, Kusuda H, Ohba K, Nakano M, 1982. Studies on the Control of the Fermentaion of the Soysauce-mash (Part 5) The Additional Effect of Yeast and Lactic Acid Bacterium in the Industrial Scale of Soysauce Brewing. J Jpn Soy Sauce Res Inst 8:108-116 (in Japanese).

28. Hulme AC, Narain R, 1931. The ferricyanide method for the determination of reducing sugars: A modification of the Hagedorn-Jensen-Hanes technique. Biochem J 25:1051-1061.

29. Yamasato K, Iizuka H, 1959. A study on bacteria in soy sauce mash (Part 1). Nippon Nogei Kagakkaishi 33:379-382 (in Japanese).

30. Abe K, Hayashi H, Maloney PC, 1996. Exchange of aspartate and alanine mechanism for development of a proton-motive force in bacteria. J Biol Chem 271:3079-3084.

31. Abe K, Ohnishi F, Yagi K., Nakajima T, Higuchi T, Sano M, Maloney PC, 2002. Plasmid-encoded asp operon confers a proton motive metabolic cycle catalyzed by an aspartate-alanine exchange reaction. J Bacteriol 184:2906-2913.

32. Lamberti C, Purrotti M, Mazzoli R, Fattori P, Barello C, Coïsson JD, Pessione E, 2011. ADI pathway and histidine decarboxylation are reciprocally regulated

in *Lactobacillus hilgardii* ISE 5211: proteomic evidence. Amino acids 41:517-527.

33. Takatsuka Y, Onoda M, Sugiyama T, Muramoto K, Tomita T, Kamio Y, 1999. Novel characteristics of *Selenomonas ruminantium* lysine decarboxylase capable of decarboxylating both L-lysine and L-ornithine. Biosci Biotechnol Biochem 63:1063-1069.

34. Kirimura J, Shimizu A, Kimizuka A, Ninomiya T, Katsuya N, 1969. Contribution of peptides and amino acids to the taste of foods. J Agric Food Chem 17:689-695.

35. Schiffman SS, Sennewald K, Gagnon J, 1981. Comparison of taste qualities and thresholds of D-and L-amino acids. Physiol Behav 27:51-59.

**SUMMARY**

The aims of this section were to isolate halophilic lactic acid bacteria possessing aspartate decarboxylase and elucidate the property of the isolates as starter cultures for fish sauce fermentation. Seventy-four strains were isolated from fermented fish foods on aspartate indicator broth containing bromocresol purple, and all isolates were identified as *Tetragenococcus halophilus* and confirmed to possess the aspartate decarboxylase gene (*aspD*) by PCR amplification. The isolates were classified into 14 groups based on their *aspD*-encoding plasmid construction. Strains selected from each group and a control strain incapable of aspartate decarboxylation were inoculated into fish sauce mash as starter cultures. Isolated strains possessing *aspD* converted aspartate into alanine almost completely in the fish sauce mash. In addition, the strains prevented the accumulation of biogenic amines, as did the control strain, whereas various amines were accumulated in fish sauce mash without starter cultures. Sensory evaluation tests indicated that converting the sour amino acid aspartate into the sweet amino acid alanine made the fish sauce taste milder. In conclusion, the use of *T. halophilus* possessing aspartate decarboxylase as a fish sauce fermentation starter causes the conversion of aspartate to alanine, accompanied by taste alteration, and prevents biogenic amine accumulation in fish sauce products.

## SECTION 2

## Transposition of IS*4* family insertion sequences IS*Teha3*, IS*Teha4*, and IS*Teha5* into the *arc* operon disrupts arginine deiminase system in *Tetragenococcus halophilus*

Insertion sequences (ISs) are small transposable elements of DNA, generally consisting of transposase and terminal inverted repeats (IRs), which function as the sites for recognition and cleavage by transposase (1). ISs are distributed in a wide range of bacteria, and many bacteria possess multiple ISs in their genome (2, 3, 4). It is well recognized that the transposition of ISs often causes gene inactivation or alteration of the expression levels of adjacent genes. Furthermore, two homologous ISs can cause recombination and generate chromosomal inversions or deletions, which lead to complex rearrangements (5). Thus, ISs contribute significantly to bacterial evolution. In addition, ISs have been utilized in transposon mutagenesis systems to disrupt genes randomly in many species, including lactic acid bacteria (6, 7). Nevertheless, no active IS has been reported in tetragenococci, though putative ISs have been found in their genome or plasmid sequences (8, 9).

*Tetragenococcus halophilus,* a homofermentative, halophilic lactic acid bacterium, is isolated as the dominant microbe from various salted and fermented foods, including soy sauce and salted anchovies (10, 11, 12). *T. halophilus* plays an important role in the fermentation of soy sauce. Lactic acid produced in soy sauce mash causes a reduction in pH, which prepares the appropriate environment for halotolerant yeasts such as *Zygosaccharomyces rouxii* (13). On the other hand, some *T. halophilus* strains can raise the pH of soy sauce mash through arginine degradation via the arginine deiminase

system (ADS) (14). The ADS converts arginine into ornithine, $CO_2$ and $NH_3$ releasing adenosine triphosphate (ATP) (Fig. 1A). $NH_3$ generation prevents pH reduction, which causes an increase of lactic acid, inhibiting the alcoholic fermentation. More importantly, citrulline, a metabolic intermediate of the ADS, is reported as the main precursor of ethyl carbamate (EC) in soy sauce (15). EC belongs to the 2A group of carcinogens and is formed through the reaction of citrulline and ethanol. Normally, the ADS converts arginine to ornithine inside the bacterial cells, and citrulline is not discharged outside the cell membrane. However, when the bacterial cells are destroyed while this pathway is in progress, citrulline leaks out of the cells and accumulated in soy sauce mash. Infection by bacteriophage is one of the factors that can induce cell lysis and citrulline accumulation (16). Therefore, selected strains of *T. halophilus* which are incapable of arginine deimination are preferred for the fermentation starter in soy sauce manufacturing.

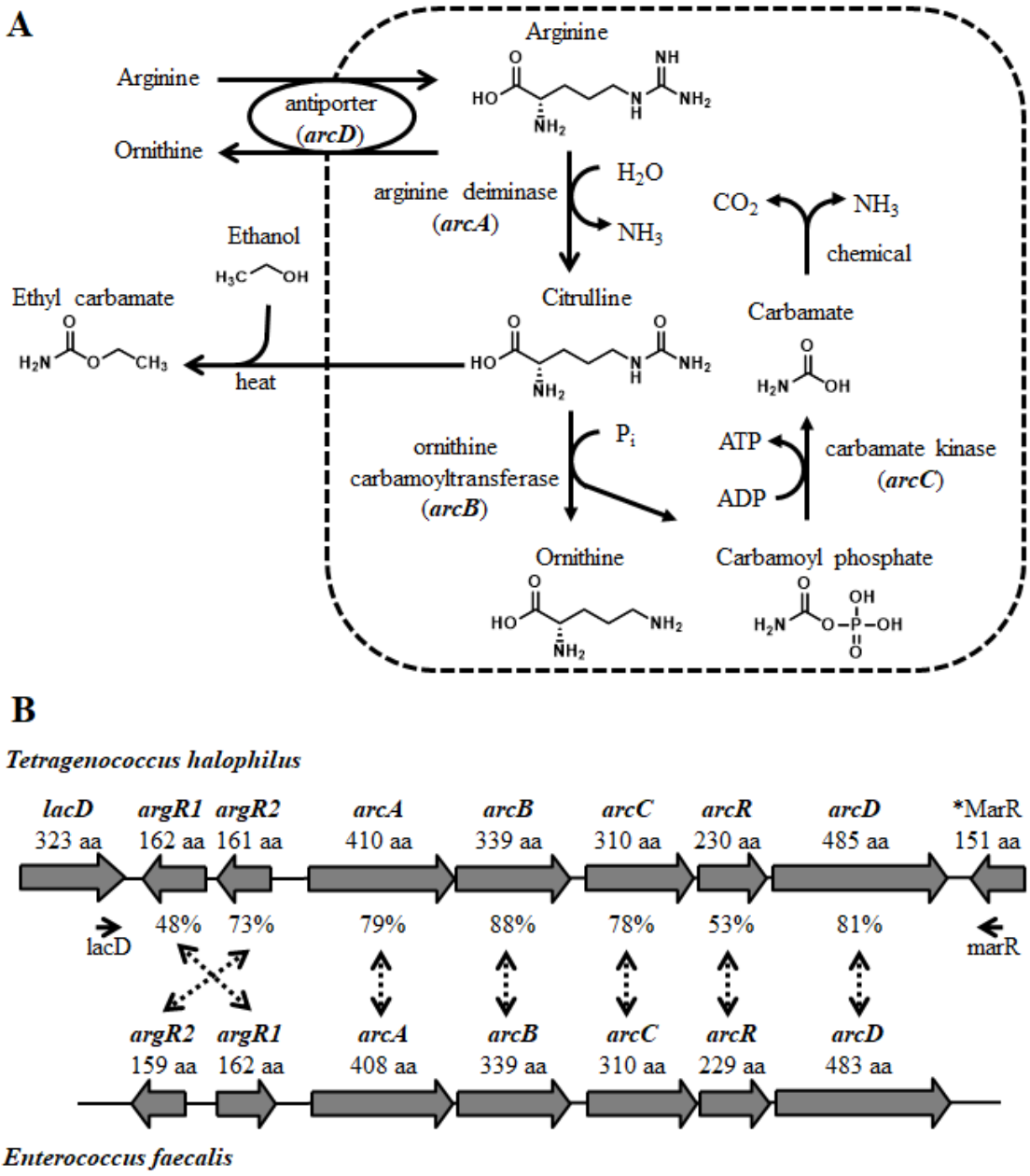


**Fig. 1:** Arginine deimination pathway in *T. halophilus* and generation of EC (A) and schematic representation of the locus of the genes around the *arc* operon in the genome of *T. halophilus* NBRC 12172 and *E. faecalis* SD10 (B). (A) The broken line represents the cell membrane. Citrulline leakage out of the cell is caused by external factors, such as bacteriophage infection. (B) *MarR represents a putative MarR family transcriptional regulator gene. The arrows under *lacD* and *MarR* indicate the position on which the

lacD and marR primers were designed. Percentage shows the amino acid identities between *T. halophilus* and *E. faecalis*.

Most of the ADS genes studied to date are organized in a single operon known as the *arc* operon (17, 18). The three cytoplasmic enzymes participating in the ADS, arginine deiminase, ornithine transcarbamylase and carbamate kinase, are encoded by the *arcA*, *arcB* and *arcC* genes, respectively (Fig. 1A). In addition to these genes, other genes may be present in the *arc* operons of lactic acid bacteria, such as genes encoding arginine/ornithine antiporter (*arcD*) and Crp/Fnr-type regulator (*arcR*) (19, 20). Recent whole genome analysis of *T. halophilus* revealed five genes of the *arc* operon, *arcABCRD*, sharing 53-88% of amino acids with those of *Enterococcus faecalis* (Fig. 1B). Two ArgR/AhrC-type regulators (*argR1* and *argR2*), located upstream of the *arc* operon, were also reported to participate in the ADS by regulating the expression of *arc* operon genes (21).

In this section, I generated *T. halophilus* mutants lacking arginine deiminase activity by UV irradiation, and I identified novel ISs by transposition into the region around the *arc* operon. Information about the structure and transposition properties of the active ISs described here will contribute not only to the understanding of IS-mediated evolution in *T. halophilus* but also to the establishment of transposon mutagenesis systems in this species.

## Materials and methods

### Bacterial strains, media and growth conditions

Bacterial strains used in this study are shown in Table 1. YA5 and A-30 were

selected from the strain collection of Yamasa Corporation, which were isolated from soy sauce mash of the factory. They were confirmed not to decrease arginine content in soy sauce medium containing 2% arginine after 7 days cultivation (data not shown). *T. halophilus* was cultured in MRS-10, soy sauce medium, arginine indicator broth or LA13 medium, as specified in individual experiments. MRS-10 is Lactobacilli MRS Broth (Difco, Detroit, USA) supplemented with 10% NaCl. Soy sauce medium is the medium for halophilic lactic acid bacteria, using soy sauce (Yamasa, Choshi, Japan) and NaCl so that the final concentration becomes 0.4% total nitrogen and 10% NaCl. The pH was adjusted to 8.0 before sterilization by autoclave. When necessary, soy sauce medium was supplemented with 2% arginine. Arginine indicator broth contains 0.5% beef extract, 0.5% Hipolypepton (Nihon Pharmaceutical, Tokyo, Japan), 0.5% yeast extract, 0.1% thioglycolic acid, 10% NaCl, 0.1% glucose, 0.004% bromocresol purple and 1% arginine. The pH was adjusted to 7.5 before sterilization by autoclave. LA13 medium contains 1% Hipolypepton (Nihon Pharmaceutical), 0.4% yeast extract, 1% $KH_2PO_4$, 12% NaCl, 0.5% glucose, 5% soy sauce (Yamasa) and 1.5% agar (14). Liquid media were incubated at 30°C without stirring, and agar plates were incubated at the same temperature with an AnaeroPack (Mitsubishi Gas Chemical, Tokyo, Japan) in a hermetically sealed box.

**Table 1. Strains used in this study.**

| Strain | Description and genotype | Source |
|---|---|---|
| *Tetragenococcus halophilus* | | |
| NBRC 12172 | ADS positive. Genome sequenced. | National Bio Resource Center |
| M1 | ADS negative. *arcD*::IS*Teha3* | NBRC 12172 derivative generated in this study. |
| M2 | ADS negative. *arcA*::IS*Teha5* | NBRC 12172 derivative generated in this study. |
| M3 | ADS negative. *arcA__pr*::IS*Teha4* | NBRC 12172 derivative generated in this study. |
| M4 | ADS negative. *arcD*::IS*Teha3* | NBRC 12172 derivative generated in this study. |
| M5 | ADS negative. *arcD*::IS*Teha4* | NBRC 12172 derivative generated in this study. |
| YA5 | ADS negative. | Isolated from soy sauce mash. Kept in my laboratory. |
| A-30 | ADS negative. | Isolated from soy sauce mash. Kept in my laboratory. |

**UV irradiation and isolation of mutants lacking arginine deiminase activity**

UV irradiation was used to induce random mutations that could affect the genes encoding the ADS. One ml of MRS-10 cultures of fully grown *T. halophilus* NBRC 12172 (Table 1) was resuspended in 9 ml of fresh MRS-10 and grown for 16 h. The cultures were then centrifuged (6,000 × *g*) for 10 min at 4°C. The pellets were washed once and resuspended in 10 ml of 10% NaCl. The 5 ml suspensions in sterile dishes (diameter 55 mm) were UV irradiated using a germicidal lamp (GL-15; Panasonic, Kadoma, Japan) at a distance of 260 mm for 10-30 sec with constant stirring to yield a 0.1-0.01% survival rate after exposure. Before and after irradiation, part of the suspension was properly diluted, spread on the LA13 medium plates, and incubated for 5 days. The survival rate was determined by counting the number of colonies on the plates. Mutants lacking arginine deiminase activity were isolated in arginine indicator broth containing bromocresol purple. pH reduction by lactic acid production changes the color of this medium to yellow, but when arginine is deiminated and the pH is increased, the color remains purple. UV-irradiated derivatives were inoculated into 80 µl of this medium in 384-well microplates, which were sealed with aluminum films (AlumaSeal II; Excel Scientific, CA, USA). After 5 days of incubation, strains which changed the color of arginine indicator broth to yellow were isolated as candidate strains for mutants lacking arginine deiminase.

**DNA manipulations and sequence analysis**

The oligonucleotide primers used in this study are listed in Table 2. PCR was performed using DNA polymerase KOD FX Neo (Toyobo, Osaka, Japan) under the optimal conditions recommended by the supplier. PCR products were separated on 0.9%

agarose gel and purified using the Wizard SV Gel and PCR Clean-Up System (Promega, Madison, USA). The DNA sequences of the fragments were determined by a commercial DNA sequencing service (Fasmac, Atsugi, Japan).

**Table 2. Primers used in this study**

| Primer name | Sequence (5'→3') |
|---|---|
| lacD | GTTACAGGAAACTGCTACACCAATTGG |
| marR | CATTCGATTGGGACTTTGTTCG |
| TEH_16330f | TGAAGCTTATCATAAGCTCCCTTAAGC |
| TEH_16330r | GGGAGGTTGGAAATGCCTCTC |
| TEH_20570f | TGGGGACCTTCCTGTTTTGC |
| TEH_20570r | GACCAGCGCCTACGATCG |
| TEH_05530f | GATTGTTTCGCAATATGCCTGTG |
| TEH_05530r | ATAGCGACTTCTATGCTCCTGAATGTG |
| TEH_21080f | AGAGGCCGATCTATGGCTTCC |
| TEH_21080r | GCTTCTGCTTTACAAAAGATCACCAG |
| TEH_08830f | GACGATCTTTTTATGAAGTGCCTGAAG |
| TEH_08830r | CGCTTTATCCCTCCCCTGC |
| TEH_24130f | ATACCATTGATCGTACCACTTGCC |
| TEH_24130r | AAAGAACTGGGCATGTGAATATGC |
| arcAf | GGCATGCTTCGTGATAAAGG |
| arcAr | CCGCATGACTACGAATACCTG |
| 16Sf | CAAAGCAACGATGCATAGCC |
| 16Sr | TTGCCGAAGATTCCCTACTG |
| probe-arcAf | TCAGAAATTGGAAAGCTTAAAACG |
| probe-arcAr | AATTGGTATTCTGGCATTTCAAC |

**mRNA expression analysis by quantitative RT-PCR**

Cells grown in 500 μl of soy sauce medium supplemented with 2% arginine were pelleted by centrifugation (6,000 × *g*) and suspended in 1 ml of Isogen RNA extraction kit (Nippon Gene, Tokyo, Japan). Cells were lysed with approximately 0.5 mg of glass beads (0.1 mm in diameter) by a beads cell disrupter at room temperature and 3,000 rpm for 3 min, and RNA extraction was carried out according to the manufacturer's instructions. The yield and purity of RNA were determined by spectrophotometric measurements of the UV absorbance at 260 and 280 nm. Total RNA was reverse transcribed with PrimeScript RT Reagent Kit with gDNA Eraser (Takara, Kusatsu, Japan), using random primers following the manufacturer's instructions. The primer set arcAf and arcAr was used for the *arcA* gene expression analysis. The 16S rRNA gene was used as the housekeeping control gene with the primer sets 16Sf and 16Sr (Table 2). Quantitative real-time PCR was performed using SYBR premix Ex Taq II (Takara) using 1 μg of the cDNA as the template. The results were analyzed using the Thermal Cycler Dice Real Time System TP900 (Takara). The cycle threshold value for each PCR was calculated by the second derivative maximum method, and the relative expression of *arcA* was calculated by the calibration curve. The specificity of reactions was determined by melting curve analysis and the electrophoresis of the PCR products. The PCR was performed in triplicate.

**Northern blotting**

Total RNA was extracted as described above. The probe was amplified by PCR using the primer set probe-arcAf and probe-arcAr (Table 2) and the genomic DNA of NBRC 12172 as a template and labeled with digoxigenin (DIG)-dUTP using PCR DIG

labeling mix (Roche, Basel, Switzerland). RNA was incubated in formaldehyde MOPS buffer for 15 min at 65°C for denaturation, subjected to electrophoresis (0.4 μg per lane) on a formaldehyde-containing 0.9% agarose gel, stained with ethidium bromide, and transferred to a Hybond-N+ nylon membrane (GE health care, Chicago, USA). Hybridization was performed with the DIG Easy Hyb system (Roche) at 50°C for 16 h with a DIG-labeled probe. For detection, the membranes were treated with anti-DIG-AP Fab fragments and CDP-Star (Roche), exposed to BioMax light film (Carestream Health, Rochester, USA), and developed by the Kodak GBX developer/fixer (Kodak China, Wuxi, China). The product size on the membrane was estimated by the 16S rRNA (1.6 kb) and 23S rRNA (2.9 kb) patterns stained with ethidium bromide.

**Soy sauce manufacturing**

Soy sauce mash was prepared as described previously (11). Briefly, steamed soy beans and roasted wheat were mixed with *Aspergillus oryzae* and incubated for 40 h to make "koji", which was then mixed with brine to make soy sauce mash (final NaCl concentration 17%). Starter strains were cultured in soy sauce medium for 5 days, and 1 ml of the cultures was added to 1 L of soy sauce mash. The mash was fermented at 15°C for 2 weeks, then at 28°C for 6 weeks. The fermentation experiment was performed in triplicate.

**Chemical analysis**

Bacterial cultures or soy sauce mash were filtered through filter paper (No. 2; Toyo Roshi, Tokyo, Japan), and the pH of the filtrate was determined using an F52 pH meter (Horiba, Kyoto, Japan). Amino acid composition was analyzed by high-performance liquid chromatography (HPLC) with ninhydrin detection. The HPLC

system used was the Hitachi ELITE LaChrom (Hitachi High-Technologies, Tokyo, Japan) equipped with a pump (L-2130), an autosampler (L-2200), a column oven (L-2300), a UV detector (L-2420) and a cation-exchange column (#2619PH) (https://www.hitachi-hightech.com/file/ca/pdf/library/application/20100209-Hitachi_AAA_Sensivate_Application_Note_stw1.pdf). Lactic acid content was determined using organic acids analysis system Shodex OA (Shodex, Tokyo, Japan) following the instructions of the manufacturer.

**Bioinformatics**

The DNA and amino acid sequences were analyzed using Blast and ISfinder (22). The thermodynamic stability of RNA secondary structures was estimated using free-energy calculations from the RNA Websuite (23).

**Nucleotide sequence accession numbers**

Sequence data was deposited in the DDBJ/EMBL/GenBank databases, with accession numbers LC430896-LC430900 (M1-M5) and LC458667-LC458668 (YA5 and A-30).

## Results and discussion

### Isolation of NBRC 12172 derivatives lacking arginine deiminase activity

Approximately 20,000 colonies of NBRC 12172 derivatives survived from UV exposure were picked up into arginine indicator broth, and five strains (M1, M2, M3, M4, and M5) changed the color of the broth to yellow. The candidate strains were cultured in soy sauce medium containing 2% arginine for 7 days. The arginine content of the cultures was then analyzed, and it was confirmed that the derivatives did not decrease

arginine content after incubation (data not shown).

**Identification and structure of IS*Teha3*, IS*Teha4* and IS*Teha5***

I assumed that the derivatives lacking arginine deiminase activity would have base substitutions and/or base insertions/deletions around the *arc* operon. So I amplified the DNA region covering the entire *arc* operon and two regulator genes (*argR1* and *argR2*) by PCR using the lacD and marR primer sets designed from the *lacD* encoding tagatose 1,6-diphosphate aldolase and putative MarR family transcriptional regulator gene (Table 2, Fig. 1B). Surprisingly, all five derivatives showed elongated PCR products (over 8.0 kb) compared with the fragment amplified from the wild-type strain of NBRC 12172 (7.4 kb; data not shown). These derivatives were expected to display active transposable elements inserted into this region.

DNA sequence analysis revealed that the elongated PCR products carried the inserted DNA fragments, but their sequences and insertion sites were not identical among the derivatives (Fig. 2A). The 1522 bp inserted elements of M1 and M4, designated IS*Teha3*, duplicated exactly the same 7 bp target sequence on *arcD* but integrated in the opposite direction each other (Table 3). The inserts showed 100% identity to each other and to two putative ISs on the genome of NBRC 12172 itself (locus tags of transposase: TEH_16330 and TEH_20570). The inserts contain a single ORF and 15 bp perfect IRs at both termini (Fig. 2B and C). The ORF encodes a putative transposase consisting of 452 amino acids. This amino acid sequence shows 43% identity to the putative transposase of IS*Dha5* in *Desulfitobacterium hafniense* DCB-2 (NC_011830; data not shown). IS*Dha5* belongs to the IS*4* family IS*Epr1* subgroup, and the amino acid sequence of the putative transposase of IS*Teha3* also shows 37% identity to that of IS*Epr1*

(NZ_AAJH01000015).

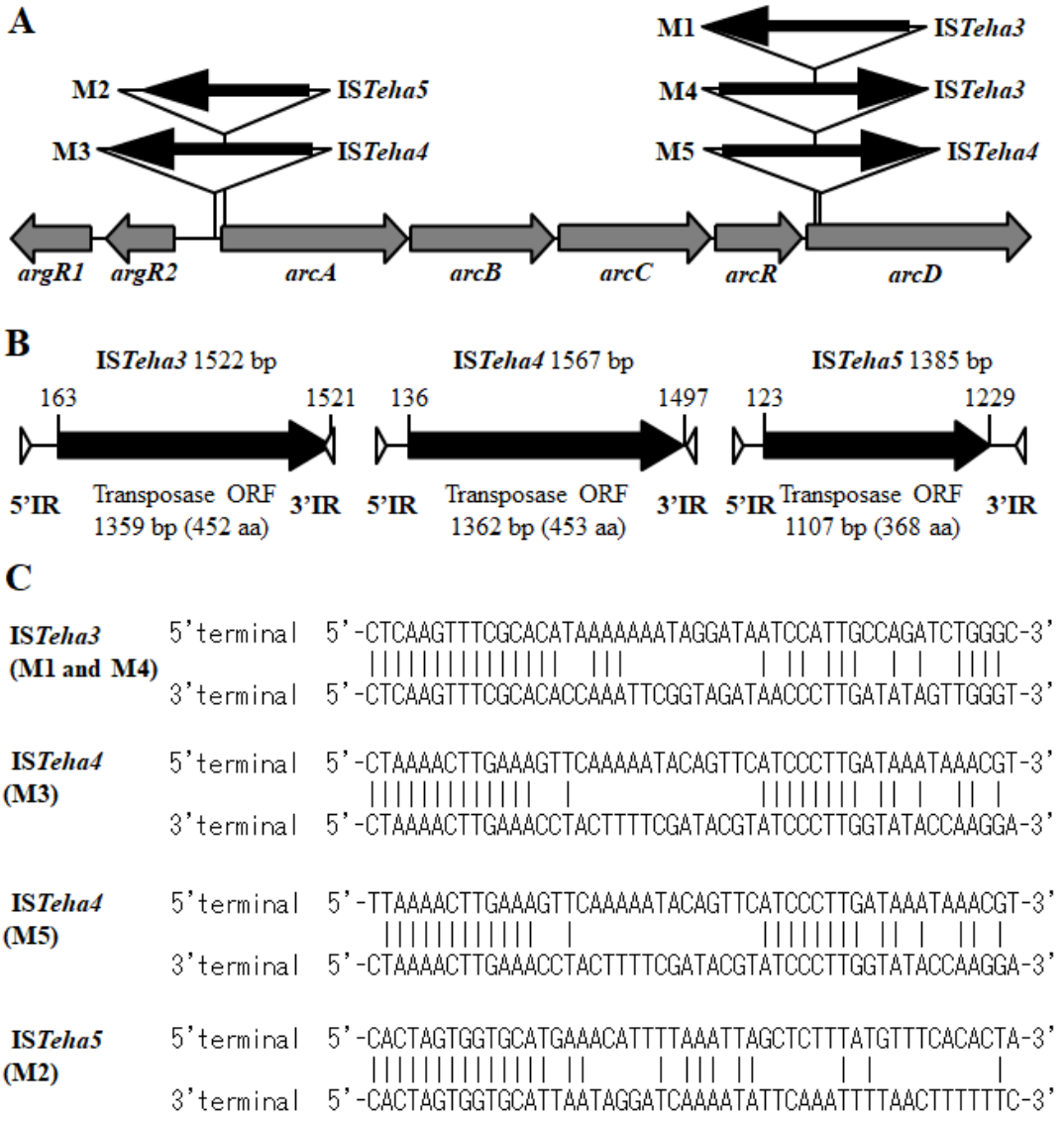


**Fig. 2:** Location and orientation of ISs transposed around the *arc* operon in each derivative (A) and genetic structures (B) and nucleotide sequences of the 5' and 3' termini (C) of IS*Teha3*, IS*Teha4* and IS*Teha5*. (A) Black arrows indicate the direction of the putative transposase transcription. The derivative names and designated IS names are indicated on the left side and right side of the arrows, respectively. (B) The black

arrows indicate ORFs that encode a putative transposase. The triangles indicate IRs at the 5' and 3' termini. The nucleotide numbers refer to the start and stop positions of the ORFs. (C) Vertical lines between the sequences denote homologous nucleotides.

**Table 3. DNA sequences of the insertion sites and their flanking regions of IS*Teha3*, IS*Teha4* and IS*Teha5*.**

| IS transposed in each derivative | Flanking sequence at 5' terminal | Insertion site (Duplicated target sequence) | Flanking sequence at 3' terminal |
|---|---|---|---|
| IS*Teha3* | | | |
| M1 | ATAAGAATAA | TAAATAA | AATACTAAAT |
| M4 | ATTTAGTATT | TTATTTA | TTATTCTTAT |
| IS*Teha4* | | | |
| M3 | CAACATAAGG | ATAATAA | ATTATCCAAT |
| M5 | TTAGGTATAC | TAACAATAA | TACTAAATGG |
| IS*Teha5* | | | |
| M2 | AACATTAATT | GGCTTACTC | ATAACTTAAG |

The 1567 bp inserted elements of M3 duplicated a 7 bp target sequence between *argR2* and *arcA*, while the same size inserted elements of M5 duplicated a 9 bp target sequence on *arcD* (Table 3). They show 96.2% identity to each other and 100% identity to the different putative ISs of NBRC 12172 (M3: TEH_05530 and TEH_21080, M5: TEH_08830). The inserts encode a putative transposase with a predicted 453 amino acid residues, sharing 98.2% identity with each other (Fig. 2B). According to ISfinder, ISs sharing more than 98% similarity in amino acid sequence or more than 95% similarity in DNA sequence are considered to be isoforms (24). Therefore, both elements transposed in M3 and M5 were designated IS*Teha4*. The insert of M3 contains 13 bp perfect IRs, whereas the IRs of M5 are imperfect (Fig. 2C). The amino acid sequence of the putative transposase in M3 shows 45% identity to that of IS*Lre1* in *Lactobacillus reuteri* 100-23 (NZ_AAPZ00000000; data not shown). IS*Lre1* also belongs to the IS*4* family IS*Pepr1* subgroup, and the amino acid sequence of the putative transposase of IS*Teha4* shows 36% identity to IS*Pepr1*. Therefore, I entered IS*Teha3* and IS*Teha4* as novel IS*4* family IS*Pepr1* subgroup members in the ISfinder database.

The 1385 bp element inserted in M2 was designated IS*Teha5*, which duplicated the 9 bp target sequence on *arcA* (Table 3). The insert showed 100% identity to a putative IS of NBRC 12172 (TEH_24130) and contains a single ORF and 14 bp perfect IRs at both termini (Fig. 2B and C). The ORF encodes a putative transposase consisting of 368 amino acids showing 44% identity to the putative transposase of IS*641* in *Bacillus halodurans* C-125 (NC_002570; data not shown). IS*641* belongs to the IS*4* family IS*4Sa* subgroup, and the amino acid sequence of the putative transposase of IS*Teha5* also shows 26% identity to that of IS*4Sa* (U38915). Hence, I entered IS*Teha5* as a novel IS*4* family IS*4Sa* subgroup member in the ISfinder database.

In the genome of NBRC 12172, at least one putative IS completely identical to the insert of each derivative is present. I amplified the DNA fragments covering these ISs from the genomic DNA of the wild-type strain and each derivative using primer sets designed at locations upstream and downstream of the fragments (data not shown). All derivatives showed the same size PCR products as the wild-type strain, suggesting that IS*Teha3*, IS*Teha4* and IS*Teha5* leave the parent sequences at the original sites and accumulate their copies in other sites (data not shown).

**mRNA expression of *arcA* in derivatives**

M1, M2, M4 and M5 carried ISs transposed into *arcA* or *arcD*, the structural genes encoding arginine deiminase and arginine/ornithine antiporter, respectively. Therefore, it is understandable that these derivatives lose arginine deiminase activity. In M3, however, an IS was transposed into the region between *arcA* and *argR2*, and no alteration was found in every ORF of *arcABCRD* and two regulators (*argR1* and *argR2*) by DNA sequence analysis (Fig. 2A). Therefore, I hypothesized that IS*Teha4* of M3 disrupted the promoter region of the *arc* operon. To investigate this hypothesis, the expression of *arcA* was analyzed at the mRNA level by quantitative RT-PCR using a primer set designed from *arcA*. As expected, the mRNA expression level of *arcA* in M3 decreased to only 2% of that of the wild-type strain (Fig. 3). Upstream of the IS*Teha4* transposition site in M3, five putative ArgR binding sequences, so-called Arg boxes (*Escherichia coli* consensus sequence, (T/A)NTGAAT(T/A)(T/A)(A/T)(A/T)ATTCAN(A/T)) (25), were found (data not shown). In addition, a putative cre box (*Bacillus subtilis* consensus sequence, TG(T/A)NANCGNTN(T/A)CA) (26) was also found between Arg boxes, indicating the possibility that the ADS is regulated by CcpA, the protein that binds to the cre box and

mediates catabolite repression in gram-positive bacteria. Although the ADS regulation mechanism in *T. halophilus* was not clarified, it was estimated that the expression level of *arcA* in M3 was reduced because of the transposition of IS*Teha4* into the region that is essential for the transcription of *arc* operon genes. The reduced *arcA* expression levels of the other derivatives compared to that of the wild-type strain may be explained by the mRNA destabilization triggered by IS transposition due to enhanced exonuclease activity (27).

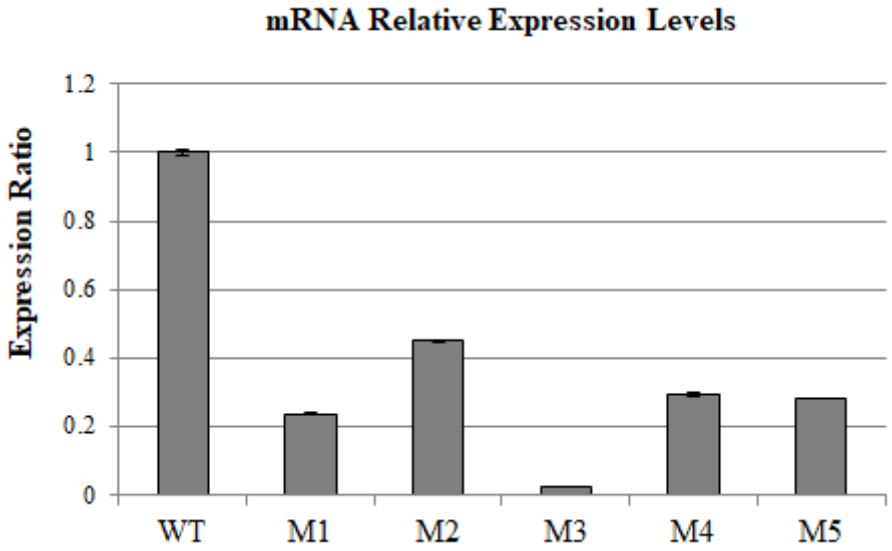


**Fig. 3:** Relative expression levels of *arcA* in the strains determined by quantitative real-time PCR. 16S rRNA gene was used as the reference. Data are expressed as the mean with error bars representing ± SD (n=3). WT: wild-type strain.

**Soy sauce fermentation with mutant strains**

To evaluate the derivatives as soy sauce fermentation starters, I performed small-scale fermentation. The five derivatives and wild-type strain of NBRC 12172 were cultured in soy sauce medium and inoculated in soy sauce mash. All derivatives, as well

as the wild-type strain, lowered the pH compared to the mash without starter cultures (Fig. 4A). After eight weeks of fermentation, the amino acid content was analyzed. All five derivatives did not convert arginine to ornithine, whereas the wild-type strain produced 11.6 mM ornithine and reduced approximately the same amounts of arginine compared to the mash with the other strains and without starter cultures (Fig. 4B). Lactic acid content was lower in the mash inoculated with the derivatives than that of the mash inoculated with the wild-type strain (Fig. 4C).

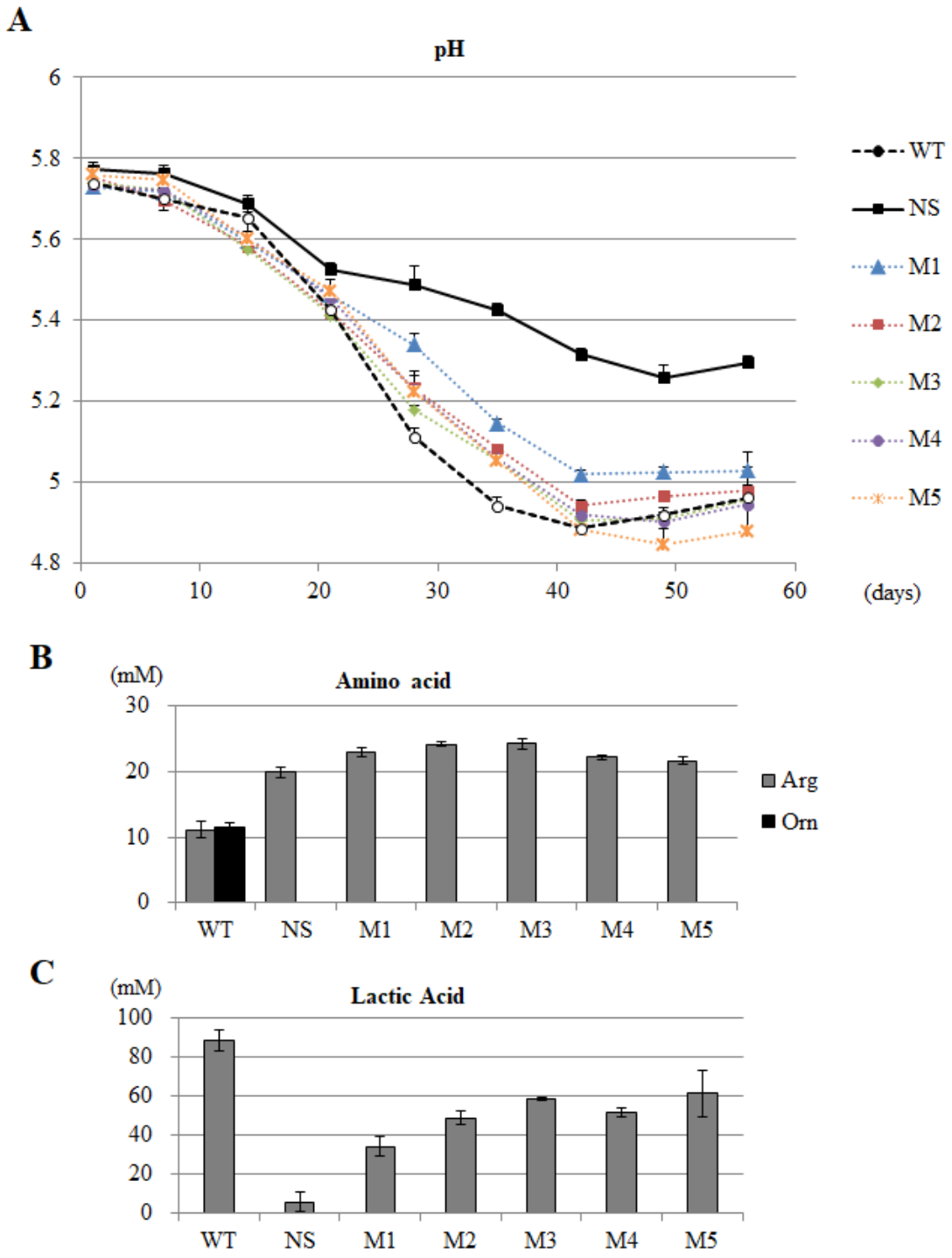


**Fig. 4:** pH transition of soy sauce mash treated with the strains (A) and arginine and ornithine content (B) and lactic acid content (C) in the soy sauce after eight weeks of fermentation. (A) Data are expressed as the mean with error bars representing +1 SD

(n=3). WT: wild-type strain. NS: Without starter cultures. (B) Gray bar and black bar indicate arginine and ornithine, respectively. Data are expressed as the mean with error bars representing ± SD. Ornithine contents were below the detection limit except for the samples treated with WT. (C) Data are expressed as the mean with error bars representing ± SD.

**Wild strains lacking arginine deiminase activity**

The DNA region around the *arc* operon of two wild strains lacking arginine deiminase activity isolated from soy sauce mash was amplified as described above. The amplified DNA fragments from these two strains, YA5 and A-30, had different lengths from that of NBRC 12172; the fragment was elongated in YA5 and shortened in A-30 (data not shown). DNA sequences of amplified fragments were analyzed (Fig. 5A). Compared to NBRC 12172, the *arc* operon genes of YA5 were completely preserved with the exception of six amino acids substitution on ArcA and two amino acids on ArcB. However, a 1522 bp element, sharing 1521 identical nucleotide bases with IS*Teha3* transposed in M1 and M4, was inserted into *argR2*. On the other hand, in A-30 *argR2* was not present in the region between *argR1* and *arcA*. The amino acid homology of ArcA between A-30 and NBRC 12172 was 80%, and *arcBCRD* was replaced by three ORFs encoding a putative acetyltransferase, arginyl-tRNA synthetase (*argS*) and a putative transposase.

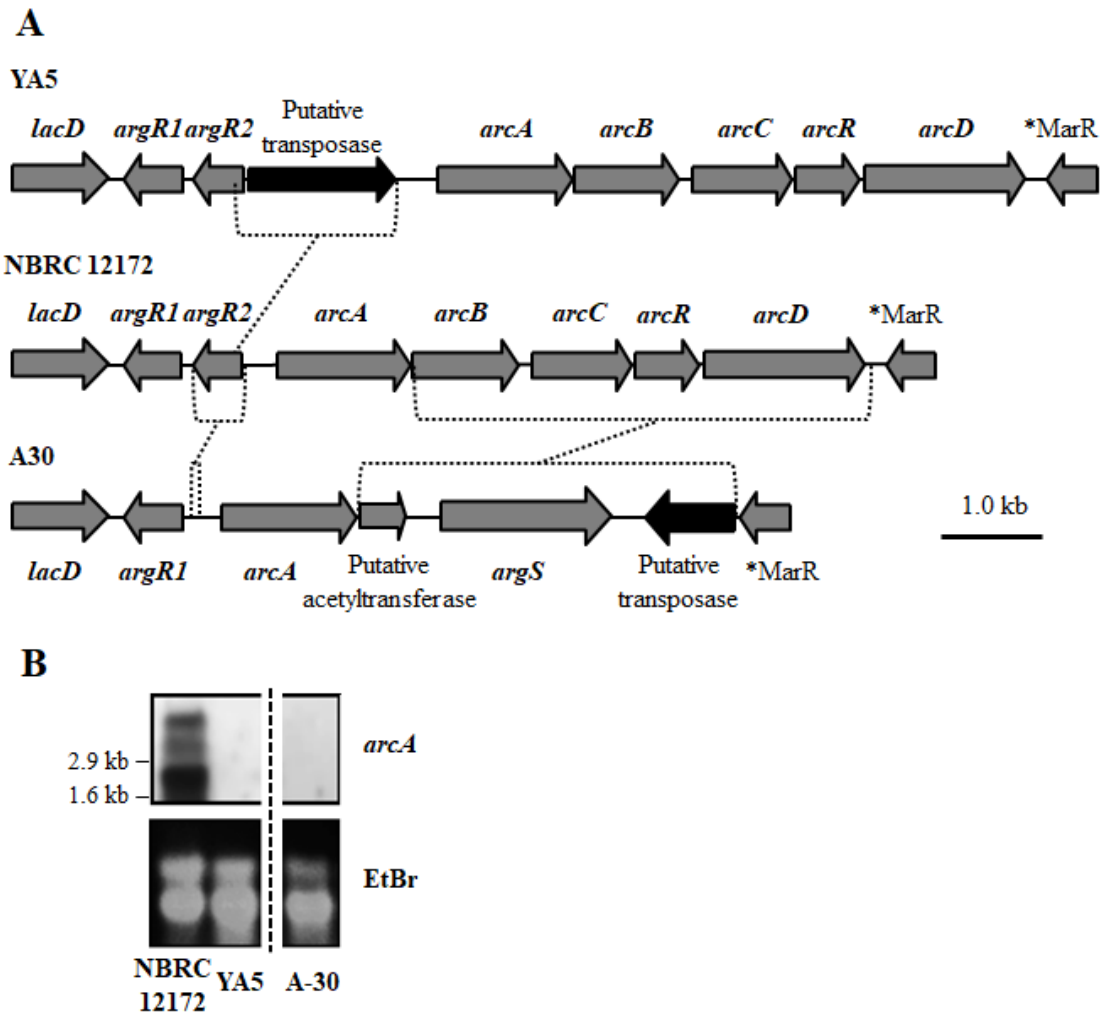


**Fig. 5:** Schematic representation of the locus of the genes between *lacD* and putative MarR family transcriptional regulator gene (A) and Northern blot analysis for *arcA* (B). (A) Broken lines represent the insertion or the replacement. *MarR represents a putative MarR family transcriptional regulator gene. (B) The result of Northern blot analysis is shown in the upper panel designated *arcA,* and the total RNA stained with ethidium bromide is shown in the lower panel designated EtBr. The RNA size on the membrane was estimated by the 16S rRNA (1.6 kb) and 23S rRNA (2.9 kb) patterns.

ArgR2 was identified as an essential activator of *arc* operon genes in

*Streptococcus pneumoniae* (28). Therefore, I assessed the *arcA* expression by Northern blot analysis, so that it could be detected even if it did not share a highly homologous nucleotide sequence with NBRC 12172, and found no *arcA* expression in YA5 and A-30 (Fig. 5B). NBRC 12172 produced three mRNAs of different lengths, which probably correspond to the transcripts of the entire or partial *arcABCRD* and are also reported in *E. faecalis* (21). A highly stable potential transcription termination hairpin (estimated minimum free energy: -250 kJ/mol) follows *arcD*, and weaker stem-loops are predicted after *arcB* and *arcR* (-113 and -26 kJ/mol, respectively), which probably act as partial terminators. Although the precise transcription start site and stop site are not clarified, the length of the three mRNA products from NBRC 12172 is not contradictory to the expected length of the fragments generated (data not shown).

EC is a topic of significant concern, especially in alcoholic beverages like wine and sake, in which urea mainly reacts with ethanol to make EC (29). The generation of non-urea-producing yeasts could minimize the accumulation of EC (30). However, the generation of yeasts or bacteria able to prevent EC accumulation in soy sauce has not been previously attempted. The main precursor of EC in soy sauce is citrulline, and here I provide an example of IS-mediated generation of noncitrulline-producing strains in *T. halophilus*, one of the main microorganism used in the production of soy sauce. DNA sequencing of the wild strains also suggested that the transposition of ISs into *argR2*, the putative activator of *arc* operon genes, disrupted the ADS, which highlighted the contribution of ISs to the natural evolution in this species.

*T. halophilus* shows physiological diversity not only in arginine deimination but also in other processes such as amino acid decarboxylation (14), carbohydrate

fermentation (31), organic acid metabolism (32) and aggregation (33). These traits severely affect the quality of fermented food products. For instance, histidine decarboxylation and tyrosine decarboxylation are responsible for histamine and tyramine accumulation, respectively (34, 35). Furthermore, bacterial bodies of *T. halophilus* can cause turbidity in soy sauce, but aggregated strains can be trapped during the squeezing process and do not flow out into soy sauce (36). The difficulty to acquire strains possessing favorable traits in all these aspects underscores the need to develop techniques for the modification of *T. halophilus*. Higuchi et al. prepared phage-insensitive strains, which is one of the few reports about modifying *T. halophilus*, but they did not describe the mutation mechanism or the genes in which the mutation occurred (37).

In this report, I identified three active IS*4* family ISs, IS*Teha3*, IS*Teha4* and IS*Teha5*. Transposases of the IS*4* family belong to the DDE transposase group, which displays three acidic residues: aspartic acid (D), aspartic acid (D) and glutamic acid (E). IS*Teha3*, IS*Teha4* and IS*Teha5* conserved these residues (data not shown). Furthermore, the main hallmark of this family's transposases is the Y-(2)-R-(3)-E-(6)-(K) motif (38). The three novel ISs displayed the complete YREK motif, suggesting that they are IS*4* family members.

The IS*4* family can be divided into seven subgroups based mainly on the amino acid sequence of transposases (38). IS*Teha3* and IS*Teha4* belong to the IS*Pepr1* subgroup, and IS*Teha5* belongs to IS*4Sa* subgroup. IR sequences of IS*Teha3* (5'-CTCAAGTTTCGCACA-3') and IS*Teha4* (5'-(C/T)TAAAACTTGAAA-3') match strongly with the consensus sequence of IS*Pepr1* subgroup IRs (5'-CTCAA+TTTCGCAG-3'). IS size (1522-1567 bp) and direct repeats (DRs) length

(7-9 bp) also show mostly typical features of the IS*Pepr1* subgroup (1,500-1,600 bp and 7-8 bp, respectively). IS*Teha4* duplicated 7 or 9 bp DRs in this study, and putative IS*Teha4* elements conserved in the genome of NBRC 12172 show 7 or 8 bp DRs (data not shown). IS*Teha3* in the genome also shows 6 or 7 bp DRs. The length of the DRs is generally fixed, but certain ISs are reported to generate atypical length of DRs (39).

The IRs sequence of IS*Teha5* (5'- CACTAGTGGTGCAT -3') matches strongly with the consensus sequence of the IS*4Sa* subgroup IRs (5'- CACTAGTGTCCGAT-3'). IS and DR length (1,385 bp and 9 bp) also supports this subgroup classification (1,150-1,750 bp and 8-10 bp in IS*4Sa* subgroup). The DR length is fixed to nine bp, including those conserved in the genome of NBRC 12172 (data not shown).

Among the 18 ISs deposited as IS*Pepr1* subgroup in the ISfinder database, only IS*2621* of *Deinococcus radiodurans* (AB001611) was demonstrated to possess transposition activity (40). Among the 41 ISs belonging to the IS*4Sa* subgroup, IS*4Bsu1* of *B. subtilis* (AB031551) and IS*5377* of *Bacillus stearothermophilus* (X67862) were demonstrated as active (41, 42). Members of the IS*4* family preferentially use a conservative (cut and paste) mechanism of transposition (1), but some examples, such as IS*4Bsu1* of *B. subtilis,* showed IS*4* family members using the replicative (copy and paste) mechanism (41). PCR amplification of the genomic region covering the ISs identified in this study supported the replicative mechanism of IS*Teha3*, IS*Teha4* and IS*Teha5* (data not shown).

The fact that all derivatives showed transposed ISs around the *arc* operon suggests that the inactivation of the ADS in *T. halophilus* is caused mainly by the transposition of transposable elements, rather than by the spontaneous mutations, such as base substitutions or deletions, associated with UV irradiation. However, although UV

irradiation has indeed been reported to induce the transposition of ISs (43), there is no direct evidence that UV irradiation actually caused the transposition in this case. It might have occurred spontaneously during the culturing before the irradiation. Further research is necessary to determine the induction factors of IS transposition.

NBRC 12172 possesses 71 copies of putative transposases in 19 different categories, except for the truncated fragments. IS*Teha1* and IS*Teha2* (AP012046) have been deposited in ISfinder, belonging to the IS*Lre2* family and the IS*6* family, respectively. However, the transposition activity of ISs in this species has not been reported previously. In tetragenococci, some reports demonstrated plasmid DNA transfer by conjugation (44, 45), but the transposon mutagenesis systems are still undeveloped. The transposon mutagenesis system is advantageous for the comprehensive characterization of gene functions that contribute to objective phenotypes. Hence, for the development of such a system in tetragenococci, the identification and characterization of active ISs are important. Other active ISs of *T. halophilus,* in addition to the three elements described here, are expected to be identified in the future.

## REFERENCES


1. Mahillon J, Chandler M. 1998. Insertion sequences. Microbiol Mol Biol Rev 62:725–774.
2. Baliga NS, Bonneau R, Facciotti MT, Pan M, Glusman G, Deutsch EW, Hung P. 2004. Genome sequence of *Haloarcula marismortui*: a halophilic archaeon from the Dead Sea. Genome Res 14:2221-2234.
3. Blattner FR, Plunkett G, Bloch CA, Perna NT, Burland V, Riley M, Gregor J. 1997. The complete genome sequence of *Escherichia coli* K-12. Science 277:1453-1462.
4. Tanizawa Y, Tohno M, Kaminuma E, Nakamura Y, Arita M. 2015. Complete genome sequence and analysis of *Lactobacillus hokkaidonensis* LOOC260 T, a psychrotrophic lactic acid bacterium isolated from silage. BMC Genomics 16:240.
5. Lee H, Doak TG, Popodi E, Foster PL, Tang H. 2016. Insertion sequence-caused large-scale rearrangements in the genome of *Escherichia coli*. Nucleic Acids Res 44:7109-7119.
6. Gury J, Barthelmebs L, Cavin JF. 2004. Random transposon mutagenesis of *Lactobacillus plantarum* by using the pGh9: ISS1 vector to clone genes involved in the regulation of phenolic acid metabolism. Arch Microbiol 182:337-345.
7. Maguin E, Prevost H, Ehrlich SD, Gruss A. 1996. Efficient insertional mutagenesis in lactococci and other gram-positive bacteria. J Bacteriol 178:931-935.
8. Nishimura I, Shiwa Y, Sato A, Oguma T, Yoshikawa H, Koyama Y. 2017.

Comparative genomics of *Tetragenococcus halophilus*. J Gen Appl Microbiol 63:369-372.

9. Satomi M, Furushita M, Oikawa H, Yano Y. 2011. Diversity of plasmids encoding histidine decarboxylase gene in *Tetragenococcus spp.* isolated from Japanese fish sauce. Int J Food Microbiol 148:60-65.

10. Tanasupawat S, Thongsanit J, Okada S, Komagata K. 2002. Lactic acid bacteria isolated from soy sauce mash in Thailand. J Gen Appl Microbiol 48:201-209.

11. Tanaka Y, Watanabe J, Mogi Y. 2012. Monitoring of the microbial communities involved in the soy sauce manufacturing process by PCR-denaturing gradient gel electrophoresis. Food Microbiol 31:100-106.

12. Amino Acid Analysis via the Hitachi Sensivate Elite Post-Column Reactor and LaChrom Elite HPLC (https://www.hitachi-hightech.com/file/ca/pdf/library/application/20100209-Hitachi_AAA_Sensivate_Application_Note_stw1.pdf)
Villar M, de Ruiz Holgado AP, Sanchez JJ, Trucco RE, Oliver G. 1985. Isolation and characterization of *Pediococcus halophilus* from salted anchovies (*Engraulis anchoita*). Appl Environ Microbiol 49:664-666.

13. Hamada T, Ishiyama T, Motai H. 1989. Continuous fermentation of soy sauce by immobilized cells of *Zygosaccharomyces rouxii* in an airlift reactor. Appl Microbiol Biotechnol 31:346-350.

14. Wakinaka T, Iwata S, Takeishi Y, Watanabe J, Mogi Y, Tsukioka Y, Shibata Y. 2019. Isolation of halophilic lactic acid bacteria possessing aspartate decarboxylase and application to fish sauce fermentation starter. Int J Food Microbiol 292:137–143.

15. Matsudo T, Aoki T, Abe K, Fukuta N, Higuchi T, Sasaki M, Uchida K. 1993. Determination of ethyl carbamate in soy sauce and its possible precursor. J Agric Food Chem 41:352-356.

16. Nakadai T. 2015. Isolation of soy sauce lactic acid bacteria from soy sauce mash and their breeding. J Jpn Soy Sauce Res Inst 41:358-376. (in Japanese)

17. Baur H, Luethi E, Stalon V, Mercenier A, Haas D. 1989. Sequence analysis and expression of the arginine-deiminase and carbamate-kinase genes of *Pseudomonas aeruginosa*. Eur J Biochem 179:53-60.

18. D'Hooghe I, Vander Wauven C, Michiels J, Tricot C, de Wilde P, Vanderleyden J, Stalon V. 1997. The arginine deiminase pathway in *Rhizobium etli*: DNA sequence analysis and functional study of the *arcABC* genes. J Bacteriol 179:7403-7409.

19. Divol B, Tonon T, Morichon S, Gindreau E, Lonvaud-Funel A. 2003. Molecular characterization of *Oenococcus oeni* genes encoding proteins involved in arginine transport. J Appl Microbiol 94:738-746.

20. Zúñiga M, del Carmen Miralles M, Pérez-Martínez G. 2002. The product of *arcR*, the sixth gene of the arc operon of *Lactobacillus sakei*, is essential for expression of the arginine deiminase pathway. Appl Environ Microbiol 68:6051-6058.

21. Barcelona-Andrés B, Marina A, Rubio V. 2002. Gene structure, organization, expression, and potential regulatory mechanisms of arginine catabolism in *Enterococcus faecalis*. J Bacteriol 184:6289-6300.

22. Siguier P, Pérochon J, Lestrade L, Mahillon J, Chandler M. 2006. ISfinder: the reference centre for bacterial insertion sequences. Nucleic Acids Res

34(suppl_1): D32-D36.

23. Gruber AR, Lorenz R, Bernhart SH, Neuböck R, Hofacker IL. 2008. The vienna RNA websuite. Nucleic Acids Res 36(suppl_2):W70-W74.

24. Siguier P, Varani A, Perochon J, Chandler M. 2012. Exploring bacterial insertion sequences with ISfinder: objectives, uses, and future developments. Mobile Genetic Elements p 91-103. Humana Press.

25. Maas WK. 1994. The arginine repressor of *Escherichia coli*. Microbiol Rev 58:631–640.

26. Weickert MJ, Chambliss GH. 1990. Site-directed mutagenesis of a catabolite repression operator sequence in *Bacillus subtilis*. Proc Natl Acad Sci USA 87:6238–6242.

27. Skorski P, Proux F, Cheraiti C, Dreyfus M, Hermann-Le Denmat S. 2007. The deleterious effect of an insertion sequence removing the last twenty percent of the essential *Escherichia coli rpsA* gene is due to mRNA destabilization, not protein truncation. J Bacteriol 189:6205-6212.

28. Schulz C, Gierok P, Petruschka L, Lalk M, Mäder U, Hammerschmidt S. 2014. Regulation of the arginine deiminase system by ArgR2 interferes with arginine metabolism and fitness of *Streptococcus pneumoniae*. MBio 5:e01858-14.

29. Zhao X, Du G, Zou H, Fu J, Zhou J, Chen J. 2013. Progress in preventing the accumulation of ethyl carbamate in alcoholic beverages. Trends Food Sci Technol 32:97-107.

30. Yoshiuchi K, Watanabe M, Nishimura A. 2000. Breeding of a non-urea producing sake yeast with killer character using a kar1-1 mutant as a killer donor. J Ind Microbiol Biotechnol 24:203-209.

31. Uchida K. 1982. Multiplicity in soy pediococci carbohydrate fermentation and its application for analysis of their flora. J Gen Appl Microbiol 28:215-223.

32. Kanbe C, Uchida K. 1982. Diversity in the metabolism of organic acids by *Pediococcus halophilus*. Agric Biol Chem 46:2357-2359.

33. Ueki T, Izawa T, Ohba K, Noda Y. 2000. Isolation and Characterization of Halotolerant Lactic Acid Bacteria with Flocculent. J Jpn Soy Sauce Res Inst 26:197-203. (in Japanese)

34. Satomi M, Furushita M, Oikawa H, Yoshikawa-Takahashi M, Yano Y, 2008. Analysis of a 30 kbp plasmid encoding histidine carboxylase gene in *Tetragenococcus halophilus* isolated from fish sauce. Int J Food Microbiol 126:202–209.

35. Satomi M, Shozen KI, Furutani A, Fukui Y, Kimura M, Yasuike M, Yano Y, 2014. Analysis of plasmids encoding the tyrosine decarboxylase gene in *Tetragenococcus halophilus* isolated from fish sauce. Fish Sci 804:849-858.

36. Ueki T, Izawa T, Ohba K, Noda Y. 2002. Mechanisms of floc formation by the halotolerant lactic acid bacteria with flocculent and its use in soy sauce brewing. J Jpn Soy Sauce Res Inst 28:105-110. (in Japanese)

37. Higuchi T, Uchida K, Abe K. 1999. Preparation of phage-insensitive strains of *Tetragenococcus halophila* and its application for soy sauce fermentation. Biosci Biotechnol Biochem 63:415-417.

38. De Palmenaer D, Siguier P, Mahillon J. 2008. IS 4 family goes genomic. BMC Evol Biol 8:18.

39. Hickman AB, Dyda F. 2015. Mechanisms of DNA Transposition. Microbiol Spectr 3: MDNA3-0034-2014.

40. Narumi I, Cherdchu K, Kitayama S, Watanabe H. 1997. The *Deinococcus radiodurans uvrA* gene: identification of mutation sites in two mitomycin-sensitive strains and the first discovery of insertion sequence element from deinobacteria. Gene 198:115-126.

41. Nagai T, Tran LSP, Inatsu Y, Itoh Y. 2000. A new IS*4* family insertion sequence, IS*4Bsu1*, responsible for genetic instability of poly-γ-glutamic acid production in *Bacillus subtilis*. J Bacteriol 182:2387-2392.

42. Xu K, He ZQ, Mao YM, Sheng RQ, Sheng ZJ. 1993. On two transposable elements from *Bacillus stearothermophilus*. Plasmid 29:1-9.

43. Eichenbaum Z, Livneh Z. 1998. UV light induces IS*10* transposition in *Escherichia coli*. Genetics 149:1173-1181.

44. Toda A, Kayahara H, Yasuhira H, Sekiguchi J. 1989. Conjugal Transfer of pIPSOl from *Enterococcus faecalis* to *Pediococcus halophilus*. Agric Biol Chem 53:3317-3318.

45. Benachour A, Flahaut S, Frère J, Novel G. 1996. Plasmid transfer by electroporation and conjugation in *Tetragenococcus* and *Pediococcus* genera and evidence of plasmid-linked metabolic traits. Curr Microbiol 32:188-194.

**SUMMARY**

*Tetragenococcus halophilus*, a halophilic lactic acid bacterium, is often used as a starter culture in the manufacturing of soy sauce. *T. halophilus* possesses an arginine deiminase system, which is responsible for the accumulation of citrulline, the main precursor of the potential carcinogen ethyl carbamate. In this study, I generated five derivatives lacking arginine deiminase activity from *T. halophilus* NBRC 12172 by UV irradiation. Using these derivatives as a fermentation starter prevented arginine deimination in soy sauce. DNA sequence analysis of the derivatives revealed that novel IS*4* family insertion sequences, designated IS*Teha3*, IS*Teha4* and IS*Teha5*, were transposed into the region around the arginine deiminase (*arc*) operon in the mutants. These insertion sequences contain a single open reading frame encoding a putative transposase and 13-15 bp inverted repeats at both termini, which are adjacent to 7-9 bp duplications of the target sequence. Investigation of wild strains isolated from soy sauce mash incapable of arginine deimination also indicated that insertion sequences are involved in the disruption of the arginine deiminase system in *T. halophilus*.

Insertion sequences play important roles in bacterial evolution and are frequently utilized in mutagenesis systems. However, the intrinsic insertion sequences of tetragenococci are not well characterized. Here, I identified three active insertion sequences of *T. halophilus* by transposition into the region around the *arc* operon. This report provides an example of insertion sequence-mediated generation and evolution of *T. halophilus* and primary information about their characteristics.

# CHAPTER III

## Studies on tetragenococcal bacteriophage susceptibility

## SECTION 1

### Ribitol-containing wall teichoic acid of *Tetragenococcus halophilus* is targeted by bacteriophage phiWJ7 as a binding receptor

*Tetragenococcus halophilus* is a Gram-positive, halophilic lactic acid bacterium that is used for the manufacturing of various salted foods, such as soy sauce and salted fish (1, 2). *T. halophilus* plays an important role in the lactic acid fermentation process of these products, and similar to cases in dairy products, bacteriophages (or "phages") have been regarded as serious threats in industry. Previously reported bacteriophages that attack *T. halophilus* have narrow host ranges and rarely infect different strains (3). Higuchi et al. successfully generated phage-insensitive mutants from *T. halophilus* D10, but the mechanisms that altered phage susceptibility were not revealed (4). Recently, CRISPR sequences were found in the genomes of *T. halophilus* and proposed as one of the defense systems against bacteriophages (5). However, the factors that determine the phage susceptibility of this species were not experimentally demonstrated.

Adsorption to host cells by bacteriophages is the first step that defines the host range. Host receptors on the cell surface are specifically recognized by their respective bacteriophages. Phage adsorption generally consists of a two-step process: a reversible binding phase and an irreversible binding phase (6). In the first step, bacteriophages reversibly adsorb to host cells, and they can still desorb from the cells and can move on the cell surface to search for an optimal site for irreversible binding. In the second step,

phages irreversibly attach to the host receptor, after which they cannot be separated from the host cells. Irreversible binding triggers phage genome ejection into the host cell, which is followed by a series of events for infection. Host receptors involved in reversible binding and irreversible binding are not always the same. For instance, λ phage that infects *Escherichia coli* targets the outer membrane protein OmpC for reversible binding and the maltose transporter protein LamB for irreversible binding (7). A few receptors of Gram-positive bacteria have been identified (8). Peptidoglycan is the main component of bacterial cell walls and is often involved in phage adsorption (9). Another important component of the cell walls in Gram-positive bacteria involved in phage adsorption is cell wall teichoic acid (WTA). In most cases, WTA consists of polymers of glycerol phosphate (Gro-P) or ribitol phosphate (Rbo-P) linked via phosphodiester bonds (called Gro-WTA and Rbo-WTA, respectively) and covalently linked to peptidoglycan. WTA is produced by many Gram-positive bacteria and usually has species- or strain-specific structural patterns both in main chain components and decoration residues (10, 11).

WTA biosynthesis genes are well understood in *Staphylococcus aureus*, namely, *tag* genes for Gro-WTA and *tar* genes for Rbo-WTA. To avoid confusion about the nomenclature, hereafter, I use '*tag*' for the genes needed for Gro-WTA biosynthesis and for the genes commonly needed for both Gro-WTA and Rbo-WTA synthesis and use '*tar*' for the genes required only for Rbo-WTA synthesis, following the policy of Xia & Peschel (12). WTA synthetic pathways in *S. aureus* are shown in Fig. 1. The structures and synthetic pathways of WTA in *T. halophilus* have not been studied to date.

In this section, I generated two phage-insensitive derivatives from *T. halophilus* WJ7 susceptible to the virulent phage phiWJ7. Both of the derivatives have mutations in

*tarL*, which is necessary for Rbo-WTA biosynthesis. The subsequent experiments in this section indicated that Rbo-WTA of WJ7 is a binding receptor for phiWJ7. The information provided here can represent a basis for dissecting the mechanisms of host-phage interactions of tetragenococci.

## Materials and methods

### Bacterial strains, bacteriophages, media and culture conditions

*T. halophilus* WJ7 was kept in my laboratory (13). The derivatives derived from WJ7 were obtained as described below. Bacteriophages lytic for WJ7 were isolated from soy sauce mash using WJ7 as the host strain. All bacterial strains and bacteriophages used in this study are summarized in Table 1. *T. halophilus* was cultured in MRS-10 or LA13 medium. MRS-10 is Lactobacilli MRS Broth (Difco, Detroit, MI) supplemented with 10% NaCl. LA13 medium contained 1% polypeptone, 0.4% yeast extract, 1% $KH_2PO_4$, 12% NaCl, 0.5% glucose, 5% soy sauce (Yamasa, Choshi, Japan), and 1.5% agar for agar plates (14). Liquid media were incubated at 30 °C without stirring, and agar plates were incubated at the same temperature with an AnaeroPack (Mitsubishi Gas Chemical, Tokyo, Japan) in a hermetically sealed box.

**Table 1. Bacterial strains and bacteriophages used in this study.**

| | Description and genotype | Source or Reference |
|---|---|---|
| *Tetragenococcus halophilus* | | |
| NBRC 12172 | Insensitive for phiWJ7. | National Bio Resource Center |
| YA5 | Insensitive for phiWJ7. | (22) |
| YA163 | Insensitive for phiWJ7. | (40) |
| YG2 | Insensitive for phiWJ7. | (40) |
| WJ7 | Sensitive for phiWJ7. | (40) |
| WJ7R1 | Insensitive for phiWJ7. *tarL*::IS*Teha3* | WJ7 derivative generated in this study. |
| WJ7R2 | Insensitive for phiWJ7. *tarL*::IS*Teha4* | WJ7 derivative generated in this study. |
| WJ7R3 | Insensitive for phiWJ7. *tarL*::IS*Teha4* | WJ7 derivative generated in this study. |
| WJ7R4 | Insensitive for phiWJ7. *tarJ*.A305G | WJ7 derivative generated in this study. |
| WJ7R5 | Insensitive for phiWJ7. *tarI*::IS*Teha3* | WJ7 derivative generated in this study. |
| WJ7R6 | Insensitive for phiWJ7. *tarJ*::IS*Teha4* | WJ7 derivative generated in this study. |
| WJ7R7 | Insensitive for phiWJ7. *tarI*::IS*Teha4* | WJ7 derivative generated in this study. |

| | | |
|---|---|---|
| WJ7R8 | Insensitive for phiWJ7. *tarJ*::IS*Teha4* | WJ7 derivative generated in this study. |
| WJ7R9 | Insensitive for phiWJ7. *tarL*::IS*Teha4* | WJ7 derivative generated in this study. |
| WJ7R10 | Insensitive for phiWJ7. *tarJ*::IS*Teha4* | WJ7 derivative generated in this study. |
| WJ7R11 | Insensitive for phiWJ7. *tarI*::IS*Teha4* | WJ7 derivative generated in this study. |
| WJ7R12 | Insensitive for phiWJ7. | WJ7 derivative generated in this study. |
| WJ7R13 | Insensitive for phiWJ7. *tarL*::IS*Teha4* | WJ7 derivative generated in this study. |
| WJ7R14 | Insensitive for phiWJ7. *tarL*::IS*Teha4* | WJ7 derivative generated in this study. |
| WJ7R15 | Insensitive for phiWJ7. *tarL*::IS*Teha4* | WJ7 derivative generated in this study. |
| WJ7R16 | Insensitive for phiWJ7. *tarI*::IS*Teha4* | WJ7 derivative generated in this study. |
| WJ7R17 | Insensitive for phiWJ7. *tarL*::IS*Teha4* | WJ7 derivative generated in this study. |
| WJ7R18 | Insensitive for phiWJ7. *tarJ.993_tarL.35*del | WJ7 derivative generated in this study. |
| WJ7R19 | Insensitive for phiWJ7. *tarJ*::IS*Teha4* | WJ7 derivative generated in this study. |
| WJ7R20 | Insensitive for phiWJ7. *tarJ*::IS*Teha4* | WJ7 derivative generated in this study. |
| WJ7R21 | Insensitive for phiWJ7. *tarJ*::IS*Teha4* | WJ7 derivative generated in this study. |
| WJ7R22 | Insensitive for phiWJ7. *tarL*::IS*Teha4* | WJ7 derivative generated in this study. |

| | | |
|---|---|---|
| WJ7R23 | Insensitive for phiWJ7. *tarL*::IS*Teha4* | WJ7 derivative generated in this study. |
| WJ7R24 | Insensitive for phiWJ7. | WJ7 derivative generated in this study. |
| WJ7R25 | Insensitive for phiWJ7. *tarI*::IS*Teha4* | WJ7 derivative generated in this study. |
| WJ7R26 | Insensitive for phiWJ7. *tarI*::IS*Teha4* | WJ7 derivative generated in this study. |
| WJ7R27 | Insensitive for phiWJ7. *tarL*::IS*Teha5* | WJ7 derivative generated in this study. |
| Bacteriophage | | |
| phiWJ7 | Lytic for WJ7. Not lytic for WJ7R1 and WJ7R2. | Isolated from soy sauce mash. |
| phiWJ7_2 | Lytic for WJ7, WJ7R1, and WJ7R2. | Isolated from soy sauce mash. |
| phiWJ7_3 | Lytic for WJ7, WJ7R1, and WJ7R2. | Isolated from soy sauce mash. |

**Manipulation of bacteriophages and generation of phage-insensitive derivatives**

Uchida & Kanbe developed a detection method for tetragenococcal phages by spreading host-phage mixtures on agar plates with a cell spreader, since the usual soft-agar overlay technique was not successful (3). I used this method with a little modification. Before the plaque forming assay, the indicator strains cultured in MRS-10 to the stationary phase were sonicated by a sonicator (AUS-01; CHO-ONPA KOGYO, Tokyo, Japan) for 30 sec to produce homogenous cell suspensions because some strains of *T. halophilus* form cell clusters (13). The suspension was diluted 6 times with 10% saline, and 600 μl of the diluted suspension was mixed with the phage specimen. The host-phage mixture was spread on the whole surface of an LA13 plate (diameter 85 mm) by tilting the plate without using a cell spreader to prevent traces of a cell spreader from disturbing plaque detection. The plate was dried on a clean bench and incubated for three days to form plaques. For the phage spot assay, the host suspension was spread in advance, and 10 μl of phage specimen was spotted afterward. If necessary, phages were collected from plaques with 10% saline, and the lysate was filtered through a polyethersulfone membrane filter (0.2 μm; Advantec, Tokyo, Japan) after removal of cell debris by centrifugation. The lysate was stored at -80 °C as a stock suspension with 16% (v/v) glycerol. To obtain spontaneous phage-insensitive derivatives, the culture of the parental strain (approximately $10^6$ cfu) was spread with $>10^7$ pfu of phages on LA13 plates, and the surviving colonies were isolated.

**Scanning electron microscopy**

WJ7 was mixed with phiWJ7, and the mixture was incubated for 1 h at room temperature. Fixation was performed by immersing the specimens in 2.5% glutaraldehyde. Fixed specimens were stepwise dehydrated in a series of ethanol

solutions (50–70–90–100–100%) in 15 min steps. Dehydrated specimens were lyophilized in *tert*-butyl alcohol. Afterward, the specimens were coated with a thin Pt layer using an autofine coater JEC-3000FC (JEOL, Ltd., Tokyo, Japan) and observed with a JSM-IT500HR InTouchScope™ scanning electron microscope (JEOL, Ltd.). Scanning electron microscopy was performed at 15 kV, and the samples were observed at a working distance of 11.0 mm.

**DNA preparation and genome sequencing**

Genomic DNA from *T. halophilus* WJ7R1 and WJ7R2 was isolated using the DNeasy PowerSoil Pro Kit (QIAGEN, Hilden, Germany) and QIAcube, an automated system (QIAGEN). Genomic DNA from bacteriophage phiWJ7 was isolated using the Phage DNA Isolation Kit (Norgen Biotek, Thorold, Canada). The quantity and purity of the genomic DNA were assessed using a Qubit dsDNA BR Assay Kit (Thermo Fisher Scientific, Waltham, MA) and NanoDrop 1000 spectrophotometer (Thermo Fisher Scientific). A genomic DNA library was prepared using the Illumina Nextera DNA Flex Library Prep Kit (Illumina, San Diego, CA) according to the manufacturer's instructions. Whole-genome sequencing of WJ7R1, WJ7R2, and phiWJ7 was performed using the Illumina MiSeq sequencing platform with a paired-end sequencing strategy (2 × 300 bp). Adapter sequences and low-quality regions in the Illumina reads were trimmed using Trim Galore! v.0.6.4 with default parameters (https://www.bioinformatics.babraham.ac.uk/projects/trim_galore/).

**Genome mapping analysis and mutation search of the derivatives**

The previously published genome sequence of the wild-type strain *T. halophilus* WJ7 (GenBank accession numbers: BLRM01000001-BLRM01000113) was used as the reference sequence for the genome mapping analysis (5). The Illumina

sequence reads of these strains were mapped to the reference sequence using BWA with default parameters (16). All single nucleotide polymorphisms (SNPs) and indels were detected using the Genome Analysis Toolkit (GATK) (17, 18). To detect the transposon insertion site of adapted genomes, breseq v.0.31.0 was used with default parameters (19). To ascertain the mutations detected in the adapted strain, the DNA regions were amplified from genomic DNA of WJ7, WJ7R1, and WJ7R2 using the primers WJ7contig68 and asnS (Table 2) with DNA polymerase KOD FX Neo (Toyobo, Osaka, Japan) under the optimal conditions recommended by the manufacturer. The PCR products were purified using the Wizard SV Gel and PCR Clean-Up System (Promega, Madison, WI), and the resulting DNA fragment was analyzed by a commercial DNA sequencing service (Fasmac, Atsugi, Japan/Eurofins Genomics, Tokyo, Japan). The primer sets tagOf-tagOr, mnaAf-mnaAr, tagGHDr-tagGHDf, tagABr-tagABf, tagFr-tagFf, and asnS-tarIJLr were used to amplify the DNA region covering WTA synthesis genes to detect the IS insertion in the additionally acquired derivatives WJ7R3-WJ7R27 (Table 2, Fig. 4B). If necessary, the resulting DNA fragment was analyzed by a DNA sequencing service (Fasmac /Eurofins Genomics).

**Table 2. Primers list.**

| Primer name | Sequence (5'→3') |
|---|---|
| WJ7contig68 | GAGGAACTACATCATAATTAAATAACTCGC |
| asnS | CGTTTATTGAATCGGATTTATCCG |
| tagOf | TGAATGCTTCGATGGAAGAG |
| tagOr | TCCCATTCGGAATCGC |
| mnaAf | GGCAAAGACCTAGATTCTATCCG |
| mnaAr | CAATGCTTGAAAGTCAATCGTC |
| tagGHDr | GCGTCGAACTTGCGG |
| tagGHDf | GGTTTAGACGTATGGGAACATGC |
| tagABr | TCTTCTGATTGGTTCTTGTCACTC |
| tagABf | AGGTGAATATCGCTCAAGGG |
| tagFr | GCCATTCATCGCCTAACTG |
| tagFf | CAGCGCCACTGGACAC |
| tarIJLr | TCGTAACCTTGTAGCCTATCGG |

**De novo assembly of phage genomes**

To remove the contaminated host genome sequence, read data were mapped onto the WJ7 genome (17, 18). Unmapped read pairs were collected and used for de novo assembly. De novo assembly was performed using SPAdes v. 3.13.0 (20). Gene detection of the draft genome assemblies was performed using the DDBJ Fast Annotation and Submission Tool with default settings (21). The resulting assemblies were used for further comparative genome analysis.

**WTA extraction and chemical analysis**

Cell walls of *T. halophilus* were prepared as described previously (13) with some modifications. The cells were grown to the stationary phase in MRS-10 medium and harvested by centrifugation (8,000 × *g*, 5 min, 4°C). The cell pellets were washed with water, resuspended in 4% sodium dodecyl sulfate, boiled for 30 min, and incubated at room temperature overnight. Then, the suspension was boiled again for 10 min, and the pellets were collected by centrifugation, washed four times with water, and treated with DNase, RNase, and trypsin. After thorough washing with water, cell walls were pelleted by centrifugation and lyophilized. WTA was extracted by following the procedure of Bron et al (22). Briefly, cell walls were treated with 10% TCA, and released WTA was precipitated by the addition of three volumes of ethanol for 24 h at 4 °C. WTA was collected by centrifugation, washed with 70% ethanol twice, and lyophilized. To extract Rbo and Gro, 50 mg of WTA was hydrolyzed in 6 M HCl at 100 °C for 3 h and neutralized with 4 M NaOH. As an internal standard, 20 μl of a 1,000 ppm solution of [1,1,2,3,3-$D_5$] glycerol (Cambridge Isotope Laboratories, Inc., Tewksbury, MA) was added to 200 μl of the neutralized hydrolysate. Samples were derivatized with benzoyl chloride according to the procedure of Bornø et al (23). Derivatized Rbo and Gro in the hydrolysates were analyzed by LC/MS. LC was performed on an ACQUITY UPLC H-Class (Waters Corporation, Milford, MA). An ACQUITY UPLC BEH C18 column (2.1x100 mm; Waters Corporation) was used at room temperature. Milli-Q water containing 10 mM ammonium formate (pH 3.5) was used as mobile phase A, and acetonitrile was used as mobile phase B. A gradient was employed starting at 60% B and increasing to 90% within 7 min and re-equilibrated at 60% B for 4.5 min followed by column washing at 90% B for 3 min. The flow rate was

set at 0.3 ml/min. Three microliters of the sample was injected. MS analysis was performed on a Xevo G2-XS Q-TOF MS (Waters Corporation). Electrospray ionization was employed at positive polarity at the following parameter settings: capillary voltage 2.0 kV, sampling cone voltage 40 V, source temperature 120 °C, and desolvation gas temperature 450 °C. The mass detection range was from *m/z* 150 to 1,000.

**Bacteriophage adsorption assay**

Phage adsorption by cell walls was measured according to the method of Baptista et al. (24). Cell walls were prepared as described above and resuspended at 10 μg/ml. Phages were mixed with cell walls and incubated at 30 °C for 10 min. Control mixtures without cell walls were used to confirm the phage input in the experiment. To assess total adsorption, the mixture was centrifuged at 6,000 × *g* for 5 min at 4 °C, and the supernatant was assayed for plaques using WJ7 as the indicator strain. Free phages (unbound phages) in the supernatants after centrifugation were measured. To assess irreversible adsorption, the mixture was diluted 100-fold in 10% NaCl, vortexed for 5 s, equilibrated for 5 min at room temperature, and centrifuged. Free phages (unbound and reversibly bound phages) in the supernatants were enumerated. For statistical analysis, the data were assessed by one-way ANOVA followed by post hoc Tukey's multiple comparison test using R software (version 3.6.0; www.r-project.org). Statistical significance was considered at $p < 0.05$.

**Bioinformatics and data availability**

The DNA and amino acid sequences were analyzed using Blast. Illumina sequence reads of WJ7R1 WJ7R2 and phiWJ7 were deposited in the DDBJ Sequence Read Archive. The DRA accession numbers for WJ7R1, WJ7R2, and phiWJ7 are DRR311734, DRR311735 and DRR311536, respectively. Other sequence data were

deposited in the DDBJ/EMBL/GenBank databases, with accession numbers LC638494-LC638497 and LC640109-LC640133. The phylogenetic tree was constructed based on the alignment of the amino acid sequences from the major capsid protein of phiWJ7 and other *Rountreeviridae* phages. Their sequence data are available in the NCBI database. The amino acid sequences were aligned with Clustal X (version 2.1), and the neighbor-joining phylogenetic tree was drawn by NJplot (version 2.3) with bootstrap analysis (1000 replicates).

## Results and discussion

### phiWJ7 is a member of the *Rountreeviridae*

PhiWJ7 lytic for *T. halophilus* WJ7 was isolated from soy sauce mash. The complete genome sequence of phiWJ7 was determined to be 17,405 bp in size with an average G+C content of 32.90% (Accession number: LC644557). The genome contains 21 possible ORFs and more than 100 bp inverted terminal repeats (Fig. 2A). The ORFs whose functions were estimated were all arranged in the same direction and exhibited clustering of related functional genes. Some ORFs of phiWJ7 show similarity with genes of staphylococcal phages, such as SLPW, Andhra, SA03-CTH2, and PSa3. These phages belonged to the *Podoviridae* family of the *Caudovirales* order and have linear double-stranded DNA genomes of 17,511–18,546 bp with 19–20 ORFs and long inverted terminal repeats (at least 81 bp) (25, 26, 27). Most staphylococcal phages characterized thus far belong to the order *Caudovirales* and had been classified into three families with different genome sizes: *Podoviridae* (16–18 kb), *Siphoviridae* (39–43 kb), and *Myoviridae* (120–140 kb) (28). Very recently, three new families, *Salasmaviridae*, *Rountreeviridae*, and *Guelinviridae* were established (29). They

include the phages previously assigned to the *Podoviridae* family. *Rountreeviridae* is mainly composed of *Staphylococcus*- and *Enterococcus*-infecting phages with genomes between 17 and 19 kb in size. The genome size and protein sequence homologies suggest the classification of phiWJ7 into *Rountreeviridae*. I aligned the sequences of major capsid protein from phiWJ7 and other *Rountreeviridae* phages and compared the phylogenetic relationships. The result confirmed phiWJ7 classification into *Rountreeviridae* (Fig. 2B). Scanning electron micrograph (SEM) images of phiWJ7 bound to WJ7 displayed an isometric capsid of approximately 44 nm in diameter and hardly observable tails, which are the typical morphological characteristics of *Rountreeviridae* (Fig. 2C).

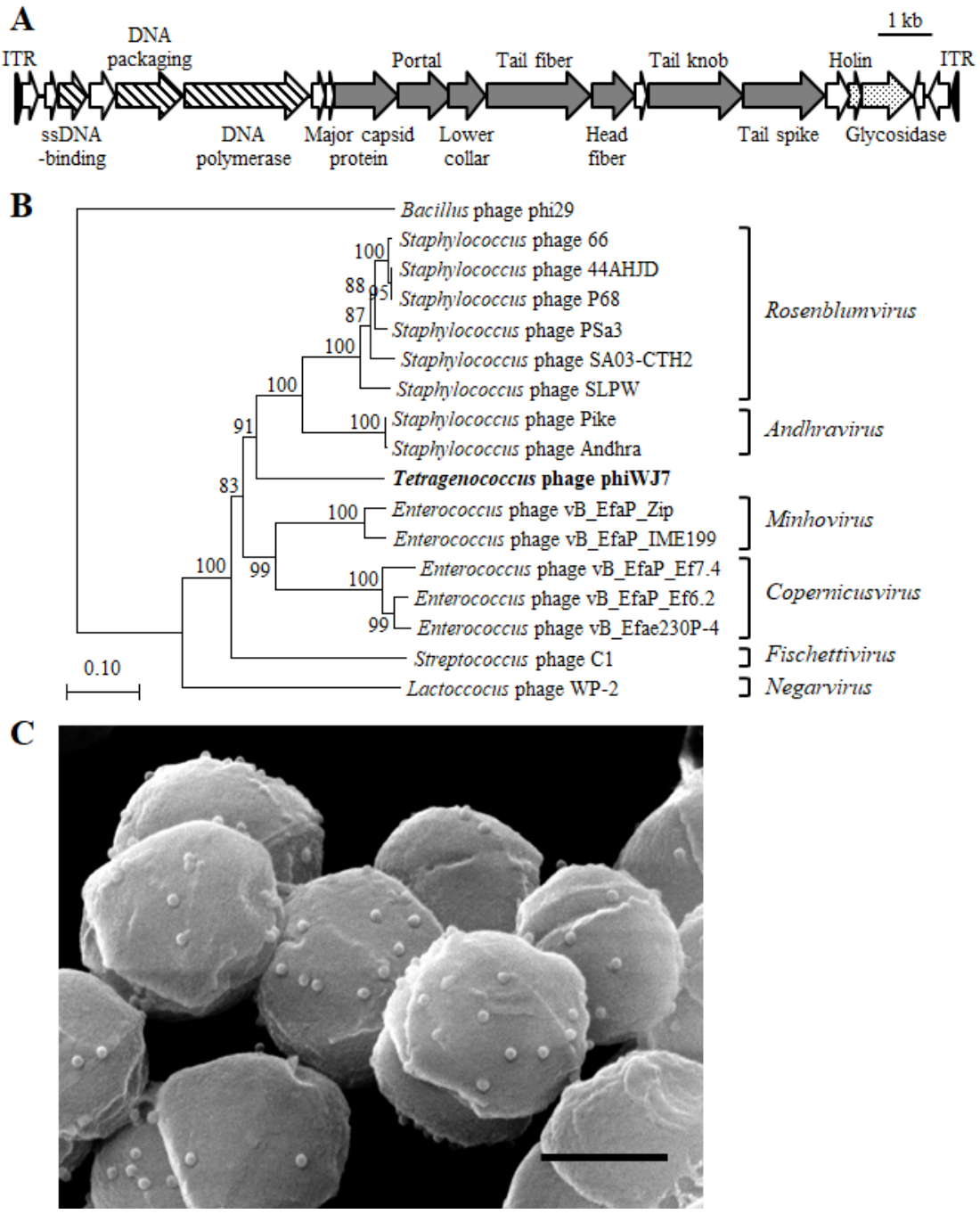


**Fig. 2:** Characterization of phiWJ7. (A) Genetic map of the phiWJ7 genome. Arrows indicate the possible ORFs. Functional groups are categorized into patterns (striped: DNA replication and packaging, gray-shaded: structural proteins, dotted: bacterial lysis, blanked: unknown). ITR indicates inverted terminal repeats and is marked by black triangles. (B) Phylogeny of phiWJ7 and other *Rountreeviridae* phages based on the

amino acid sequence relatedness of major capsid protein. The names of the six genera belonging to the family *Rountreeviridae* are denoted on the right side of each phage. *Bacillus* phage phi29 belongs to the family *Salasmaviridae*. (C) SEM image of WJ7 treated with phiWJ7. Black bar represents 500 nm.

**Generation of phiWJ7-insensitive derivatives and other bacteriophages lytic for WJ7**

Spontaneous phiWJ7-insensitive derivatives WJ7R1 and WJ7R2 were selected from the parental strain WJ7 as colonies growing in the presence of phiWJ7 on LA13 agar plates. PhiWJ7 forms clear plaques to WJ7, but even with $10^9$ pfu phiWJ7, no plaques were formed to these derivatives (Fig. 3). However, they were infected with other bacteriophages, phiWJ7_2 and phiWJ7_3, which were also isolated from soy sauce mash. PhiWJ7_2 made similar plaques to phiWJ7 in clearance and size and infected WJ7 and its derivatives. Interestingly, phiWJ7_3 formed a smaller size and a lower number of plaques to WJ7 than to WJ7R1 and WJ7R2, which suggests that the derivatives were more vulnerable to phiWJ7_3 instead of acquiring resistance to phiWJ7. According to the genome sequence, phiWJ7_2 belongs to the family *Siphoviridae* (unpublished data), and phiWJ7_3 is not characterized yet.

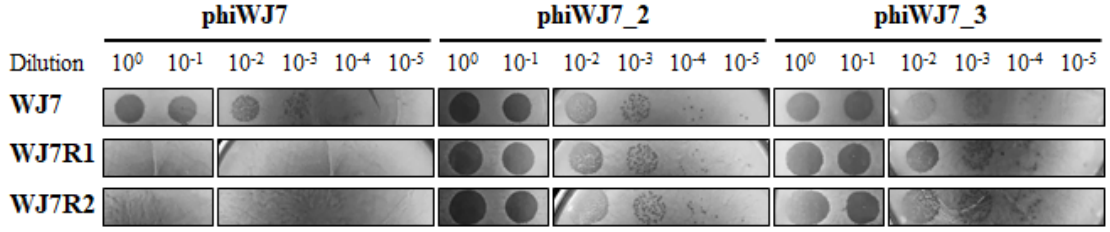


**Fig. 3:** Phage susceptibility of the host strains toward phiWJ7, phiWJ7_2, and

phiWJ7_3. Each phage specimen was diluted and spotted on each host strain indicated on the left side of the panel. The various dilutions of a phage were spotted on the same plate of a strain, though it is divided.

**Detection of mutational and IS insertion sites in the two adapted genomes**

To investigate the mechanism that altered the phage susceptibility of the derivatives, whole-genome sequences of WJ7R1 and WJ7R2 were analyzed, and the mutation sites of the derivatives were clarified by genome mapping analysis. A single base insertion was commonly observed in both derivatives but not in ORFs (178 bp upstream of an ORF; locus tag WJ7_08810). I considered that this mutation had presumably occurred during the culture of the parent strain and was unlikely to contribute to the phenotypical change. Only one other mutation was found in each derivative. Both WJ7R1 and WJ7R2 contained a transposed insertion sequence (IS) in the same ORF (WJ7_16330); IS*Teha3* in WJ7R1 and IS*Teha4* in WJ7R2 (Fig. 4A). In a previous study, I found that the transposition of these IS*4* family ISs plays an important role in the disruption of the arginine deiminase system in *T. halophilus* NBRC 12172 (15). Transposition activities of the ISs in WJ7 were also demonstrated here, and they targeted a TA-rich 7 bp sequence on the ORF, which is a typical feature of these ISs. The amino acid sequence of this mutated ORF showed 68% similarity with poly(ribitol phosphate) polymerase (TarL) of *S. aureus*, and two ORFs located upstream of *tarL* also showed high amino acid similarity with ribitol-5-phosphate cytidylyltransferase (TarI) and ribulose 5-phosphate reductase (TarJ) of *S. aureus*. TarIJL is responsible for the biosynthesis of Rbo-WTA (Fig. 1).

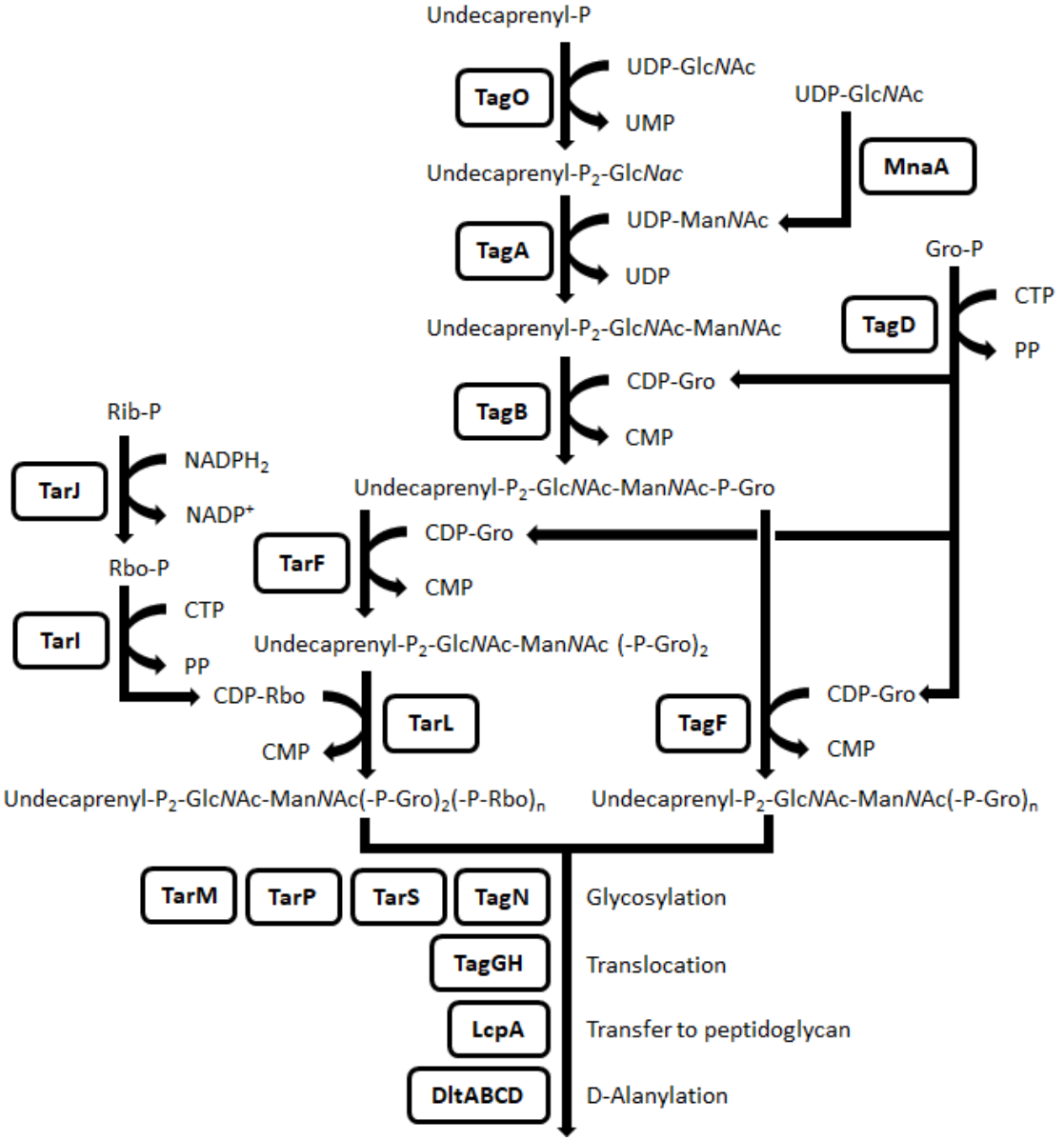


**Fig. 1:** Biosynthetic pathways of Rbo- and Gro-WTA in *S. aureus,* adapted from previous reports (30, 31, 32, 33). WTA synthesis is initiated with consecutive transfer of *N*-acetylglucosamine (Glc*N*Ac) phosphate and *N*-acetylmannosamine (Man*N*Ac) to the lipid carrier undecaprenylphosphate by TagO and TagA, on the cytoplasmic side of the cell membrane. UDP-Man*N*Ac is generated from UDP-Glc*N*Ac by MnaA. In Gro-WTA synthesis, the primase TagB adds the first Gro-P to the disaccharide unit and the polymerase TagF extends the Gro-P chain. The precursor CDP-glycerol is generated by

TagD. In Rbo-WTA synthesis, the TagB reaction is followed by the addition of only one Gro-P unit by TarF. Subsequently, TarL polymerizes Rbo-P, and TarIJ is responsible for the generation of the precursor CDP-ribitol. Finally, the complete WTA polymers are translocated to the extracellular space by TagGH, and are linked to the *N*-acetylmuramic acid residue of peptidoglycan by Lcp family proteins, primarily LcpA. The basic WTA polymers can be decorated with glycosyl residues and/or D-alanyl moieties. (Rib-P, ribulose 5-phosphate; Rbo, ribitol; Gro, glycerol; P, phosphate; PP, diphosphate.)

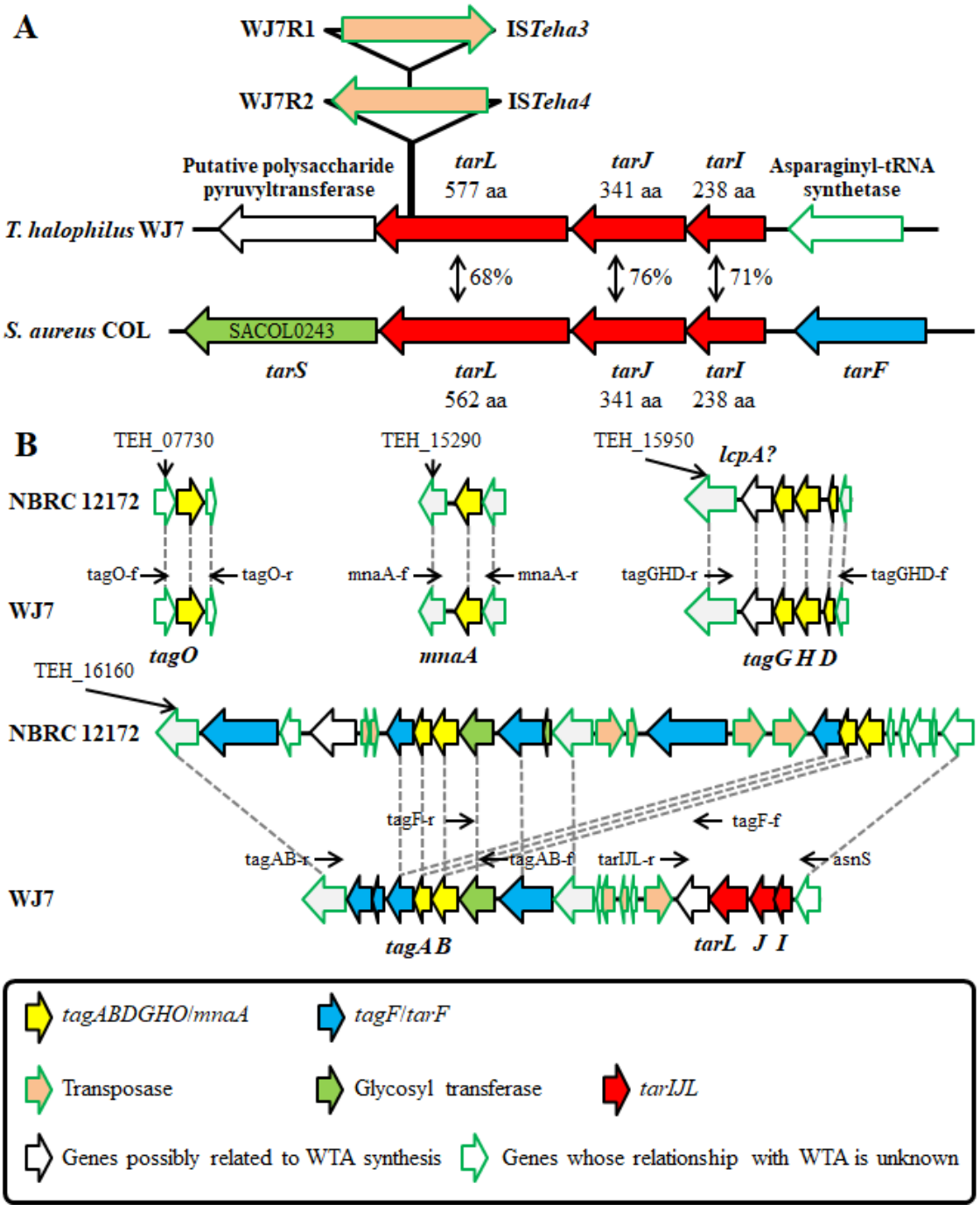


**Fig. 4:** WTA synthesis genes of WJ7. (A) Schematic representation of *tarIJL* in *T. halophilus* WJ7 and *S. aureus* COL, and the location of ISs transposed into *tarL* in WJ7R1 and WJ7R2. Percentage shows the amino acid identities between *T. halophilus* and *S. aureus*. The derivative names and IS names are indicated on the left side and right side of the arrows that represent the putative transposase, respectively. (B)

Chromosomal organization of the four loci harboring the genes involved in WTA synthesis in the NBRC 12172 and WJ7 genomes. Homologous ORFs with amino acid sequence identities above 90% are connected with gray dotted lines, except for transposases. The black arrows above each ORF indicate the position at which the primers were designed.

### *In silico* analysis of the WTA biosynthesis genes in *T. halophilus*

Since IS transpositions independently occurred into *tarL* in the two phage-insensitive derivatives, it is most likely that the disruption of the Rbo-WTA synthetic pathway altered phage susceptibility. However, there has not been systematic consideration of WTA synthesis genes in *T. halophilus* before. Therefore, I first carried out *in silico* analysis of the WTA biosynthetic pathways in *T. halophilus* NBRC 12172, whose complete genome was deposited in the DDBJ database (Accession number: AP012046). The genes involved in WTA synthesis were searched by BLASTP using the amino acid sequences of the genes in *S. aureus* COL as queries. As a result, the genome of NBRC 12172 contains homologs of *tagO*, *mnaA*, *tagADB*, *tarF*, and *tagGH*, which are scattered over four chromosomal loci (Fig. 4B). There are five homologs of *tarF*, one of which might be *tagF* since *tarF* and *tagF* are homologous to each other (34). NBRC 12172 possesses three Lcp family proteins, and one of them is assumed to be mainly responsible for the transfer of WTA to peptidoglycan; TEH_15960, adjoining *tagG*, is the most likely candidate. Thus, it was estimated that NBRC 12172 possesses the gene set for Gro-WTA synthesis. However, it does not contain *tarIJL* required for Rbo-WTA synthesis. The counterparts of these genes were searched in the genome of WJ7. WJ7 was also estimated to contain the gene set for Gro-WTA synthesis, and *tarIJL*

was located in the same chromosomal locus as *tagAB* and *tagF*/*tarF* (Fig. 4B). In conclusion, it was estimated that WJ7 is endowed with gene sets for both Gro- and Rbo-WTA synthesis. I compared the *tagAB*-containing locus with three other strains, YA5, YA163, and YG2, for which draft genome sequences are available (5). The three strains did not contain *tarIJL* in their genomes, similar to NBRC 12172, and all of them were insusceptible to phiWJ7 (data not shown).

**Alditol detection from WTA of WJ7 and WJ7R1**

Since WJ7 possessed gene sets for Gro- and Rbo-WTA synthesis and the Rbo-WTA synthesis gene was disrupted in WJ7R1, I assessed the presence of Rbo and Gro in extracted WTA from WJ7 and WJ7R1. WTA extracted from the cell walls by trichloroacetic acid (TCA) was hydrolyzed and derivatized with benzoyl chloride followed by analysis with liquid chromatography (LC)/mass spectrometry (MS). Derivatized Rbo and Gro were detected as ammonium adducts, and their exact masses were *m/z* 422.16 and 690.23, respectively. The derivatization efficiencies of the samples were normalized by comparing the peak intensities of $D_5$-glycerol. Extracted ion chromatograms of *m/z* 690.23 showed a clear peak only in the hydrolysate sample of WJ7 at the same elution time corresponding to the standard Rbo peak (Fig. 5). I also confirmed that extracted ion chromatograms of *m/z* 422.16 showed clear peaks with almost the same intensities in both the WJ7 and WJ7R1 samples at the elution time of standard Gro. These results suggest that WJ7 produces Rbo-WTA, but the phage-insensitive derivative WJ7R1 does not, while both strains produce Gro-WTA at almost the same level.

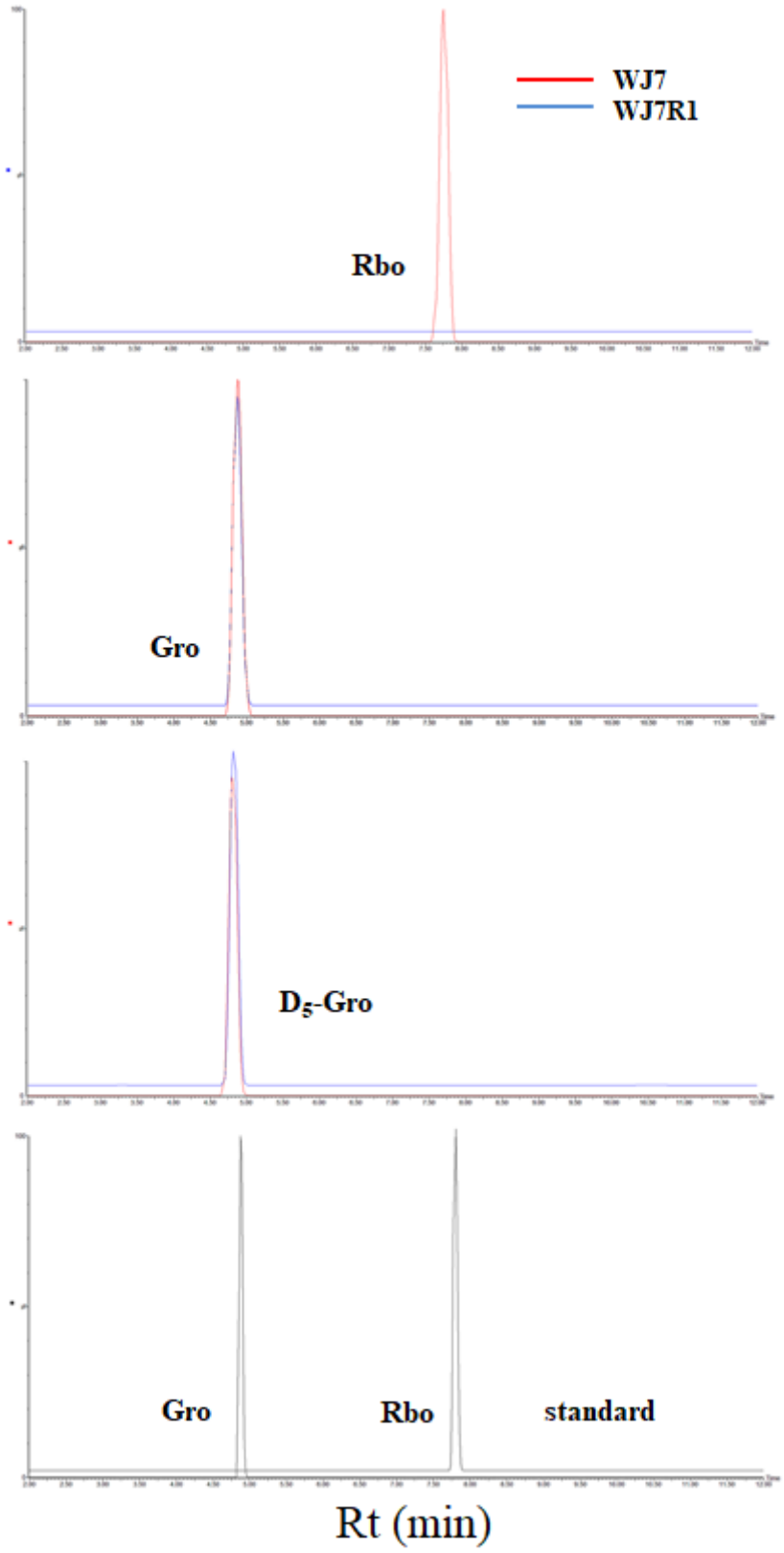


**Fig. 5:** Extracted ion chromatogram of the benzoyl derivatives of Rbo (*m/z* 690.23), Gro

(*m/z* 422.16) and $D_5$-Gro (1,1,2,3,3-D5-glycerol; *m/z* 437.19) in the cell wall samples of WJ7 and WJ7R1. Extracted ion chromatograms of Gro and Rbo in the reference standard sample are also shown.

**Bacteriophage adsorption by cell walls**

The WTA of Gram-positive bacteria could be the host receptor for bacteriophage adsorption (8). Therefore, I performed a phage adsorption assay with cell walls of WJ7 and the two derivatives. The cell walls were mixed with phiWJ7, and the bound phages were removed by centrifugation. The phage adsorption was calculated from the free phage titer of the supernatant. Almost 99% of phiWJ7 adsorbed to the cell walls of WJ7 (Fig.6A), which verifies a presence of a binding receptor for phiWJ7. Yet, 34-39% of phiWJ7 adsorbed to WJ7R1 and WJ7R2, which indicates a binding receptor for phiWJ7 is impaired in the derivatives but the derivatives still adsorb to phiWJ7. Next, I observed irreversible phage adsorption by diluting the cell wall-phage mixtures 100-fold prior to centrifugation, a procedure that releases reversibly bound phages (35). After the dilution, the number of free phages was increased. However, 89% of phiWJ7 still adsorbed to the cell walls of WJ7, whereas phiWJ7 that adsorbed to WJ7R1 and WJ7R2 were totally released (Fig.6B), which demonstrates that WJ7 contains the irreversible binding receptor for phiWJ7, and the derivatives lack this receptor. Considering these results along with the fact that the derivatives have IS transposition in *tarL* and that WJ7R1 lacks Rbo in the extracted WTA, it was estimated that Rbo-WTA is an indispensable binding receptor for phiWJ7. Since the derivatives were reversibly adsorbed by phiWJ7, there must be another cell wall component than Rbo-WTA involved in primary reversible attachment.

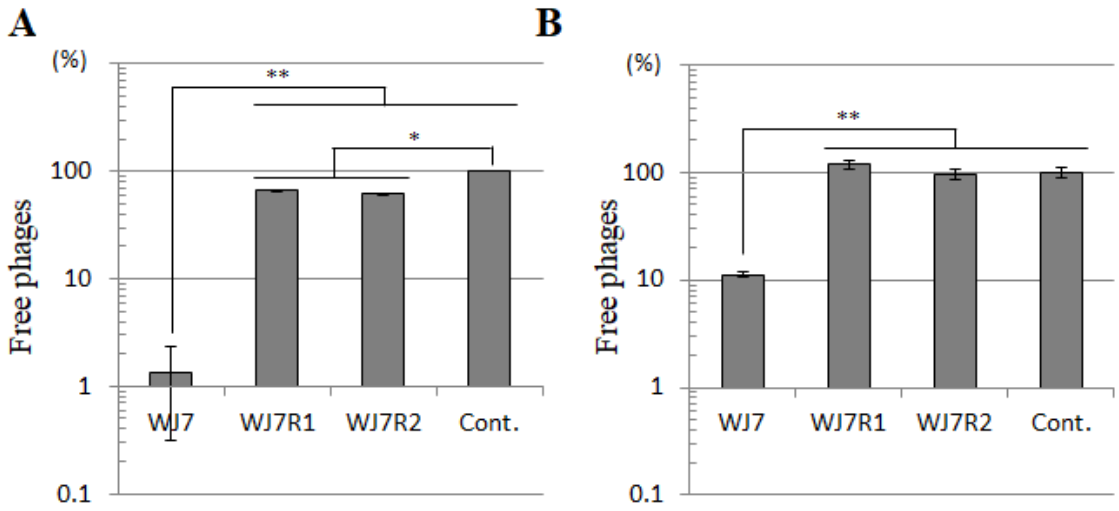


**Fig. 6:** PhiWJ7 adsorption to the cell walls of WJ7 and the derivatives. Free phage titers were calculated as percentages of the control (without cell walls). Cont. means control sample. Data are expressed as the mean with error bars representing ± SD (n=3). Bars with asterisks are significantly different by Tukey's multiple comparison test (*: $p$<0.05, **: $p$<0.01). (A) Free phages represent total adsorption (the sum of phages reversibly and irreversibly adsorbed). (B) Free phages after 100-fold dilution of the samples represent irreversible adsorption.

**Additional acquisition of phiWJ7-insensitive derivatives and identification of the mutation sites**

Suppose that Rbo-WTA is an indispensable binding receptor for phiWJ7, and mutants that lack any genes participating in Rbo-WTA synthesis are expected to be acquired as phiWJ7-insensitive derivatives. When these genes are disrupted by IS transposition, the mutants could easily be found by comparing the length of PCR-amplified DNA fragments containing the disrupted genes. Thus, I acquired additional 25 phiWJ7-insensitive derivatives (WJ7R3-WJ7R27) in the same way as

WJ7R1 and WJ7R2 were obtained, and amplified the DNA region covering the WTA synthesis genes with the primers indicated in Fig. 4B and Table 2. Surprisingly, 21 of 25 derivatives displayed elongated PCR products in the *tarL*-containing region compared with the product amplified from the parental strain of WJ7, and none of the derivatives showed apparently different lengths of PCR products covering other regions (data not shown). DNA sequence analyses revealed that the 21 derivatives had IS transposition into either *tarI*, *tarJ*, or *tarL* (data not shown). These 21 derivatives showed the same phage susceptibility as WJ7R1: insensitive to phiWJ7, sensitive to phiWJ7_2 the same as WJ7, and more sensitive to phiWJ7_3 than WJ7 (data not shown). Among the remaining four derivatives, WJ7R12 and WJ7R24 were less sensitive to phiWJ7_2 and phiWJ7_3 than WJ7R1. I considered that these two derivatives have different mechanisms of altered phage susceptibility than WJ7R1. The other two strains, WJ7R4 and WJ7R18, showed the same phage susceptibility as WJ7R1. Hence, I analyzed the DNA sequence of *tarIJL* and found one base substitution in *tarJ* of WJ7R4 causing the amino acid replacement Y102C and a 102 bp deletion from *tarJ* to *tarL* in WJ7R18. In conclusion, all 23 additionally acquired derivatives that displayed the same phage susceptibility as WJ7R1 contained mutations in *tarIJL*. Lack of *tarIJ* also disrupts Rbo-P polymerization by abstaining to provide the donor substrate CDP-ribitol (Fig. 1).

Bacteriophages are a significant concern for fermentation industries. Industries have dealt with this problem for many years and are now implementing a variety of approaches to control phages, such as factory design changes, sanitation improvement, sterilization of raw materials, and culture rotation. However, since soy sauce is generally manufactured in imperfectly closed facilities, it is difficult to completely exclude bacteriophages from factories. *T. halophilus* severely affects the quality of soy

sauce products, not only by lactic acid production but also by other traits. For instance, most *T. halophilus* strains produce citrulline as a metabolic intermediate of the arginine deiminase system. Citrulline is reported as the main precursor of the potential carcinogen ethyl carbamate in soy sauce (36). Normally, citrulline is converted to ornithine inside bacterial cells, but when the cells are lysed by bacteriophages, it is discharged outside the cells and makes ethyl carbamate in soy sauce (15). Thus, phage infection of fermentation starters remains one of the most common causes of incomplete fermentation and product downgrading.

Extensive efforts have been made to acquire many strains suitable for starters as a preparation for the appearance of bacteriophages (4). The use of phage-insensitive derivatives is one of the solutions, but a mutated strain resistant to a particular phage is not necessarily resistant to other phages, as the results clearly demonstrated, which highlights the importance of understanding the host-phage interaction mechanisms. Some bacterial antiphage defense systems are known, such as restriction/modification (37), toxin/antitoxin (38), and CRISPR-Cas systems (39). In addition, cell surface structure alterations are an important phage defense mechanism. Genetic mutations affecting the structures or expression of phage binding receptors prevent the adsorption of a particular phage and change phage susceptibility (40, 41). Previous studies identified a few phage receptor molecules of Gram-positive bacteria, such as cell membrane-associated proteins, peptidoglycan, lipoteichoic acid, and WTA (9, 42, 43). Here, I demonstrated that phiWJ7 requires Rbo-WTA as a host receptor for irreversible binding and that WJ7 becomes resistant to phiWJ7 by mutating Rbo-WTA synthesis genes. Many staphylococcal *Rountreeviridae* phages also use Rbo-WTA as a binding receptor (28).

The difference in WTA structures is established as one of the determining factors of phage susceptibility in *T. halophilus*. Staphylococcal phages usually infect strains with common WTA structures, whereas previously studied tetragenococcal phages showed narrow host ranges and were reported to be almost "strain-specific" (3). It was estimated that phiWJ7 recognizes its hosts by combining Rbo-WTA and the still-unknown reversible binding receptor. The receptors of phiWJ7_2 and phiWJ7_3 are not known, but they are not Rbo-WTA. Accordingly, other receptors in addition to Rbo-WTA should also play an important role in host recognition by tetragenococcal phages. In this study, however, most of the derivatives obtained for phiWJ7 resistance contained a mutation in *tarIJL*. The reason why the derivatives devoid of reversible binding receptors for phiWJ7 could scarcely be acquired is perhaps because the reversible binding receptor is not essential for infection of some phages and only allows their rapid recognition of irreversible binding receptors (35). Another possibility is that the reversible binding receptor for phiWJ7 is indispensable for the cell viability of WJ7. WJ7 becomes more vulnerable to phiWJ7_3 when Rbo-WTA synthesis genes are disrupted. The reason is unclear, but possibly Rbo-WTA masks the receptor for phiWJ7_3 and prevents phiWJ7_3 adsorption, or the expression level of the receptor for phiWJ7_3 is changed as Rbo-WTA synthesis is impaired.

The *in silico* analysis of the WJ7 genome and the chemical analysis of the WTA extracted from WJ7 suggested the presence of both Gro- and Rbo-WTA, but their structures and synthetic pathways are not fully clarified. In *S. aureus*, *tarIJL* is located upstream of *tarS* encoding a glycosyltransferase that attaches β-Glc*N*Ac residues to Rbo-WTA (44), while *tarIJL* of WJ7 is followed by a putative polysaccharide pyruvyltransferase (Fig. 4A). *Nocardiopsis metallicus* actually produces Rbo-WTA with

pyruvate residues (45). Further research is necessary to fully understand the structures and biosynthetic pathways of WTA in *T. halophilus*.

In the context of host-phage interactions, WTA is often regarded as the host receptor for phage adsorption, and I added additional evidence to show this. Additionally, various roles of WTA were proposed, such as protection of pathogens from host defense and antibiotics, regulation of cell division, ion homeostasis, adhesion, and biofilm formation (10). The WTA function for *T. halophilus* is unclear. The deletion of *tagO*, whose product catalyzes the first step in WTA synthesis, results in a complete lack of WTA in cell walls and is not lethal for *S. aureus* (46). Nevertheless, *tagO* mutants were not obtained in this study, suggesting that WTA may play some important roles in *T. halophilus* and that *tagO* mutants may severely be compromised, as in *Bacillus subtilis* (47). In *S. aureus*, the disruption of late-stage Rbo-WTA synthesis genes such as *tagBDGH* and *tarFIJL* is lethal, probably because the accumulation of undecaprenol-linked intermediates depletes lipid carriers that are also needed for peptidoglycan synthesis (48). In *T. halophilus*, *tarIJL* mutants were obtained, and under laboratory conditions, WJ7R1 and WJ7R2 were not different in growth rate and morphology from WJ7 (data not shown). I hypothesized this is because *tarIJL* mutants do not accumulate the intermediates but use them for Gro-WTA production. *Lactiplantibacillus plantarum* activates Rbo-WTA synthesis genes when *tagF* is impaired (49).

Despite notable industrial concern, little is known about tetragenococcal phages. Only three phages, Φ7116 (*Myoviridae*), ΦD-86, and ΦD10 (both *Siphoviridae*), have been characterized thus far, but their genomic sequences have not been published (3, 4). I present the complete genome sequence of phiWJ7 belonging to the

*Rountreeviridae* family. The phiWJ7 genome resembles those of some staphylococcal *Rountreeviridae* phages in genome size, protein sequence homology, and the presence of long inverted terminal repeats. PhiWJ7 presumably evolved from a common ancestor of such phages. I compared the genome of phiWJ7 with that of *Staphylococcus* phage P68 (see Fig. 2B) in which the virion-constituting proteins were identified and the virion-structures were elucidated (50). Among ten structural proteins of P68, six showed similarity with the proteins of phiWJ7 by BLASTP search. P68 binds to Rbo-WTA and the tail fiber is responsible for the adsorption. The ORF12 of phiWJ7 showed 34% amino acid similarity to the tail fiber of P68, which suggests ORF12 of phiWJ7 is involved in the interaction with Rbo-WTA. The head fiber of P68 is considered to function in the primary reversible attachment of the phages to cells. Although none of the proteins of phiWJ7 showed similarity with the entire head fiber of P68, the N-terminal part of ORF13 of phiWJ7 was similar to that part of P68 head fiber. The head fiber of P68 contains N-terminal capsid-binding domain and the C-terminal receptor binding domain. Hence, ORF13 of phiWJ7 is likely to code the head fiber but bind to a different receptor from P68.

In this study, IS*Teha3*, IS*Teha4*, and IS*Teha5* played important roles in the disruption of the Rbo-WTA synthetic pathway, which emphasizes the contribution of ISs to mutations and the evolution of *T. halophilus.* First, I discovered the transposition of these ISs in UV-irradiated derivatives (15), but it was shown here that transposition occurred spontaneously without UV irradiation. Unfortunately, the lack of an established transformation technique in *T. halophilus* makes it difficult to adopt cloning strategies to analyze gene functions. In this study, I adopted a strategy utilizing intrinsic ISs, which is similar to a transposon mutagenesis system. It is advantageous that the

transposition of ISs can be easily detected by PCR amplification if the transposition site is predicted and that the mutant strains do not contain foreign genes so they can immediately be available in a food grade form. On the other hand, the disadvantage is that the transposition is uncontrollable in frequency and location. The ISs used here preferentially target AT-rich regions and are relatively difficult to insert into shorter ORFs. Since a number of genes other than *tarIJL* contribute to Rbo-WTA synthesis and their total length is sufficiently long compared with *tarIJL*, I think the unsuccessful acquisition of mutants in which such genes were disrupted by ISs is likely to be caused by the reason described above. However, when expecting short genes without sufficient AT-rich regions to be disrupted, the necessity to consider the difficulty of IS insertion increases. I hope to understand the nature of these ISs better, and hope that the technique will be developed in the future to obtain derivatives in which a particular gene is impaired by the ISs. Such a technique will contribute to the development of efficient strategies against bacteriophage infections.

**REFERENCES**


1. Higuchi T, Uchida K, Abe K. 1998. Aspartate decarboxylation encoded on the plasmid in the soy sauce lactic acid bacterium, *Tetragenococcus halophila* D10. Biosci Biotechnol Biochem 62:1601-1603.
2. Kuda T, Izawa Y, Ishii S, Takahashi H, Torido Y, Kimura B. 2012. Suppressive effect of *Tetragenococcus halophilus*, isolated from fish-*nukazuke*, on histamine accumulation in salted and fermented fish. Food Chem 130: 569-574.
3. Uchida K, Kanbe C. 1993. Occurrence of bacteriophages lytic for *Pediococcus halophilus*, a halophilic lactic-acid bacterium, in soy sauce fermentation. J Gen Appl Microbiol 39:429-437.
4. Higuchi T, Uchida K, Abe K. 1999. Preparation of phage-insensitive strains of *Tetragenococcus halophila* and its application for soy sauce fermentation. Biosci Biotechnol Biochem 63:415-417.
5. Matsutani M, Wakinaka T, Watanabe J, Tokuoka M, Ohnishi A. 2021. Comparative genomics of closely related *Tetragenococcus halophilus* strains elucidate the diversity and microevolution of CRISPR elements. Front microbiol 12:1605.
6. Hancock RW, Braun V. 1976. Nature of the energy requirement for the irreversible adsorption of bacteriophages T1 and Φ80 to *Escherichia coli*. J Bacteriol 125:409-415.
7. Letarov AV, Kulikov EE. 2017. Adsorption of bacteriophages on bacterial cells. Biochemistry 82:1632-1658.
8. Bertozzi Silva J, Storms Z, Sauvageau D. 2016. Host receptors for bacteriophage adsorption. FEMS Microbiol lett. 363:fnw002.

9. Wendlinger G, Loessner MJ, Scherer S. 1996. Bacteriophage receptors on *Listeria monocytogenes* cells are the *N*-acetylglucosamine and rhamnose substituents of teichoic acids or the peptidoglycan itself. Microbiology 142:985-992.

10. Brown S, Santa Maria JP, Walker S. 2013. Wall teichoic acids of gram-positive bacteria. Annu Rev Microbiol 67:313-336.

11. Tomita S, Furihata K, Tanaka N, Satoh E, Nukada T, Okada S. 2012. Determination of strain-specific wall teichoic acid structures in *Lactobacillus plantarum* reveals diverse α-D-glucosyl substitutions and high structural uniformity of the repeating units. Microbiology 158:2712-2723.

12. Xia G, Peschel A. 2008. Toward the pathway of *S. aureus* WTA biosynthesis. Chem Biol 15:95-96

13. Shirakawa D, Wakinaka T, Watanabe J. 2020. Identification of the putative *N*-acetylglucosaminidase CseA associated with daughter cell separation in *Tetragenococcus halophilus*. Biosci Biotechnol Biochem 84:1724-1735.

14. Wakinaka T, Iwata S, Takeishi Y, Watanabe J, Mogi Y, Tsukioka Y, Shibata Y. 2019. Isolation of halophilic lactic acid bacteria possessing aspartate decarboxylase and application to fish sauce fermentation starter. Int J Food Microbiol 292:137-143.

15. Wakinaka T, Watanabe J. 2019. Transposition of IS*4* family insertion sequences IS*Teha3*, IS*Teha4*, and IS*Teha5* into the *arc* operon disrupts arginine deiminase system in *Tetragenococcus halophilus*. Appl Environ Microbiol 85: e00208-19.

16. Li H, Durbin R. 2010. Fast and accurate long-read alignment with Burrows–Wheeler transform. Bioinformatics 26:589-595.

17. McKenna A, Hanna M, Banks E, Sivachenko A, Cibulskis K, Kernytsky A, Garimella K, Altshuler D, Gabriel S, Daly M, DePristo MA. 2010. The Genome Analysis Toolkit: a MapReduce framework for analyzing next-generation DNA sequencing data. Genome Res 20:1297-1303.

18. DePristo MA, Banks E, Poplin R, Garimella KV, Maguire JR, Hartl C, Philippakis AA, del Angel G, Rivas MA, Hanna M, McKenna A, Fennell TJ, Kernytsky AM, Sivachenko AY, Cibulskis K, Gabriel SB, Altshuler D, Daly MJ. 2011. A framework for variation discovery and genotyping using next-generation DNA sequencing data. Nat Genet 43:491-498.

19. Deatherage DE, Barrick JE. 2014. Identification of mutations in laboratory-evolved microbes from next-generation sequencing data using breseq. Methods Mol Biol 1151:165-188.

20. Bankevich A, Nurk S, Antipov D, Gurevich AA, Dvorkin M, Kulikov AS, Lesin VM, Nikolenko SI, Pham S, Prjibelski AD, Pyshkin AV, Sirotkin AV, Vyahhi N, Tesler G, Alekseyev MA, Pevzner PA. 2012. SPAdes: a new genome assembly algorithm and its applications to single-cell sequencing. J Comput Biol 19:455–477.

21. Tanizawa Y, Fujisawa T, Kaminuma E, Nakamura Y, Arita M. 2016. DFAST and DAGA: Web-based integrated genome annotation tools and resources. Biosci Microbiota Food Health 35:173–184.

22. Bron PA, Tomita S, van S II, Remus DM, Meijerink M, Wels M, Okada S, Wells JM, Kleerebezem M. 2012. *Lactobacillus plantarum* possesses the capability for wall teichoic acid backbone alditol switching. Microb Cell Fact 11:123.

23. Bornø A, Foged L, van Hall G. 2014. Glucose and glycerol concentrations and their tracer enrichment measurements using liquid chromatography tandem mass spectrometry. J Mass Spectrom 49:980-988.

24. Baptista C, Santos MA, São-José C. 2008. Phage SPP1 reversible adsorption to *Bacillus subtilis* cell wall teichoic acids accelerates virus recognition of membrane receptor YueB. J Bacteriol 190:4989-4996.

25. Kraushaar B, Thanh MD, Hammerl JA, Reetz J, Fetsch A, Hertwig S. 2013. Isolation and characterization of phages with lytic activity against methicillin-resistant *Staphylococcus aureus* strains belonging to clonal complex 398. Arch Virol 158:2341–2350.

26. Wang Z, Zheng P, Ji W, Fu Q, Wang H, Yan Y, Sun J. 2016. SLPW: a virulent bacteriophage targeting methicillin-resistant *Staphylococcus aureus* in vitro and in vivo. Front Microbiol 7:934.

27. Cater K, Dandu VS, Bari SM, Lackey K, Everett GF, Hatoum-Aslan A. 2017. A novel *staphylococcus* podophage encodes a unique lysin with unusual modular design. mSphere 2(2):e00040-17.

28. Azam AH, Tanji Y. 2019. Peculiarities of *Staphylococcus aureus* phages and their possible application in phage therapy. Appl Microbiol Biotechnol 103:4279-4289.

29. Krupovic M, Turner D, Morozova V, Dyall-Smith M, Oksanen HM, Edwards R,Dutilh BE, Lehman SM, Reyes A, Baquero DP, Sullivan MB, Uchiyama J, Nakavuma J, Barylski J, Young MJ, Du S, Alfenas-Zerbini P, Kushkina A, Kropinski AM, Kurtboke I, Brister JR, Lood C, Sarkar BL, Yigang T, Liu Y, Huang L, Wittmann J, Chanishvili N, van Zyl LJ, Rumnieks J, Mochizuki T,

Jalasvuori M, Aziz RK, ?obocka M, Stedman KM, Shkoporov AN, Gillis A, Peng X, Enault F, Knezevic P, Lavigne R, Rhee SK, Cvirkaite-Krupovic V, Moraru C, Switt AIM, Poranen MM, Millard A, Prangishvili D, Adriaenssens EM. 2021. Bacterial Viruses Subcommittee and Archaeal Viruses Subcommittee of the ICTV: update of taxonomy changes in 2021. Arch Virol 2021: 1-6

30. Xia G, Kohler T, Peschel A. 2010. The wall teichoic acid and lipoteichoic acid polymers of *Staphylococcus aureus*. Int J Med Microbiol 300:148-154

31. Winstel V, Sanchez-Carballo P, Holst O, Xia G, Peschel A. 2014. Biosynthesis of the unique wall teichoic acid of *Staphylococcus aureus* lineage ST395. mBio 5:e00869-14.

32. Schaefer K, Matano LM, Qiao Y, Kahne D, Walker S. 2017. In vitro reconstitution demonstrates the cell wall ligase activity of LCP proteins. Nat Chem Biol 13:396-401.

33. van Dalen R, Peschel A, van Sorge NM. 2020. Wall teichoic acid in *Staphylococcus aureus* host interaction. Trends Microbial 28:985-998

34. Qian Z, Yin Y, Zhang Y, Lu L, Li Y, Jiang Y. 2006. Genomic characterization of ribitol teichoic acid synthesis in *Staphylococcus aureus*: genes, genomic organization and gene duplication. BMC Genomics 7:74.

35. Baptista C, Santos MA, São-José C. 2008. Phage SPP1 reversible adsorption to *Bacillus subtilis* cell wall teichoic acids accelerates virus recognition of membrane receptor YueB. J Bacteriol 190:4989-4996.

36. Matsudo T, Aoki T, Abe K, Fukuta N, Higuchi T, Sasaki M, Uchida K. 1993. Determination of ethyl carbamate in soy sauce and its possible precursor. J Agric

Food Chem 41:352-356.

37. Rocha EP, Danchin A, Viari A. 2001. Evolutionary role of restriction/modification systems as revealed by comparative genome analysis. Genome Res 11:946-958.

38. Fineran PC, Blower TR, Foulds IJ, Humphreys DP, Lilley KS, Salmond GP. 2009. The phage abortive infection system, ToxIN, functions as a protein-RNA toxin-antitoxin pair. Proc Natl Acad Sci USA 106: 894-899

39. Barrangou R, Fremaux C, Deveau H, Richards M, Boyaval P, Moineau S, Romero DA, Horvath P. 2007. CRISPR provides acquired resistance against viruses in prokaryotes. Science 315:1709-1712.

40. Castillo D, Rørbo N, Jørgensen J, Lange J, Tan D, Kalatzis PG, Svenningsen SL, Middelboe M. 2019. Phage defense mechanisms and their genomic and phenotypic implications in the fish pathogen *Vibrio anguillarum*. FEMS Microbiol Ecol 95:fiz004.

41. Chatterjee AN. 1969. Use of bacteriophage-resistant mutants to study the nature of the bacteriophage receptor site of *Staphylococcus aureus*. J Bacteriol 98:519-527.

42. Davison S, Couture-Tosi E, Candela T, Mock M, Fouet A. 2005. Identification of the *Bacillus anthracis* γ phage receptor. J Bacteriol 187:6742-6749.

43. Kaneko J, Narita-Yamada S, Wakabayashi Y, Kamio Y. 2009. Identification of ORF636 in phage φSLT carrying Panton-Valentine leukocidin genes, acting as an adhesion protein for a poly (glycerophosphate) chain of lipoteichoic acid on the cell surface of *Staphylococcus aureus*. J Bacteriol 191:4674-4680.

44. Brown S, Xia G, Luhachack LG, Campbell J, Meredith TC, Chen C, Winstel V,

Gekeler C, Irazoqui JE, Peschel A, Walker S. 2012. Methicillin resistance in *Staphylococcus aureus* requires glycosylated wall teichoic acids. Proc Natl Acad Sci USA 109:18909-18914.

45. Tul'skaya EM, Shashkov AS, Streshinskaya GM, Potekhina NV, Evtushenko LI. 2014. New structures and composition of cell wall teichoic acids from *Nocardiopsis synnemataformans*, *Nocardiopsis halotolerans*, *Nocardiopsis composta* and *Nocardiopsis metallicus*: a chemotaxonomic value. Antonie van Leeuwenhoek 106:1105-1117.

46. D'Elia MA, Pereira MP, Chung YS, Zhao W, Chau A, Kenney TJ, Sulavik MC, Black TA, Brown ED. 2006. Lesions in teichoic acid biosynthesis in *Staphylococcus aureus* lead to a lethal gain of function in the otherwise dispensable pathway. J Bacteriol 188:4183-4189.

47. D'Elia MA, Millar KE, Beveridge TJ, Brown ED. 2006. Wall teichoic acid polymers are dispensable for cell viability in *Bacillus subtilis*. J Bacteriol 188:8313.

48. Sewell EWC, Brown ED. 2014. Taking aim at wall teichoic acid synthesis: new biology and new leads for antibiotics. J Antibiot 67:43-51.

49. Tomita S, de Waard P, Bakx EJ, Schols HA, Kleerebezem M, Bron PA. 2013. The structure of an alternative wall teichoic acid produced by a *Lactobacillus plantarum* WCFS1 mutant contains a 1,5-linked poly(ribitol phosphate) backbone with 2-alpha-D-glucosyl substitutions. Carbohydr. Res. 370:67-71.

50. Hrebík D, Štveráková D, Škubník K, Füzik T, Pantůček R, Plevka P. 2019. Structure and genome ejection mechanism of *Staphylococcus aureus* phage P68. Sci Adv, 5:eaaw7414.

**SUMMARY**

*Tetragenococcus halophilus*, a halophilic lactic acid bacterium, is used in the fermentation process of soy sauce manufacturing. For many years, bacteriophage infections of *T. halophilus* have been a major industrial problem that causes fermentation failure. However, studies focusing on the mechanisms of tetragenococcal host-phage interactions are not sufficient. In this study, I generated two phage-insensitive derivatives from the parental strain *T. halophilus* WJ7, which is susceptible to the virulent phage phiWJ7. Whole-genome sequencing of the derivatives revealed that insertion sequences were transposed into a gene coding poly(ribitol phosphate) polymerase (TarL) in both derivatives. TarL is responsible for the biosynthesis of ribitol-containing wall teichoic acid, and WJ7 was confirmed to contain ribitol in extracted wall teichoic acid, but the derivative was not. Cell walls of WJ7 irreversibly adsorbed phiWJ7, but those of the phage-insensitive derivatives did not. Additionally, 25 phiWJ7-insensitive derivatives were obtained, and they showed mutations not only in *tarL* but also in *tarI* and *tarJ,* which are responsible for the synthesis of CDP-ribitol. These results indicate that phiWJ7 targets the ribitol-containing wall teichoic acid of host cells as a binding receptor.

Information about the mechanisms of host-phage interactions is required for the development of efficient strategies against bacteriophage infections. Here, I identified the ribitol-containing wall teichoic acid as a host receptor indispensable for bacteriophage infection. The complete genome sequence of tetragenococcal phage phiWJ7 belonging to the family *Rountreeviridae* is also provided here. This study could become the foundation for a better understanding of host-phage interactions of tetragenococci.

## SECTION 2

## Identification of capsular polysaccharide synthesis loci determining bacteriophage susceptibility in *Tetragenococcus halophilus*

*Tetragenococcus halophilus*, a Gram-positive halophilic lactic acid bacterium, plays an important role in the fermentation process of a variety of salted and fermented foods, such as salted fish, vegetable pickles, and soy sauce (1, 2, 3). Bacteriophages infecting *T. halophilus* can impede lactic acid fermentation and decrease the quality of food products (4, 5, 6). Tetragenococcal phages typically display narrow host ranges, but the genetic background for this phenotypical characteristic has been poorly studied thus far. To develop efficient strategies against bacteriophage infections, the mechanisms of tetragenococcal host-phage interactions must be understood in detail.

The first step of phage infection is a highly specific attachment to binding receptors on the host cell surface. Some phage receptors of Gram-positive bacteria have been identified, such as peptidoglycan, membrane-associated proteins, wall teichoic acid (WTA), and lipoteichoic acid (LTA) (7, 8, 9). The presence of specific receptor molecules is necessary for phage infections, which largely dictates the host ranges of the respective phages. Tetragenococcal phage receptors have not been well characterized. In the previous section, I identified ribitol-containing WTA as a receptor for *T. halophilus* phage phiWJ7, but another cell wall component was presumed to be involved in phage adsorption since phiWJ7 and other phages could still adsorb to the strains lacking ribitol-containing WTA (6).

The cell walls of lactic acid bacteria frequently contain diverse polysaccharides in addition to peptidoglycan and WTA (10). Such polysaccharides can be divided into

three major groups: capsular polysaccharides (CPSs), exopolysaccharides (EPSs) and cell wall polysaccharides (CWPSs); note that this grouping is not strictly defined. CPSs are covalently attached to peptidoglycan and form a capsule around the bacterium. EPSs are secreted into the environment and loosely associated with the cells. CWPSs are attached to the cell wall but do not form a capsule. These polysaccharides can also interact with phages. For instance, a CWPS of *Lactococcus lactis* was identified as a receptor for some phages (11), whereas EPSs of *L. lactis* can act as a physical barrier against phage infection and protect bacteria (12).

The majority of CPSs are produced via the so-called Wzx/Wzy-dependent pathway (13). In this pathway, synthesis of a repeat unit occurs in the cytoplasm. Then, the repeat units are translocated to the outer side of the cell membrane by the Wzx flippase. The Wzy polymerase connects the repeat units and extends the sugar chain. The mature CPSs are finally attached to peptidoglycan. The gene clusters for the production of CPSs known as *cap/cps* loci have been described in many Gram-positive bacteria, including lactic acid bacteria (14, 15). Despite numerous structural and compositional varieties of CPSs, the overall organization and the core genes of *cap/cps* loci are well conserved in species and are similar even beyond genera. *Streptococcus pneumoniae*, in which CPS structures and synthesis genes are best studied, conserves *cpsABCD* as the first four genes of the *cps* locus (16). *cpsABCD* is implicated in CPS regulation and posttranslational synthesis modulation (17), and the immediately downstream region contains genes encoding glycosyltransferases, acyltransferases and other modifying enzymes, nucleotide sugar synthesis enzymes, Wzx flippase, and Wzy polymerase. The genes located downstream of *cpsABCD* are highly diverse among strains and thereby generate a variety of CPS patterns in *S. pneumoniae*. The repeating

units of CPSs in *S. pneumoniae* have two to eight saccharide residues and are often decorated with *O*-acetyl, pyruvyl, and phosphoglycerol substitutions (18). More than 100 serotypes were distinguished based on the structures of CPS in *S. pneumoniae* (19). Many other Gram-positive bacteria possess genes homologous to *cpsABCD* as the core genes of *cap/cps* loci.

The purpose of this study was to clarify the genes determining phage susceptibilities in *T. halophilus*, especially the genes affecting adsorption by phages, and to reveal the reason for the narrow host ranges of tetragenococcal phages. As a result, I discovered the *cps* loci responsible for CPS synthesis and demonstrated that mutations in the *cps* loci can change phage susceptibilities in *T. halophilus*. Moreover, it was suggested that tetragenococcal phages utilize CPSs as a binding receptor and/or degrade CPSs to approach other receptors. These findings will serve as an important basis for future studies on tetragenococcal host-phage interactions and for the development of industrial countermeasures against bacteriophage infections.

## Materials and methods

### Bacterial strains, bacteriophages, media and culture conditions

The bacterial strains and phages mainly used in this study are summarized in Table 1. The derivatives derived from YA5 and YG2 were obtained as described below. *T. halophilus* strains were cultured in MRS-10 or LA13 medium (20). MRS-10 is Lactobacilli MRS Broth (Difco, Detroit, MI) supplemented with 10% NaCl. Liquid media were statically incubated, and agar plates were incubated under anaerobic conditions using AnaeroPack (Mitsubishi Gas Chemical, Tokyo, Japan) at 30 °C. Cell morphology was observed with a BX53 optical microscope (Olympus, Tokyo, Japan).

**Table 1. Bacterial strains and bacteriophages mainly used in this study.**

| | Description | Source or Reference |
|---|---|---|
| *Tetragenococcus halophilus* | | |
| YA5 | Sensitive for phiYA5 and phiYA5_2. | (21) |
| YA5R1 | PhiYA5-resistant derivative from YA5. | Generated in this study. |
| YA5R1R1 | PhiYA5_2-resistant derivative from YA5R1. | Generated in this study. |
| YA5R2 (YA5_pyruvylTrfase::IS) | PhiYA5_2-resistant derivative from YA5. | Generated in this study. |
| YG2 | Sensitive for phiYG2_4. | (22) |
| YG2R1 (YG2_pgm::IS) | PhiYG2_4-resistant derivative from YG2. | Generated in this study. |
| YG2R2 (YG2_wzy::IS) | PhiYG2_4-resistant derivative from YG2. | Generated in this study. |
| YG2R48 (YG2_acylTrfase::IS) | PhiYG2_4-resistant derivative from YG2. | Generated in this study. |
| Bacteriophage | | |
| phiYA5 | Lytic for YA5. | Isolated from soy sauce mash. |
| phiYA5_2 | Lytic for YA5. *Rountreeviridae*. | Isolated from soy sauce mash. |
| phiYG2_4 | Lytic for YG2. | Isolated from soy sauce mash. |

**Manipulation of bacteriophages and generation of phage-resistant mutants**

Uchida & Kanbe developed a manipulation method for tetragenococcal phages (4), and I modified this method as described previously (6). Briefly, instead of using the general soft agar overlay technique, the bacterial suspension was diluted with saline and spread on LA13 agar plates by tilting the plate to form plaques. To obtain spontaneous phage-resistant mutants, the parental strain was incubated with $>10^7$ pfu of phages on LA13 plates, and the surviving colonies were selected. To observe the enzymatic activity of the virions, phage particles were UV irradiated using a germicidal lamp (GL-15; Panasonic, Kadoma, Japan) at a distance of 50 mm for 10 min.

**DNA preparation and genome sequencing**

Genomic DNA from *T. halophilus* was isolated using the DNeasy PowerSoil Pro Kit (QIAGEN, Hilden, Germany) and QIAcube, an automated system (QIAGEN). Genomic DNA from bacteriophage phiYA5_2 was isolated using the Phage DNA Isolation Kit (Norgen Biotek, Thorold, Canada). The quantity and purity of the DNA were assessed with a Qubit dsDNA BR Assay Kit (Thermo Fisher Scientific, Waltham, MA) and NanoDrop 1000 spectrophotometer (Thermo Fisher Scientific). An Illumina Nextera DNA Flex Library Prep Kit (Illumina, San Diego, CA) was used to prepare the genomic DNA library. Whole-genome sequencing was conducted using the Illumina MiSeq sequencing platform with a paired-end sequencing strategy (2 × 300 bp). Adapter sequences and low-quality regions in the Illumina reads were trimmed using Trim Galore! v.0.6.4 with default parameters (https://www.bioinformatics.babraham.ac.uk/projects/trim_galore/). De novo assembly of phage genomes was conducted as previously described (6). Briefly, read data were mapped onto the host genome to remove the contaminated host genome sequence, and

unmapped read pairs were used for the de novo assembly with SPAdes v. 3.13.0 (23). The DDBJ Fast Annotation and Submission Tool was used for gene detection and genome annotation of the draft genome assemblies with default settings (24).

**Genome mapping analysis and mutation search of the derivatives**

To detect the mutation sites of YA5R1, YA5R1R1, and YG2R1, the genome data of *T. halophilus* YA5, YA5R1, and YG2 were used as the reference sequence for the genome mapping analysis. The genome sequences of YA5 (DRA accession numbers: DRR424329) and YG2 (DRR220997) were previously published (25). The Illumina sequence reads of the derivatives were mapped to the reference sequence of the parental strain using BWA with default parameters (26). Single nucleotide polymorphisms and indels were detected by the Genome Analysis Toolkit (GATK) (27, 28). For the detection of the transposon insertion sites, breseq v.0.31.0 was used with default parameters (29). To find the IS transposition in the additionally acquired derivatives YA5R2-YA5R17 and YG2R2-YG2R49, the primer sets YA5_22620 and YA5_22670, YA5_22670-2 and YA5_22740, YA5_22740-2 and YA5_22800, YA5_22800-2 and YA5_22880, YA5_22670-2 and YG2_06590, YG2_06590-2 and YG2_06630, and YG2_16110 and YG2_16130 were used to amplify the DNA region covering CPS synthesis genes (Table 2, Fig. 1). The PCR products amplified with DNA polymerase KOD FX Neo (Toyobo, Osaka, Japan) were purified using the Wizard SV Gel and PCR Clean-Up System (Promega, Madison, USA), and the resulting DNA fragment was analyzed by a commercial DNA sequencing service (Fasmac, Atsugi, Japan/Eurofins Genomics, Tokyo, Japan).

**Table 2. Primers used in this study.**

| Primer name | Sequence (5'→3') |
|---|---|
| YA5_22620 | TCGCGTTGGTAACGCAG |
| YA5_22670 | GTGCGCATCCGAAGC |
| YA5_22670-2 | AAACAGCGCAAGAAATGGTAG |
| YA5_22740 | TTTAATTGAACTGCATTACGTACCC |
| YA5_22740-2 | TCTGTTGTAGATGAAGTCGAGGG |
| YA5_22800 | CCACACTCCGAATCTTCTCC |
| YA5_22800-2 | TCGACAGTTCCGGTTGG |
| YA5_22880 | TCAGCATGGCGGGG |
| YG2_06590 | AATGAATGGTACTAACAACTCTCGG |
| YG2_06590-2 | GGGAATTCGGACGCG |
| YG2_06630 | CAAAGGTAACAGCTTTTTAGGGATG |
| YG2_16110 | CCAGTACGATTTTCAAACGAGTC |
| YG2_16130 | GGTACACTCGCTCGCTCC |

**CPS extraction and analysis**

CPSs were roughly quantified following the method of Ha et al. (30). Briefly, cells were grown to stationary phase in MRS-10 medium and harvested by centrifugation (8,000 × g, 5 min, 4 °C). The pellets (0.2 g) were washed with sodium phosphate buffer (50 mM, pH 7.0) and suspended in 2 mL of sodium phosphate buffer containing 70 mg lysozyme. After incubation at 37 °C for 24 h, the supernatant was recovered by centrifugation and treated with DNase, RNase, and Proteinase K. The supernatant was adjusted to a concentration of 30% (v/v) ethanol and cooled at 4 °C for

2 h, and the precipitate was removed by centrifugation. Then, the supernatant was adjusted to a concentration of 80% ethanol and precipitated. CPSs were collected by centrifugation and lyophilized. For quantification analysis of CPSs, a modified phenol–sulfuric acid method was employed. The dried pellet was resuspended in 600 μL of water, and 300 μL of 5% phenol was added. Then, 1.5 mL of 95% sulfuric acid was mixed and allowed to develop color for 10 min at room temperature. Finally, the intensity of the color was measured at 490 nm with a spectrophotometer. The concentration of the extracted CPSs was calculated based on the color intensity of the glucose standard. For sugar composition analysis, hydrolysates of CPSs (2 M HCl, 100 °C, 3 h) were analyzed with a reducing sugar analysis system LC-20 (Shimadzu, Kyoto, Japan). For imaging, cells cultured in MRS-10 medium were collected by centrifugation, fixed with 2% glutaraldehyde in 0.1 M cacodylate buffer (pH 7.0) and stained with 2% osmium tetroxide containing 0.8% sucrose. The cells were then stepwise dehydrated in ethanol solutions of increasing concentration and embedded in Epon 812. Ultrathin sections were prepared and stained with 2% uranyl acetate and lead. TEM observation was carried out with an H-7600 microscope (Hitachi Ltd., Tokyo, Japan) at Hanaichi UltraStructure Research Institute (Okazaki, Japan).

**Bacteriophage adsorption assay**

Phage adsorption by cells was measured by the method of Baptista et al. (31). Cells were grown in LA13 liquid medium to OD=0.5 and sterilized by heating at 60 °C for 30 min. Phages were mixed with cells and incubated at 30 °C for 2 h. Control mixtures without cells were used to confirm the phage input in the experiment. After incubation, the mixture was centrifuged (6,000 × *g*, 5 min, 4 °C), and the supernatant was assayed for plaques using YA5 for phiYA5 and phiYA5_2 and YG2 for phiYG2_4

as the indicator strain. Unbound free phages in the supernatants after centrifugation were enumerated.

**Statistical analysis**

The data were analyzed using R software (version 3.6.0; www.r-project.org). Comparisons of the two groups were performed using an unpaired t test. The data involving more than two groups were assessed by one-way ANOVA followed by post hoc Tukey's multiple comparison test. Statistical significance was considered at $p < 0.05$.

**Bioinformatics and data availability**

BLAST was used for the DNA and amino acid sequence analysis. Illumina sequence reads of YA5R1, YA5R1R1, and YG2R1 were deposited in the DDBJ Sequence Read Archive. The DRA accession numbers for YA5R1, YA5R1R1, YG2R1, and phiYA5_2 are DRR424330, DRR424331, DRR424332, and DRR424333, respectively. The BioProject number is; PRJDB9642 for DRR424330, DRR424331, and DRR424332; PRJDB12096 for DRR424333. Other sequence data were deposited in the DDBJ database with accession numbers LC720293-LC720358.

**Results and discussion**

**Generation of phage-resistant derivatives and detection of mutational sites**

To investigate the genes determining phage susceptibility in *T. halophilus*, I tried the acquisition of spontaneous phage-resistant derivatives and determination of their mutated sites. Two host strains, YA5 and YG2, and phages infecting these strains were mainly used in this study (Table 1). Phage-resistant derivatives derived from these strains were selected as colonies growing in the presence of the phages, and the mutation

sites of the derivatives were clarified by whole-genome sequence analysis. A YA5 derivative resistant to phage phiYA5 was obtained, which I refer to as YA5R1 (data not shown). The genome mapping analysis revealed no mutation sites in YA5R1 (data not shown). The mutation responsible for the phenotypical change in YA5R1 might have occurred in a region missing from the draft genome analysis. Unfortunately, I could not determine the mutation site and did not conduct further investigation because the adsorption to YA5R1 by phiYA5 was not impaired, which shows that YA5R1 does not have a mutation involved in phage adsorption (data not shown). Intriguingly, another phage, phiYA5_2, formed larger plaques to YA5R1 than to YA5 (data not shown). Subsequently, a YA5R1-dirivative resistant to phage phiYA5_2 was obtained, which I refer to as YA5R1R1. YA5R1R1 contained only one mutation: transposition of an insertion sequence (IS) in an ORF encoding putative polysaccharide pyruvyltransferase (locus tag; YA5_022780). Another host strain, YG2, is susceptible to phage phiYG2_4, and the phiYG2_4-resistant derivative YG2R1 was obtained from YG2 (cf. Fig. 3). YG2R1 contained an 8 bp deletion outside ORFs (744 bp upstream of YG2_08150) and a transposed IS in an ORF encoding α-phosphoglucomutase (YG2_16120).

**Identification of capsular polysaccharide synthesis (*cps*) loci**

The gene mutated in YA5R1R1 (putative polysaccharide pyruvyltransferase) clustered with the genes similar to *cpsACDB* of *Enterococcus faecium*, the core genes to CPS synthesis loci (Fig. 1A). The *cps* locus of *E. faecium* contains *cpsACDB* and an unnamed gene adjacent to *cpsA*. These five genes are well conserved in *E. faecium* and are flanked by genes that are nonhomologous among strains (32). The comparison of the *cps* loci of YA5 and YG2, and those of six *T. halophilus* strains whose complete genomes had been deposited in the DDBJ database, revealed that *T. halophilus* also

conserves the five genes upstream of the variable regions that contain genes for various glycosyl transferases, modifying enzymes, sugar precursor synthesis enzymes, a repeat unit flippase (Wzx), and a polysaccharide polymerase (Wzy) (Fig. 1A). Generally, genetic variation of *cps* loci can create different CPS patterns (16), which implies the structural difference of CPSs between YA5 and YG2. I extracted CPSs from YA5 and YG2 and analyzed their sugar composition by high-performance liquid chromatography (HPLC) (data not shown). Only glucose was detected in the hydrolysates from both strains, but they should contain other types of components, such as amino sugars, uronic acids, sialic acids, and sugar alcohols. Polysaccharide pyruvyltransferase of YA5 is presumed to be one of the modifying enzymes for CPS synthesis, indicating that the mutation might have affected the structure and/or expression of CPSs. The gene that contained a transposed IS in YG2R1 (α-phosphoglucomutase) was not located in the *cps* locus, but α-phosphoglucomutase contributes to the generation of sugar precursors such as UDP-glucose and UDP-glucuronic acid for CPS synthesis (33). Based on these results, I hypothesized that CPSs of *T. halophilus* would be involved in the interactions with phages.

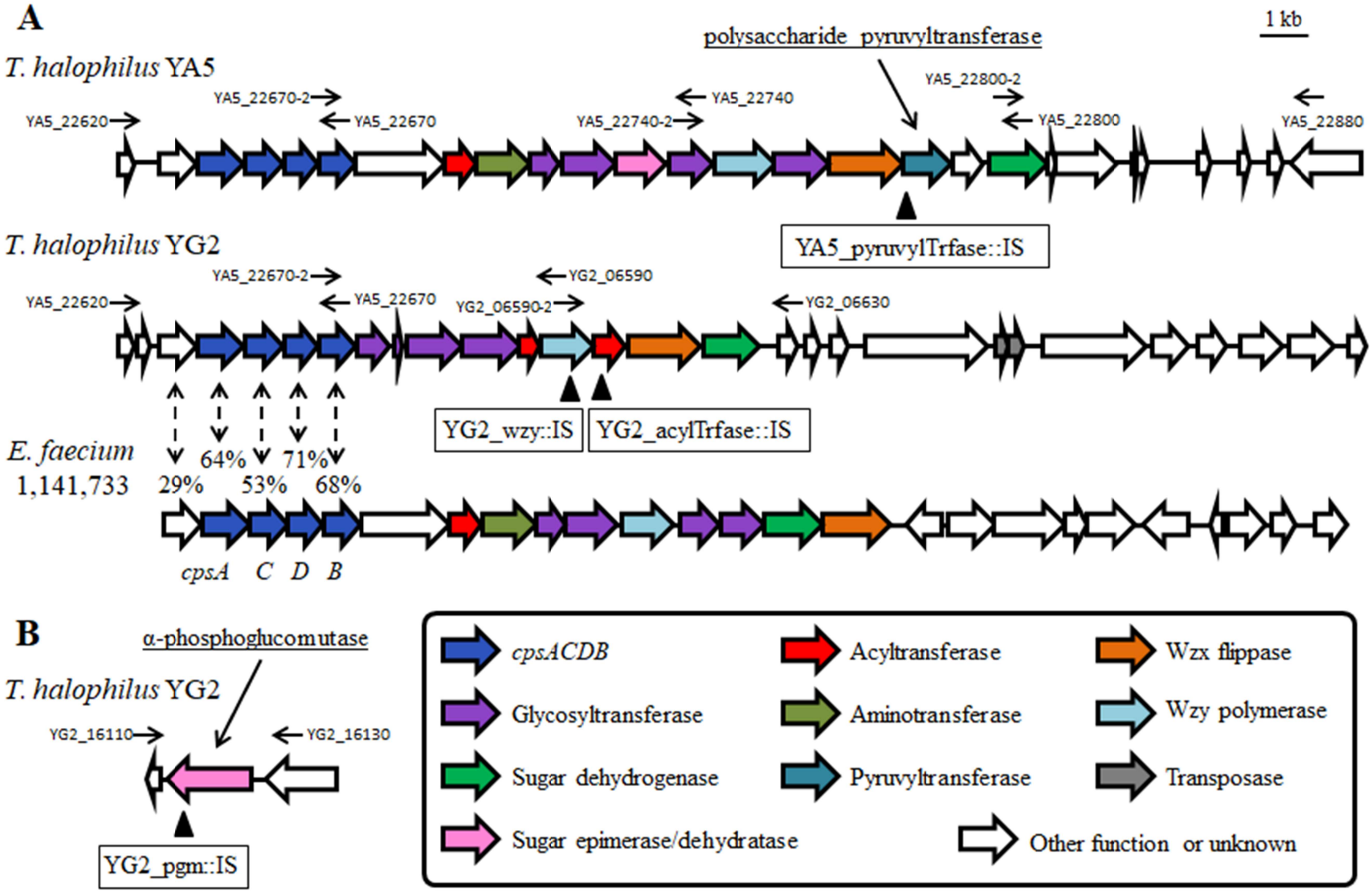
A
1 kb
polysaccharide_pyruvyltransferase
T. halophilus YA5
YA5_22620
YA5_22670-2
YA5_22670
YA5_22740-2
YA5_22740
YA5_22800-2
YA5_22800
YA5_22880
YA5_pyruvylTrfase::IS
T. halophilus YG2
YA5_22620
YA5_22670-2
YA5_22670
YG2_06590-2
YG2_06590
YG2_06630
YG2_wzy::IS
YG2_acylTrfase::IS
E. faecium
1,141,733
29%
64%
53%
71%
68%
cpsA
C
D
B
B
α-phosphoglucomutase
T. halophilus YG2
YG2_16110
YG2_16130
YG2_pgm::IS
cpsACDB
Glycosyltransferase
Sugar dehydrogenase
Sugar epimerase/dehydratase
Acyltransferase
Aminotransferase
Pyruvyltransferase
Other function or unknown
Wzx flippase
Wzy polymerase
Transposase

**Fig. 1:** Schematic representation of CPS synthesis genes in *T. halophilus*. The black arrows above ORFs represent the position at which the primers were designed. The location of ISs transposed in each derivative is indicated by black triangles below ORFs. (A) Comparison of *cps* loci in *T. halophilus* YA5, YG2, and *E. faecium* 1,141,733. The percentage shows the amino acid identities between *T. halophilus* and *E. faecium*. (B) Schematic representation of the α-phosphoglucomutase gene in YG2.

**Screening of additional *cps* derivatives**

Unfortunately, a feasible transformation technique for *T. halophilus* has not been established thus far (6), which did not allow me to use a general gene deletion and complementation strategy for the analysis of gene function. However, intrinsic ISs of *T. halophilus* jump within the genomes quite actively, and the transposition of ISs can be detected by comparing the length of PCR-amplified DNA fragments covering the targeted genes between the derivative and the parental strain (6, 21). Suppose that the deletion or structural alteration of CPSs is responsible for the altered phage susceptibility in the derivatives, and other additional phage-resistant derivatives with transposed ISs into the *cps* loci are expected to be found easily. Hence, I obtained additional phiYA5_2-resistant derivatives from YA5 and phiYG2_4-resistant derivatives from YG2 and amplified their DNA region covering the *cps* loci and α-phosphoglucomutase gene with the primers shown in Fig. 1 and Table 2. As expected, 16 of 31 phiYA5_2-resistant derivatives showed elongated PCR products covering a part of the *cps* locus (data not shown), and they were named YA5R2-YA5R17. DNA sequence analyses revealed that all 16 derivatives contained ISs on the polysaccharide pyruvyltransferase gene, similar to YA5R1R1 (data not shown). For YG2, among

approximately 700 phiYG2_4-resistant derivatives, 41 derivatives had ISs on α-phosphoglucomutase, the same as YG2R1; two ISs, IS*Teha7* and IS*Teha8*, were identified as active for the first time here. In addition, one derivative had an IS on the *wzy* polymerase gene (YG2_06590), and six derivatives had ISs on a putative acyltransferase gene (YG2_06600). The additional phiYG2_4-resistant derivatives were named YG2R2-YG2R49. The successful acquisition of the additional *cps* derivatives from both host strains strongly suggests the involvement of *cps* loci with host-phage interactions in *T. halophilus*. I picked four derivatives containing an IS in each gene and used them for further investigation. Hereafter, I will refer to these selected derivatives as YA5_pyruvylTrfase::IS (YA5R2), YG2_pgm::IS (YG2R1), YG2_wzy::IS (YG2R2), and YG2_acylTrfase::IS (YG2R48) (Fig. 1, Table 1). Under laboratory conditions, YG2_pgm::IS and YG2_acylTrfase::IS grew as fast as the parental strain YG2 (data not shown). The growth of YG2_wzy::IS was delayed, possibly because the *wzy* mutation accumulates synthetic intermediates and depletes lipid carriers that are also needed for peptidoglycan synthesis (34, 35). This might explain the infrequent acquisition of the *wzy* mutant in this study. YA5 and YG2 form cell clusters due to the lack of peptidoglycan hydrolase activity required for daughter cell separation (22). CPSs have also been suggested to be involved in the bacterial aggregation phenotype (36), but *cps* derivatives from YG2 form cell clusters the same as YG2 (data not shown), which denies the relation between CPSs and the cluster-forming phenotype in this case.

**CPS analysis of the derivatives**

To assess the CPS production of the *cps* derivatives, cell surface polysaccharides from YA5, YG2, and their derivatives were extracted and quantified by a phenol–sulfuric acid method (Fig. 2AB). YA5_pyruvylTrfase::IS produced no less

polysaccharides than the parental strain YA5. Therefore, YA5_pyruvylTrfase::IS is likely to produce adequate amounts of CPS, but it probably has a structural alteration. The three YG2 derivatives produced fewer glycopolymers than the parental strain, which shows that CPS production by the derivatives was severely damaged. α-phosphoglucomutase prepares donor substrates for CPS synthesis, and Wzy polymerase polymerizes CPS chains, which suggests that both genes are essential for CPS synthesis. Accordingly, I considered that the CPS production of these derivatives is almost completely lost. The remaining reactants in these derivatives could be other types of cell surface polysaccharides, such as WTA. On the other hand, acyltransferase is predicted to be involved in the decoration of CPSs and not indispensable for CPS synthesis, and YG2_acylTrfase::IS produced slightly more polysaccharides than YG2_pgm::IS and YG2_wzy::IS, which implies the possibility that the CPS production of YG2_acylTrfase::IS is not completely lost. YG2 and its derivatives were visualized through transmission electron microscopy (TEM) (Fig. 2C). Filamentary structures (>400 nm for long ones) were observed outside the cell walls of YG2, but the three derivatives forfeited such structures. These results demonstrated that the *cps* loci in *T. halophilus* are responsible for the production of CPSs, which were observed as filamentary capsule structures. Although I expected YG2_acylTrfase::IS to display a slight capsule, it seems that the CPS amounts of YG2_acylTrfase::IS were not enough to be observed. Since some parts of the filaments are bleary, it is likely that the visible filaments are only a part of the CPSs and that the CPSs, though invisible by TEM, possibly form a layer around cells. Particularly thick filaments might have been created by aggregation of CPSs during TEM fixation/staining. The cell wall thickness of YG2_pgm::IS was decreased, probably because α-phosphoglucomutase contributes not

only to the synthesis of CPS but also other polysaccharides, such as WTA and LTA (37).

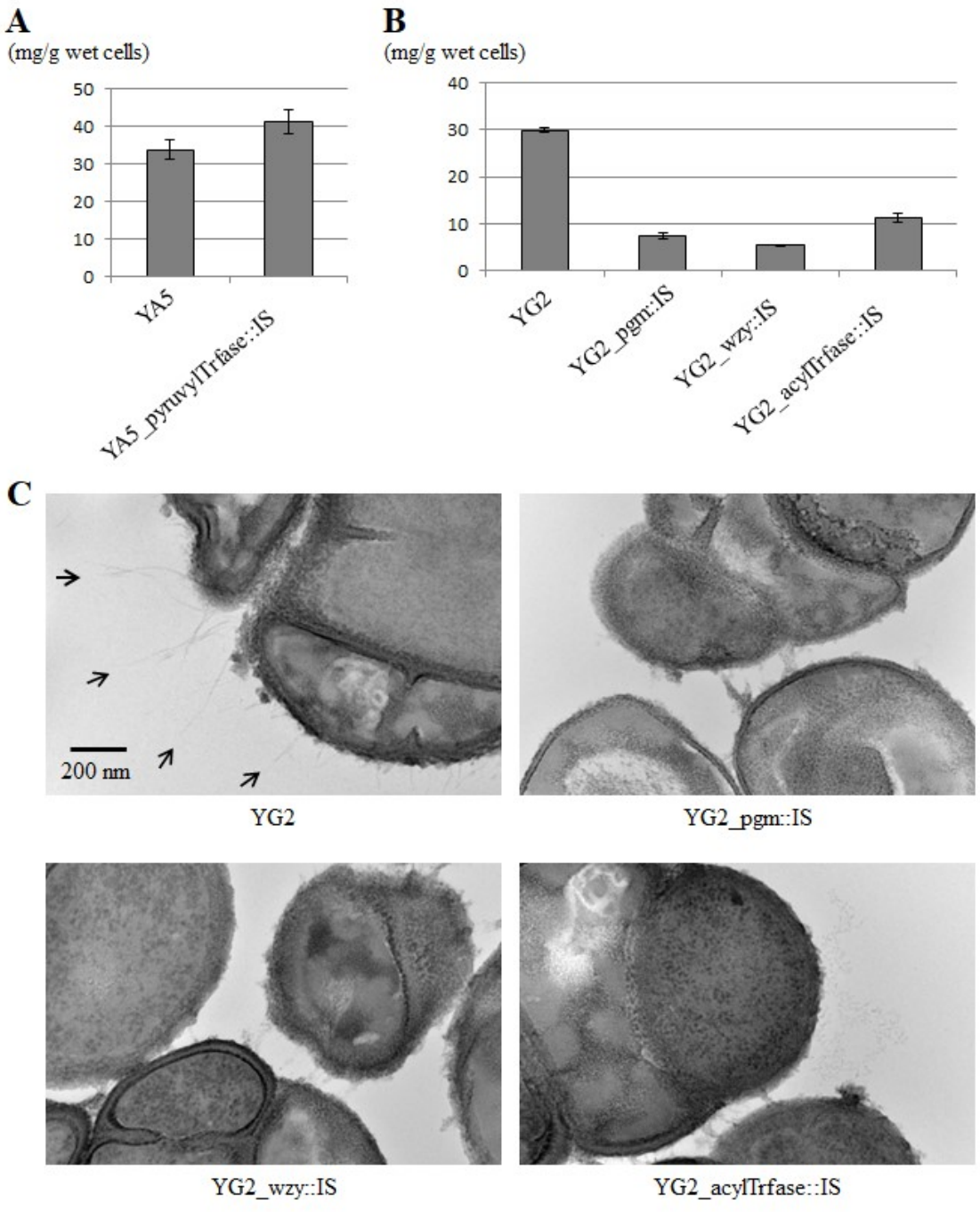


**Fig. 2:** Cell surface polysaccharide analysis in *T. halophilus*. (A) Quantification of polysaccharides in YA5 and its derivative. Data are expressed as the mean with error bars representing ± SD (n=3). (B) Quantification of polysaccharides in YG2 and its

derivatives. Data are expressed as the mean with error bars representing ± SD (n=3). (C) TEM image of YG2 and its derivatives. Arrows indicate the filamentous structures outside the cell walls of YG2.

### *cps* derivatives have altered phage susceptibility

The susceptibility of the *cps* derivatives to phiYA5_2 and phiYG2_4 was investigated by plaque formation assays (Fig. 3A). As expected, YA5_pyruvylTrfase::IS was not infected by phiYA5_2. Surprisingly, the three *cps* derivatives from YG2 were susceptible to phiYA5_2, although the parent strain was not. YG2_pgm::IS and YG2_wzy::IS became resistant to phiYG2_4, but curiously, YG2_acylTrfase::IS was still susceptible to phiYG2_4 as well as the parent strain, although it had been obtained as a phiYG2_4-resistant strain. To address this discrepancy, the cultures of YG2 and its derivatives were diluted and spotted on LA13 agar plates with or without phiYG2_4 (Fig. 3B). YG2_pgm::IS and YG2_wzy::IS were not affected by the presence of phiYG2_4. The growth of YG2_acylTrfase::IS was slightly inhibited, but the parent strain YG2 was further obstructed by phiYG2_4. Taken together, it was concluded that YG2_acylTrfase::IS acquired resistance to phiYG2_4 but was not insensitive.

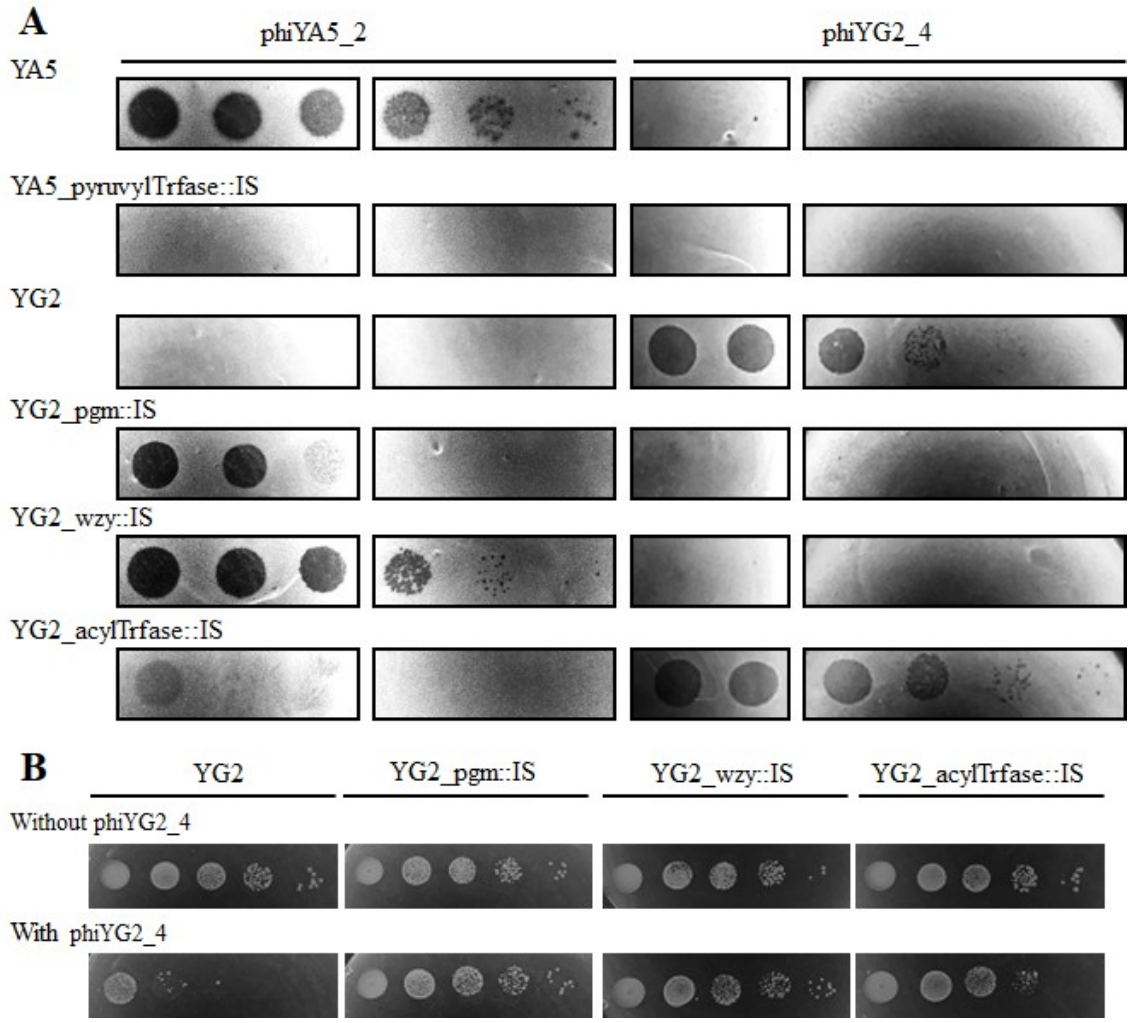


**Fig. 3:** Phage susceptibility of YA5, YG2, and their derivatives. (A) PhiYA5_2 and phiYG2_4 specimens were serially diluted 10-fold from left to right and spotted on each host strain. (B) YG2 and its derivatives were grown with or without phiYG2_4. More than $10^6$ pfu of phiYG2_4 was plated prior to spotting cells. The cells were serially diluted 10-fold from left to right.

**Bacteriophage adsorption to the *cps* derivatives**

Bacterial CPSs are reported to act as barriers and/or receptors for phages (38, 39). Hence, I speculated that the adsorption to the *cps* derivatives by the phages was

affected in some way, which conferred phage resistance to the derivatives. I performed a phage adsorption assay with YA5, YG2, and their derivatives. The cells were mixed with the phages, and the bound phages were removed by centrifugation. Phage adsorption was measured from the free phage titers of the supernatant. YA5, YG2_pgm::IS, and YG2_wzy::IS were adsorbed by phiYA5_2 (Fig. 4A), consistent with the results of the plaque formation assay (Fig. 3A). These data verify the presence of a binding receptor for phiYA5_2 in both YA5 and YG2. The structural change in CPSs that occurred in YA5_pyruvylTrfase::IS could possibly have prevented adsorption by phiYA5_2, but the loss of CPSs of YG2 allowed phiYA5_2 to adsorb. These results indicated that CPSs are a barrier rather than a receptor to phiYA5_2. It is likely that CPSs hide the other receptor molecules on the cell surface, but phiYA5_2 specifically breaks through the CPSs of YA5 and approaches the receptor (see below results). The adsorption by phiYG2_4 to YG2 was also confirmed, but the three *cps*-derivatives from YG2 were not. This is consistent with the resistance to phiYG2_4 (Fig. 3B). The fact that the CPSs of YG2 are required for adsorption by phiYG2_4 suggests that the CPSs of YG2 are a specific receptor for phiYG2_4. The lack of structural decoration in CPSs of YG2_acylTrfase::IS perhaps made the adsorption by phiYG2_4 less efficient and conferred resistance against phiYG2_4 on YG2_acylTrfase::IS. It can also be guessed that phages could bind to hosts less efficiently when they were dispersed in liquid compared to when they were densely packed on an agar plate. The reason for the strong plaque formation to YG2_acylTrfase::IS by phiYG2_4 (Fig. 3A), despite the decreased adsorption efficiency, may be because the thinning of capsule facilitates phage infection; even if the phage targets capsule (40).

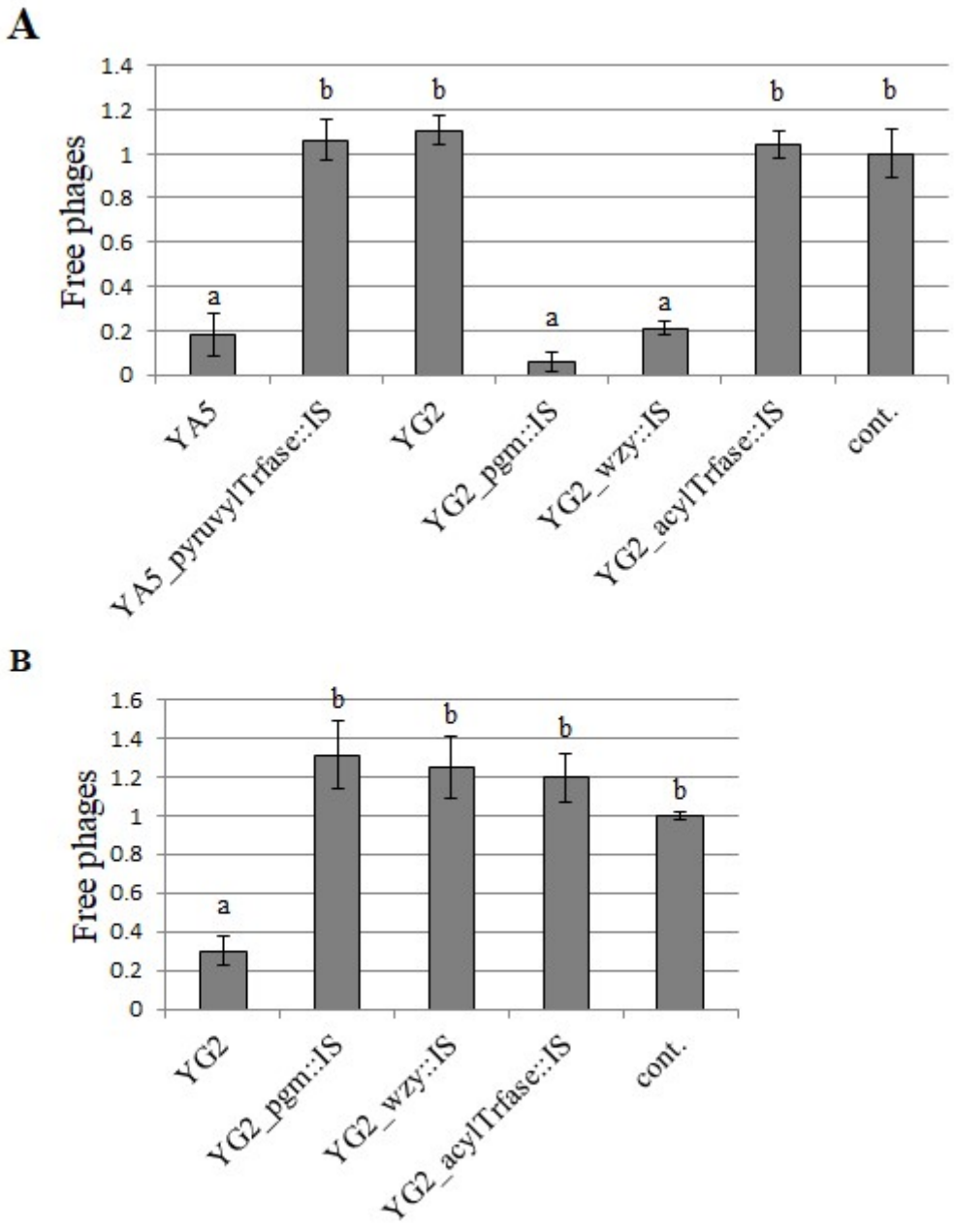


**Fig. 4:** Phage adsorption to the host cells. Free phage titers after centrifugation were calculated as the ratio of the control (without cells). Cont. means control sample. Data are expressed as the mean with error bars representing ± SD (n=3). Bars with different letters are significantly different by Tukey's multiple comparison test. (A) Adsorption by

phiYA5_2. (B) Adsorption by phiYG2_4.

**PhiYA5_2 possesses the CPS depolymerase**

As described above, it was estimated that CPSs prevented the adsorption to host cells by phiYA5_2, but phiYA5_2 specifically overcame the CPSs of YA5. CPSs have been reported to act as physical barriers against phages, and phages are equipped with various virion-associated enzymes to penetrate CPSs, termed polysaccharide depolymerases (41). Virions of phiYA5_2 were spotted on each strain after UV irradiation, which renders the virion noninfective but leaves the enzymatic activity of viral proteins (42). The phage particles formed no plaques but created translucent zones on YA5, YG2_pgm::IS, and YG2_wzy::IS, which clearly shows that the virions of phiYA5_2 possess the activity to degrade cell components of the host strains (Fig. 5A). This result is in good agreement with the adsorption experiment (Fig. 4A), suggesting that cell component degradation by virion-associated enzymes is a prerequisite for phage adsorption to receptors (or vice versa). Since these zones were formed not only on YA5 but also on CPS-deficient derivatives from YG2, I hypothesized that the zones were brought about by peptidoglycan degradation. Adsorption by multiple phages that cleave a pore in the bacterial cell walls causes instant cell lysis (43). Depolymerases can cause CPS degradation prior to infection and result in plaque-surrounding halos, which are the typical hallmark for the presence of depolymerases (41). I carefully observed the plaques of phiYA5_2 and noticed turbid halos around the plaques on YA5 (Fig. 5B). Such halos were not formed around the plaques on YG2_pgm::IS, YG2_wzy::IS, and YG2_acylTrfase::IS, which suggests that phiYA5_2 possesses the depolymerase digesting the CPSs of YA5. The fact that YG2 were not lysed but the *cps* derivatives

from YG2 were lysed by UV-inactivated phiYA5_2 supports that CPSs are a barrier for peptidoglycan hydrolase to contact cell walls. Taken together, I consider that the cell lysis of YA5 by inactivated phiYA5_2 was synergistically caused by CPS depolymerase and peptidoglycan hydrolase, while the cell lysis of YG2_pgm::IS and YG2_wzy::IS was caused by peptidoglycan hydrolase alone. YG2_pgm::IS was more susceptible to the UV-inactivated virion of phiYA5_2 than YA5 and YG2_wzy::IS, possibly because the disruption of α-phosphoglucomutase affects the other cell wall components and makes YG2_pgm::IS more vulnerable to peptidoglycan hydrolase. Given the possibility that YA5_pyruvylTrfase::IS has a structural alteration in CPSs, the specific depolymerase of phiYA5_2 may not be able to recognize the altered CPS structure of YA5_pyruvylTrfase::IS, which probably explains why phiYA5_2 cannot approach the cell surface of YA5_pyruvylTrfase::IS and cannot infect it. To predict the gene encoding the depolymerase from phiYA5_2, I compared the genome of phiYA5_2 to that of phiWJ7, which belongs to the same genus as phiYA5_2. Overall, the structures of the two phage genomes were quite similar, but the ORFs encoding phage tail fiber proteins were remarkably different, which suggests that tail fibers might be responsible for host specificity. Considering that most depolymerases are encoded within the ORF of the tail spike or tail fiber (44), the tail fiber of phiYA5_2 is likely to possess depolymerase activity, degrading the CPSs of YA5. I previously indicated that the tail spike of phiWJ7 is homologous to the peptidoglycan-degrading enzyme of staphylococcal phages (6), and phiYA5_2 also possessed a similar tail spike, suggesting that the tail spike of phiYA5_2 is responsible for peptidoglycan digestion.

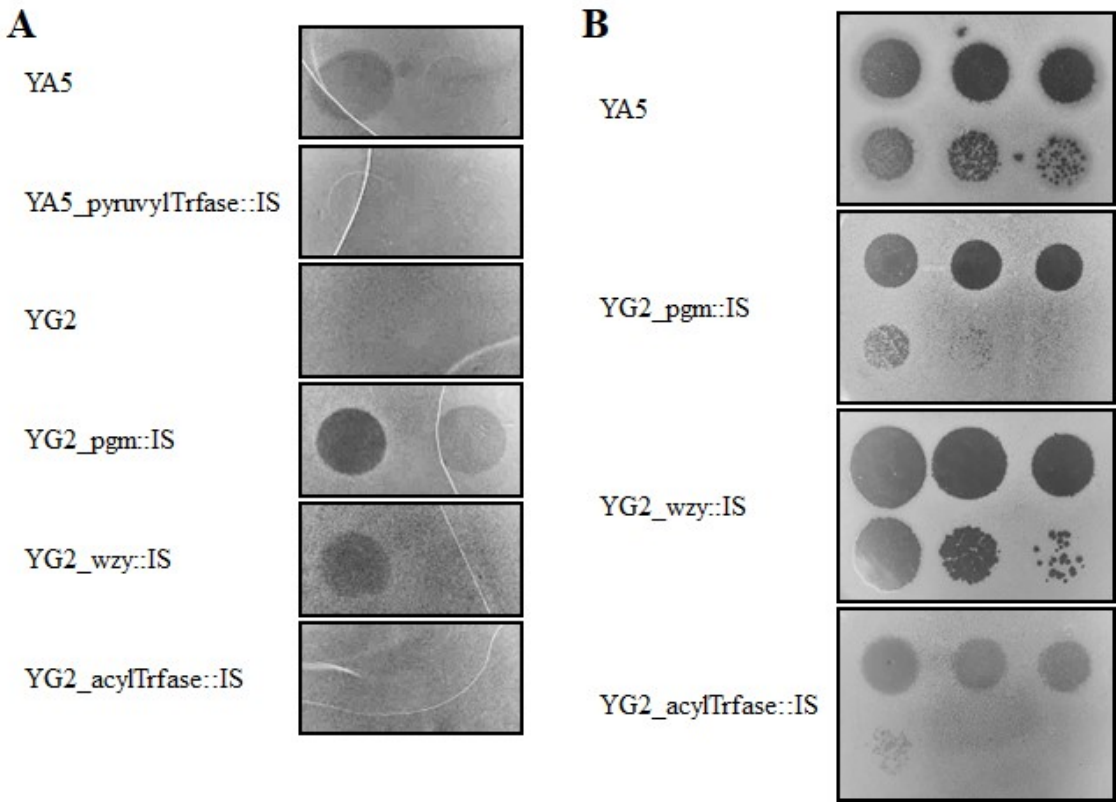


**Fig. 5:** Cell-degrading enzyme activities of phiYA5_2. (A) UV-inactivated virions of phiYA5_2 were spotted on each strain. The left spot contained $1.9 \times 10^7$ pfu of virions (before UV irradiation), and the right spot contained 1/10 of that. (B) Plaques of phiYA5_2 were observed by shining light from behind the plates. The spotted phage specimens were serially diluted 10-fold from top left to bottom right.

## DISCUSSION

### Identification of CPS

In this section, I identified CPS as the determinant factor for phage susceptibility in *T. halophilus*. This information could help establish effective strategies to avoid fermentation failure caused by phage-induced lysis of the starter strains, e.g., preparing a mixture of strains with different phage susceptibilities as a starter culture.

In section 1, I identified WTA as an indispensable irreversible binding receptor for the *T. halophilus* phage phiWJ7, but another cell wall component was estimated to be involved in the first reversible attachment (6). Moreover, the genetic diversity of WTA synthesis genes was not high enough to explain the observed narrow host ranges of tetragenococcal phages. Therefore, I conducted this study and concluded that the *cps* loci contributing to CPS synthesis were the genetic determinants of phage susceptibility in *T. halophilus* and that the variability in the *cps* loci is, at least partially, responsible for the narrow host ranges of tetragenococcal phages. The structural diversity of CPSs from Gram-negative bacteria often limits the host range of phages, but this study is meaningful in that it suggested a similar mechanism in Gram-positive bacteria.

Bacterial CPSs exhibit great diversity in sugar composition, linkage, and branching. Determination of the detailed CPS structures is particularly challenging, as the diversity of CPS components and branching complicate the structural analysis. Very recently, EPS structures from *T. halophilus* were analyzed, and they contained various components, such as glucose, galactose, mannose, arabinose, xylose, fucose, and glucuronic acid (45, 46). Structural analysis of CPSs in *T. halophilus* is expected to be conducted in other studies.

Capsules are produced by many bacterial species, including both Gram-positive and Gram-negative bacteria, but their morphological characteristics are diverse. For instance, some strains of *Staphylococcus aureus* produce a thick capsule that can be visualized by light microscopy with India ink staining (47). On the other hand, a capsule from *E. faecium* cannot be seen without immunogold labeling even by TEM (48). The capsule from *T. halophilus* was not detectable by light microscopy (data not shown) but a part of it could be observed as filamentary structures by TEM (Fig.

2C). Similar filamentary structures from *T. halophilus* were previously observed by Ueki et al., although their identification has not been obtained (49).

**CPS as receptor/barrier**

CPSs are known to act as a protective barrier against stress factors such as ethanol, low pH, lysozyme, and antibiotics (50, 51). In this study, it was shown that CPSs can protect *T. halophilus* against phage infections, and other roles of CPSs for *T. halophilus* will be revealed in the future.

Since phiYG2_4 could not bind to *cps* derivatives from YG2, I considered that CPSs are the binding receptor for phiYG2_4 (Fig. 4B). Several types of cell surface polysaccharides of Gram-positive bacteria, in addition to peptidoglycan, WTA, and LTA, have been reported to be receptors for phage adsorption. For instance, CWPSs, so-called "pellicles" of *L. lactis,* are targeted by phages and mainly define phage susceptibility in this species (52). EPSs of *Streptococcus thermophilus* are the receptor for streptococcal phage CHPC926 (53). Enterococcal phage ΦNPV1 utilizes a complex polysaccharide called "enterococcal polysaccharide antigen (EPA)" of *Enterococcus faecalis* (54). Thus, various glycopolymers can serve as phage binding receptors, and CPSs are also reported as receptors in many Gram-negative bacteria, such as *Escherichia coli*, *Campylobacter jejuni*, and *Salmonella enterica* (38, 55). However, only *Clostridium perfringens* phage CPS1 is known to date as a phage infecting Gram-positive bacteria using CPS as a receptor (30). To my knowledge, phages infecting lactic acid bacteria have not yet been reported to target CPSs as receptors. To irrefutably prove that CPS is the binding receptor for phiYG2_4, I preincubated phiYG2_4 with CPSs extracted from YG2 prior to infection, but a decrease in pfu was not observed (data not shown). Ho et al. obtained a similar result when ΦNPV1 was preincubated with EPA, and they speculated that EPA

is not the only requirement for ΦNPV1 adsorption or that the availability of EPA for ΦNPV1 differs in whole cells versus EPA extracts (54). In any case, further research is necessary to elucidate the detailed mechanism by which CPSs in *T. halophilus* are involved in phage adsorption.

It is also known that CPSs act as a barrier to sterically inhibit phage adsorption (39). To break through this barrier, phages utilize CPSs as a receptor and/or degrade CPSs by CPS depolymerases (40). The depolymerases digest CPSs, thereby drilling a tunnel through the capsules and enabling phage particles to contact the receptors under the capsules. The high diversity of CPS structures can contribute to the narrow host spectrum, as phage-carried CPS depolymerases recognize specific CPS structures. A considerable number of putative depolymerases encoded by phages infecting Gram-negative pathogens such as *Klebsiella pneumoniae*, *Pseudomonas aeruginosa*, and *Acinetobacter baumannii* have been identified, but only scarce information is available about depolymerases from Gram-positive phages (56). Hyaluronidases that act on hyaluronan capsules from *Streptococcus pyogenes* and *Streptococcus equi* and γ-glutamyl hydrolases that act on poly-γ-glutamate capsules from *Bacillus subtilis* are known (57, 58, 59). I predicted that the tail fiber gene of phiYA5_2 encodes the depolymerase, and the precise identification of phage-encoded depolymerases that digest strain-specific CPSs of Gram-positive bacteria, including *T. halophilus*, will be an interesting topic for future studies.

**Insertion sequences**

ISs played important roles in this section. In chapter 2, I reported the very frequent transposition of three IS*4* family ISs, IS*Teha3*, IS*Teha4*, and IS*Teha5,* in *T. halophilus* (6, 21). Here, I discovered two additional active ISs named IS*Teha7* and

IS*Teha8* for transposition into the α-phosphoglucomutase gene of YG2. Based on the amino acid sequence relatedness of transposases, I entered IS*Teha7* as a novel IS*5* family IS*5* subgroup member and IS*Teha8* as a novel IS*4* family IS*Pepr1* subgroup member in the ISfinder database. Four of five ISs identified as active in *T. halophilus* to date are IS*4* family members, and IS*Teha7* is the only IS*5* family member. The previously described three ISs are distributed in the genomes of all six *T. halophilus* strains whose complete genomes were determined. However, one strain among the six does not possess IS*Teha7*, and two strains among the six do not possess IS*Teha8*, suggesting that these ISs are minor mutagens compared to the other three ISs. ISs are utilized in transposon mutagenesis systems for the characterization of gene functions (60). They are also used for the identification of phage receptors (61). Usually, transposon mutagenesis is accomplished by inserting ISs with a drug resistance marker gene from an extrinsic plasmid into the host chromosome, but I could execute this study with intrinsic ISs without marker genes due to the surprisingly high transposition frequency of ISs in *T. halophilus*. I will continue to pursue research to understand the basic features of ISs in *T. halophilus* and to develop their utility.

**REFERENCES**


1. Kuda T, Izawa Y, Ishii S, Takahashi H, Torido Y, Kimura B. 2012. Suppressive effect of *Tetragenococcus halophilus*, isolated from fish-*nukazuke*, on histamine accumulation in salted and fermented fish. Food Chem 130:569-574.
2. Chen YS, Yanagida F, Hsu JS. 2006. Isolation and characterization of lactic acid bacteria from suan-tsai (fermented mustard), a traditional fermented food in Taiwan. J Appl Microbiol 101:125-130.
3. Tanaka Y, Watanabe J, Mogi Y. 2012. Monitoring of the microbial communities involved in the soy sauce manufacturing process by PCR-denaturing gradient gel electrophoresis. Food Microbiol 31:100-106.
4. Uchida K, Kanbe C. 1993. Occurrence of bacteriophages lytic for *Pediococcus halophilus*, a halophilic lactic-acid bacterium, in soy sauce fermentation. J Gen Appl Microbiol 39:429-437.
5. Higuchi T, Uchida K, Abe K. 1999. Preparation of phage-insensitive strains of *Tetragenococcus halophila* and its application for soy sauce fermentation. Biosci Biotechnol Biochem 63:415-417.
6. Wakinaka T, Matsutani M, Watanabe J, Mogi Y, Tokuoka M, Ohnishi A. 2022. Ribitol-containing wall teichoic acid of *Tetragenococcus halophilus* is targeted by bacteriophage phiWJ7 as a binding receptor. Microbiol Spectr 10:e00336-22.
7. Geller BL, Ivey RG, Trempy JE, Hettinger-Smith B. 1993. Cloning of a chromosomal gene required for phage infection of *Lactococcus lactis* subsp. *lactis* C2. J Bacteriol 175:5510-5519.
8. Räisänen L, Schubert K, Jaakonsaari T, Alatossava T. 2004. Characterization of

lipoteichoic acids as *Lactobacillus delbrueckii* phage receptor components. J Bacteriol 186:5529-5532.

9. Wendlinger G, Loessner MJ, Scherer S. 1996. Bacteriophage receptors on *Listeria monocytogenes* cells are the *N*-acetylglucosamine and rhamnose substituents of teichoic acids or the peptidoglycan itself. Microbiology 142:985-992.

10. Chapot-Chartier MP, Kulakauskas S. 2014. Cell wall structure and function in lactic acid bacteria. Microb Cell Factories 13:1-23.

11. Theodorou I, Courtin P, Palussière S, Kulakauskas S, Bidnenko E, Péchoux C, Fenaille F, Penno C, Mahony J, van Sinderen D, Chapot-Chartier MP. 2019. A dual-chain assembly pathway generates the high structural diversity of cell-wall polysaccharides in *Lactococcus lactis*. J Biol Chem 294:17612-17625.

12. Forde A, Fitzgerald GF. 1999. Analysis of exopolysaccharide (EPS) production mediated by the bacteriophage adsorption blocking plasmid, pCI658, isolated from *Lactococcus lactis* ssp. *cremoris* HO2. Int Dairy J 9:465-472.

13. Islam ST, Lam JS. 2014. Synthesis of bacterial polysaccharides via the Wzx/Wzy-dependent pathway. Can J Microbiol 60:697-716.

14. Standish AJ, Morona R. 2014. The role of bacterial protein tyrosine phosphatases in the regulation of the biosynthesis of secreted polysaccharides. Antioxid Redox Signal 20:2274-2289.

15. Zeidan AA, Poulsen VK, Janzen T, Buldo P, Derkx PM, Øregaard G, Neves AR. 2017. Polysaccharide production by lactic acid bacteria: from genes to industrial applications. FEMS Microbiol Rev 41:S168-S200.

16. Bentley SD, Aanensen DM, Mavroidi A, Saunders D, Rabbinowitsch E, Collins M, Donohoe K, Harris D, Murphy L, Quail MA, Samuel G, Skovsted IC, Kaltoft MS, Barrell B, Reeves PR, Parkhill J, Spratt BG. 2006. Genetic analysis of the capsular biosynthetic locus from all 90 pneumococcal serotypes. PLoS Genet 2:e31.

17. Varvio SL., Auranen K, Arjas E, Mäkelä PH. 2009. Evolution of the capsular regulatory genes in *Streptococcus pneumoniae*. J Infect Dis 200:1144-1151.

18. Geno KA, Gilbert GL, Song JY, Skovsted IC, Klugman KP, Jones C, Konradsen HB, Nahm MH. 2015. Pneumococcal capsules and their types: past, present, and future. Clin Microbiol Rev 28:871-899.

19. Sempere J, Llamosí M, Román F, Lago D, González-Camacho F, Pérez-García C, Yuste J, Domenech M. 2022. Clearance of mixed biofilms of *Streptococcus pneumoniae* and methicillin-susceptible/resistant *Staphylococcus aureus* by antioxidants *N*-acetyl-L-cysteine and cysteamine. Sci Rep 12:1-12.

20. Wakinaka T, Iwata S, Takeishi Y, Watanabe J, Mogi Y, Tsukioka Y, Shibata Y. 2019. Isolation of halophilic lactic acid bacteria possessing aspartate decarboxylase and application to fish sauce fermentation starter. Int J Food Microbiol 292:137-143.

21. Wakinaka T, Watanabe J. 2019. Transposition of IS*4* family insertion sequences IS*Teha3*, IS*Teha4*, and IS*Teha5* into the *arc* operon disrupts arginine deiminase system in *Tetragenococcus halophilus*. Appl Environ Microbiol 85:e00208-19.

22. Shirakawa D, Wakinaka T, Watanabe J. 2020. Identification of the putative *N*-acetylglucosaminidase CseA associated with daughter cell separation in *Tetragenococcus halophilus*. Biosci Biotechnol Biochem 84:1724-1735.

23. Bankevich A, Nurk S, Antipov D, Gurevich AA, Dvorkin M, Kulikov AS, Lesin VM, Nikolenko SI, Pham S, Prjibelski AD, Pyshkin AV, Sirotkin AV, Vyahhi N, Tesler G, Alekseyev MA, Pevzner PA. 2012. SPAdes: a new genome assembly algorithm and its applications to single-cell sequencing. J Comput Biol 19:455–477.

24. Tanizawa Y, Fujisawa T, Kaminuma E, Nakamura Y, Arita M. 2016. DFAST and DAGA: Web-based integrated genome annotation tools and resources. Biosci Microbiota Food Health 35:173–184.

25. Matsutani M, Wakinaka T, Watanabe J, Tokuoka M, Ohnishi A. 2021. Comparative genomics of closely related *Tetragenococcus halophilus* strains elucidate the diversity and microevolution of CRISPR elements. Front microbiol 12:1605.

26. Li H, Durbin R. 2010. Fast and accurate long-read alignment with Burrows–Wheeler transform. Bioinformatics 26:589-595.

27. McKenna A, Hanna M, Banks E, Sivachenko A, Cibulskis K, Kernytsky A, Garimella K, Altshuler D, Gabriel S, Daly M, DePristo MA. 2010. The Genome Analysis Toolkit: a MapReduce framework for analyzing next-generation DNA sequencing data. Genome Res 20:1297-1303.

28. DePristo MA, Banks E, Poplin R, Garimella KV, Maguire JR, Hartl C, Philippakis AA, del Angel G, Rivas MA, Hanna M, McKenna A, Fennell TJ, Kernytsky AM, Sivachenko AY, Cibulskis K, Gabriel SB, Altshuler D, Daly MJ. 2011. A framework for variation discovery and genotyping using next-generation DNA sequencing data. Nat Genet 43:491-498.

29. Deatherage DE, Barrick JE. 2014. Identification of mutations in

laboratory-evolved microbes from next-generation sequencing data using breseq. Methods Mol Biol 1151:165-188.

30. Ha E, Chun J, Kim M, Ryu S. 2019. Capsular polysaccharide is a receptor of a *Clostridium perfringens* bacteriophage CPS1. Viruses 11:1002.

31. Baptista C, Santos MA, São-José C. 2008. Phage SPP1 reversible adsorption to *Bacillus subtilis* cell wall teichoic acids accelerates virus recognition of membrane receptor YueB. J Bacteriol 190:4989.

32. Palmer KL, Godfrey P, Griggs A, Kos VN, Zucker J, Desjardins C, Cerqueira G, Gevers D, Walker S, Wortman J, Feldgarden M, Haas B, Birren B, Gilmore MS. 2012. Comparative genomics of enterococci: variation in *Enterococcus faecalis*, clade structure in *E. faecium*, and defining characteristics of *E. gallinarum* and *E. casseliflavus*. MBio 3:e00318-11.

33. Gilbert C, Robinson K, Le Page RW, Wells JM. 2000. Heterologous expression of an immunogenic pneumococcal type 3 capsular polysaccharide in *Lactococcus lactis*. Infect Immun 68:3251-3260.

34. Liu D, Cole RA, Reeves PR. 1996. An O-antigen processing function for Wzx (RfbX): a promising candidate for O-unit flippase. J Bacteriol 178:2102-2107.

35. Sewell EWC, Brown ED. 2014. Taking aim at wall teichoic acid synthesis: new biology and new leads for antibiotics. J Antibiot 67:43-51.

36. Burdman S, Jurkevitch E, Soria-Díaz ME, Serrano AMG, Okon Y. 2000. Extracellular polysaccharide composition of *Azospirillum brasilense* and its relation with cell aggregation. FEMS Microbiol Lett 189:259-264.

37. Lazarevic V, Soldo B, Médico N, Pooley H, Bron S, Karamata D. 2005. *Bacillus subtilis* α-phosphoglucomutase is required for normal cell morphology

and biofilm formation. Appl Environ Microbiol 71:39-45.

38. Gong Q, Wang X, Huang H, Sun Y, Qian X, Xue F, Ren J, Dai J, Tang F. 2021. Novel host Recognition mechanism of the K1 capsule-specific phage of *Escherichia coli*: capsular polysaccharide as the first receptor and Lipopolysaccharide as the secondary receptor. J Virol 95:e00920-21.

39. Knecht LE, Veljkovic M, Fieseler L. 2020. Diversity and function of phage encoded depolymerases. Front microbiol 10:2949.

40. Pelkonen S, Aalto J, Finne J. 1992. Differential activities of bacteriophage depolymerase on bacterial polysaccharide: binding is essential but degradation is inhibitory in phage infection of K1-defective *Escherichia coli*. J Bacteriol 174:7757-7761.

41. Latka A, Maciejewska B, Majkowska-Skrobek G, Briers Y, Drulis-Kawa Z. 2017. Bacteriophage-encoded virion-associated enzymes to overcome the carbohydrate barriers during the infection process. Appl Microbiol Biotechnol 101:3103-3119.

42. Cornelissen A, Ceyssens PJ, T'syen J, Van Praet H, Noben JP, Shaburova OV, Krylov VN, Volckaert G, Lavigne R. 2011. The T7-related *Pseudomonas putida* phage φ15 displays virion-associated biofilm degradation properties. PLoS One 6:e18597.

43. Delbrück M. 1940. The growth of bacteriophage and lysis of the host. J Gen Physiol 23:643.

44. Liu Y, Mi Z, Mi L, Huang Y, Li P, Liu H, Yuan X, Niu W, Jiang N, Bai C, Gao Z. 2019. Identification and characterization of capsule depolymerase Dpo48 from *Acinetobacter baumannii* phage IME200. PeerJ 7:e6173.

45. Yang X, Wu J, An F, Xu J, Bat-Ochir M, Wei L, Li M, Bilige M, Wu R. 2022. Structure characterization, antioxidant and emulsifying capacities of exopolysaccharide derived from *Tetragenococcus halophilus* SNTH-8. Int J Biol Macromol 208:288-298.

46. Zhang M, Zeng S, Hao L, Yao S, Wang D, Yang H, Wu C. 2022. Structural characterization and bioactivity of novel exopolysaccharides produced by *Tetragenococcus halophilus*. Food Res Int 155:111083.

47. Foster TJ. 1991. Potential for vaccination against infections caused by *Staphylococcus aureus*. Vaccine 9:221-227.

48. Huebner J, Wang Y, Krueger WA, Madoff LC, Martirosian G, Boisot S, Goldmann DA, Kasper DL, Tzianabos AO, Pier GB. 1999. Isolation and chemical characterization of a capsular polysaccharide antigen shared by clinical isolates of *Enterococcus faecalis* and vancomycin-resistant *Enterococcus faecium*. Infect Immun 67:1213-1219.

49. Ueki T, Izawa T, Ohba K, Noda Y. 2002. Mechanisms of floc formation by the halotolerant lactic acid bacteria with flocculent and its use in soy sauce brewing. J Jpn Soy Sauce Res Inst 28:105-110. (in Japanese).

50. Fernebro J, Andersson I, Sublett J, Morfeldt E, Novak R, Tuomanen E, Normark S, Normark BH. 2004. Capsular expression in *Streptococcus pneumoniae* negatively affects spontaneous and antibiotic-induced lysis and contributes to antibiotic tolerance. J Infect Dis 189:328-338.

51. Caggianiello G, Kleerebezem M, Spano G. 2016. Exopolysaccharides produced by lactic acid bacteria: from health-promoting benefits to stress tolerance mechanisms. Appl Microbiol Biotechnol 100:3877-3886.

52. Ainsworth S, Sadovskaya I, Vinogradov E, Courtin P, Guerardel Y, Mahony J, Grard T, Cambillau C, Chapot-Chartier MP, van Sinderen D. 2014. Differences in lactococcal cell wall polysaccharide structure are major determining factors in bacteriophage sensitivity. MBio 5:e00880-14.

53. Szymczak P, Filipe SR, Covas G, Vogensen FK, Neves AR, Janzen T. 2018. Cell wall glycans mediate recognition of the dairy bacterium *Streptococcus thermophilus* by bacteriophages. Appl Environ Microbiol 84:e01847-18.

54. Ho K, Huo W, Pas S, Dao R, Palmer KL. 2018. Loss-of-function mutations in *epaR* confer resistance to ϕNPV1 infection in *Enterococcus faecalis* OG1RF. Antimicrob Agents Chemother 62:e00758-18.

55. Sørensen MCH, van Alphen LB, Harboe A, Li J, Christensen BB, Szymanski C. M, Brøndsted L. 2011. Bacteriophage F336 recognizes the capsular phosphoramidate modification of *Campylobacter jejuni* NCTC11168. J Bacteriol 193:6742-6749.

56. Shen Y, Loessner MJ. 2021. Beyond antibacterials–exploring bacteriophages as antivirulence agents. Curr Opin Biotechnol 68:166-173.

57. Baker JR, Dong S, Pritchard DG. 2002. The hyaluronan lyase of *Streptococcus pyogenes* bacteriophage H4489A. Biochem J 365:317-322.

58. Kimura K, Itoh Y. 2003. Characterization of poly-γ-glutamate hydrolase encoded by a bacteriophage genome: possible role in phage infection of *Bacillus subtilis* encapsulated with poly-γ-glutamate. Appl Environ Microbiol 69:2491-2497.

59. Lindsay AM, Zhang M, Mitchell Z, Holden MT, Waller AS, Sutcliffe IC, Black GW. 2009. The *Streptococcus equi* prophage-encoded protein SEQ2045 is a

hyaluronan-specific hyaluronate lyase that is produced during equine infection. Microbiology 155:443-449.

60. Van Opijnen T, Camilli A. 2013. Transposon insertion sequencing: a new tool for systems-level analysis of microorganisms. Nat Rev Microbiol 11:435-442.

61. Kortright KE, Chan BK, Turner PE. 2020. High-throughput discovery of phage receptors using transposon insertion sequencing of bacteria. Proc Natl Acad Sci U S A 117:18670-18679.

## SUMMARY

Bacteriophages infecting *Tetragenococcus halophilus*, a halophilic lactic acid bacterium, have been a major industrial concern due to their detrimental effect on the quality of food products. Previously characterized tetragenococcal phages displayed narrow host ranges, but there is little information on these mechanisms. Here, I revealed the host's determinant factors for phage susceptibility using two virulent phages, phiYA5_2 and phiYG2_4, that infect *T. halophilus* YA5 and YG2, respectively. Phage-resistant derivatives were obtained from these host strains, and mutations were found at the capsular polysaccharide synthesis (*cps*) loci. Quantification analysis verified that capsular polysaccharide production by the *cps* derivatives from YG2 was impaired. Transmission electron microscope observation confirmed the presence of filamentous structures outside the cell walls of YG2 and their absence in the *cps* derivatives from YG2. Phage adsorption assays revealed that phiYG2_4 adsorbed to YG2 but not to its *cps* derivatives, which suggests that the capsular polysaccharide of YG2 is the specific receptor for phiYG2_4. Interestingly, phiYA5_2 adsorbed and infected *cps* derivatives from YG2, although neither adsorption nor infection by phiYA5_2 to the parental strain YG2 was observed. The plaque-surrounding halos formed by phiYA5_2 implied the presence of the virion-associated depolymerase that degrades capsular polysaccharide of YA5. These results indicated that the capsular polysaccharide is a physical barrier rather than a binding receptor to phiYA5_2 and that phiYA5_2 specifically overcomes the capsular polysaccharide of YA5. Thus, it was suggested that tetragenococcal phages utilize CPSs as a binding receptor and/or degrade CPSs to approach host cells.

*T. halophilus* is a halophilic lactic acid bacterium that contributes to the

fermentation process of various salted foods. Bacteriophage infections of *T. halophilus* have been a major industrial problem causing fermentation failure. Here, I identified the *cps* loci in *T. halophilus* as genetic determinants of phage susceptibility. The structural diversity of the capsular polysaccharide is responsible for the narrow host ranges of tetragenococcal phages. The information provided here could facilitate future studies on tetragenococcal phages and the development of efficient methods to prevent bacteriophage infections.

## CONCLUSIONS

As described in the GENERAL INTRODUCTION, lactic acid bacteria and bifidobacteria are used for various fermented foods and industrially important. Therefore, I studied on sugar metabolism in *Bifidobacterium bifidum*, and on amino acid metabolism and bacteriophage susceptibility in *Tetragenococcus halophilus*.

In CHAPTER I SECTION 1, an α-galactosidase of *B. bifidum* that degrades blood group B antigens on sugar termini of human gastrointestinal mucin was investigated. The recombinant α-galactosidase hydrolyzed α1,3-linked galactose in branched blood group B antigen, and the enzyme also acted on group B human salivary mucin and erythrocytes. The α-galactosidase conteins a carbohydrate-binding module (CBM) 51 domain, and I revealed that CBM51 specifically binds blood group B antigen and enhances the affinity of the enzyme toward substrates with multivalent B antigens. It was concluded that this enzyme plays an important role in degrading B antigens to acquire nutrients from mucin oligosaccharides in the gastrointestinal tracts.

In CHAPTER II, amino acid metabolism in *T. halophilus* was studied. In CHAPTER II SECTION 1, *T. halophilus* strains possessing aspartate decarboxylase were isolated and their property as starter cultures for fish sauce fermentation was elucidated. The isolates converted aspartate into alanine almost completely in the fish sauce mash. In addition, the strains prevented the accumulation of biogenic amines, whereas various amines were accumulated in fish sauce mash without starter cultures. Sensory evaluation tests indicated that converting the sour amino acid aspartate into the sweet amino acid alanine made the fish sauce taste milder. In conclusion, *T. halophilus* possessing aspartate decarboxylase can be used as a favorable fish sauce fermentation starter.

In CHAPTER II SECTION 2, I generated derivatives lacking arginine deiminase activity from a wild-type strain of *T. halophilus*. Using these derivatives as a fermentation starter prevented arginine deimination in soy sauce. DNA sequence analysis of the derivatives revealed that novel IS*4* family insertion sequences, designated IS*Teha3*, IS*Teha4* and IS*Teha5*, were transposed into the region around the arginine deiminase operon. These are the first active insertion sequences found in *T. halophilus*.

In CHAPTER III, the mechanism determining bacteriophage susceptibility in *T. halophilus* was investigated. In CHAPTER III SECTION 1, ribitol-containing wall teichoic acid was identified as a host receptor indispensable for bacteriophage phiWJ7 infection. This is the first experimentally confirmed factor that determines the phage susceptibility in *T. halophilus*. However, it was thought that the structural diversity of wall teichoic acid is not high enough to explain the observed narrow host ranges of tetragenococcal phages.

In CHAPTER III SECTION 2, it was suggested that tetragenococcal phages utilize CPSs as a binding receptor and/or degrade CPSs to approach host cells. The variety in capsular polysaccharide structures is concluded to be responsible for the narrow host ranges of tetragenococcal phages. Bacteriophage infections of *T. halophilus* have been a major industrial problem causing fermentation failure, and these findings could facilitate future studies on tetragenococcal phages and the development of efficient methods to prevent bacteriophage infections.

## ACKNOWLEDGEMENTS

I sincerely acknowledge Prof. Jun Ogawa of Kyoto University for his nice and precise instruction.

I thank Prof. Hisashi Ashida of Kindai University for his kind and practical teaching.

I am grateful to the NODAI Genome Research Center, Tokyo University of Agriculture for sequencing and analysis, and to Mr. Kazuki Hayashi and Ms. Harumi Tanabe for their excellent technical assistance.

I thank Dr. Satoru Tomita of Food Research Institute, National Agriculture and Food Research Organization, for the helpful discussions and comments.

I would like to express my deepest gratitude to my co-workers for their support throughout this study, especially Prof. Jun Watanabe of Fukushima University, Dr. Masataka Satomi of Japan Fisheries Research and Education Agency, Prof. Minenosuke Matsutani of Tokyo University of Agriculture, Prof. Masafumi Tokuoka of Tokyo University of Agriculture, Prof. Akihiro Ohnishi of Tokyo University of Agriculture, Mr. Yoshinobu Mogi of Yamasa Corporation.

**Takura Wakinaka**

## LIST OF PUBLICATIONS

**Takura Wakinaka**, Masashi Kiyohara, Shin Kurihara, Akiko Hirata, Thida Chaiwangsri, Takayuki Ohnuma, Tamo Fukamizo, Takane Katayama, Hisashi Ashida, Kenji Yamamoto: Bifidobacterial α-galactosidase with unique carbohydrate-binding module specifically acts on blood group B antigen. Glycobiol., **23**, 232-240 (2013)

**Takura Wakinaka**, Satomi Iwata, Yuya Takeishi, Jun Watanabe, Yoshinobu Mogi, Yuichiro Tsukioka, Yuki Shibata: Isolation of halophilic lactic acid bacteria possessing aspartate decarboxylase and application to fish sauce fermentation starter. Int. J. Food Microbiol., **292**, 137-143 (2019)

**Takura Wakinaka**, Jun Watanabe: Transposition of IS*4* family insertion sequences IS*Teha3*, IS*Teha4*, and IS*Teha5* into the *arc* operon disrupts arginine deiminase system in *Tetragenococcus halophilus*. Appl. Environ. Microbiol., **85**, e00208-19 (2019)

**Takura Wakinaka**, Minenosuke Matsutani, Jun Watanabe, Yoshinobu Mogi, Masafumi Tokuoka, Akihiro Ohnishi: Ribitol-Containing Wall Teichoic Acid of *Tetragenococcus halophilus* is targeted by bacteriophage phiWJ7 as a binding receptor. Microbiol. Spectr., **10**, e00336-22 (2022)

**Takura Wakinaka**, Minenosuke Matsutani, Jun Watanabe, Yoshinobu Mogi, Masafumi Tokuoka, Akihiro Ohnishi: Identification of capsular polysaccharide synthesis loci determining bacteriophage susceptibility in *Tetragenococcus halophilus*. Microbiol. Spectr., **11**, e00385-23 (2023)